

# **Geological Survey Ireland**

## **Airborne Geophysical Survey – Pilot Studies 2006**

**(Cavan-Monaghan, Castleisland &  
Silvermines, Ireland)**

*Geological Survey Ireland is a division of the Department  
of Communications, Climate Action & Environment.*



**Geological Survey**  
Suirbhéireacht Gheolaíochta  
Ireland | Éireann

## TABLE OF CONTENTS

<b>SUMMARY.....</b>	<b>II</b>
<b>1 SURVEY: LOCATION AND DETAILS.....</b>	<b>3</b>
1.1 SURVEY SCHEME.....	3
1.1.1 Cavan-Monaghan-Leitrim survey .....	4
1.1.2 Castleisland and Silvermines surveys .....	4
1.2 COORDINATE SYSTEM.....	6
1.3 REFLIGHT SPECIFICATIONS.....	7
1.4 SURVEY OPERATIONS.....	7
1.4.1 Survey Duration .....	7
1.4.2 Personnel .....	9
1.4.3 Exceptions to Specifications .....	10
<b>2 EQUIPMENT .....</b>	<b>13</b>
2.1 GROUND-BASED EQUIPMENT .....	14
2.1.1 Base station at Enniskillen airport.....	15
2.1.2 Base station at Kerry airport.....	16
<b>3 CALIBRATION DATA .....</b>	<b>19</b>
3.1 MAGNETIC COMPENSATION .....	19
3.1.1 Compensations for Cavan-Monaghan-Leitrim area.....	20
3.1.2 Compensation for Castleisland and Silvermines areas .....	21
3.2 RADIOMETRIC CALIBRATION DATA .....	22
3.2.1 Cosmic and background coefficients .....	22
3.2.2 Stripping ratios .....	22
3.2.3 Height attenuation .....	23
3.2.4 Concentration coefficients.....	23
3.2.5 Resolution of the spectrometer.....	23
3.3 ELECTROMAGNETIC CALIBRATIONS .....	24
3.3.1 Coefficient Calibration .....	24
3.3.2 EM System orthogonality.....	26
3.3.3 EM Transmitter Effect on Magnetic Sensors .....	26
<b>4 DATA HANDLING, QC PROCEDURES AND PROCESSING .....</b>	<b>28</b>
4.1 QC AND FIELD PROCESSING.....	29
4.2 FINAL PROCESSING .....	31
<b>5 DELIVERABLES.....</b>	<b>33</b>
5.1 XYZ FILES .....	33
5.2 GRID FILES.....	36
<b>6 REFERENCES .....</b>	<b>38</b>
<b>APPENDIX 1: SURVEY EQUIPMENT .....</b>	<b>39</b>
AIRCRAFT.....	39
GEOPHYSICAL EQUIPMENT.....	39
<b>APPENDIX 2: MAPS OF THE SURVEY AREA.....</b>	<b>41</b>
OVERVIEW .....	41
CAVAN-MONAGHAN-LEITRIM .....	43
CASTLEISLAND.....	53
SILVERMINES .....	63
<b>APPENDIX 3: COMMENTS ON THE DATA .....</b>	<b>74</b>
CAVAN-MONAGHAN-LEITRIM .....	74
CASTLEISLAND.....	76

# Summary

This report provides an overview of the Republic of Ireland trial airborne geophysical survey conducted in June 2006 in three selected sites in Ireland. The Joint Airborne Geoscience Capability (JAC) established between the Geological Survey of Finland (GTK) and British Geological Survey (BGS), carried out the survey under contract to the Geological Survey of Ireland. The survey is being conducted at high resolution (a flight line spacing of 200 m and 100 m) and at low altitude (56 m) across the selected survey areas in Cavan-Monaghan-Leitrim, Castleisland in Kerry and Silvermines in Tipperary.

The three main data sets being acquired are magnetic, radiometric (gamma ray spectrometry) and active frequency domain electromagnetic. The aim of the present report is to provide data and descriptions of the logistical elements of the survey operations.

In Espoo 13 September 2006

---

Maija Kurimo  
Project Manager

# 1 Survey: Location and details

## 1.1 SURVEY SCHEME

The Republic of Ireland high-resolution trial airborne geophysical survey was designed using the boundaries provided by Geological Survey of Ireland as shown in Figure 1. The survey comprises three areas: Cavan-Monaghan-Leitrim, Castleisland and Silvermines. Originally a fourth area north of Dublin was also included in the plans but later left out.

The idealised survey lines provided the parameters of the survey shown in Table 1.

*Figure 1. Location of the survey areas Cavan-Monaghan-Leitrim, Castleisland and Silvermines.*

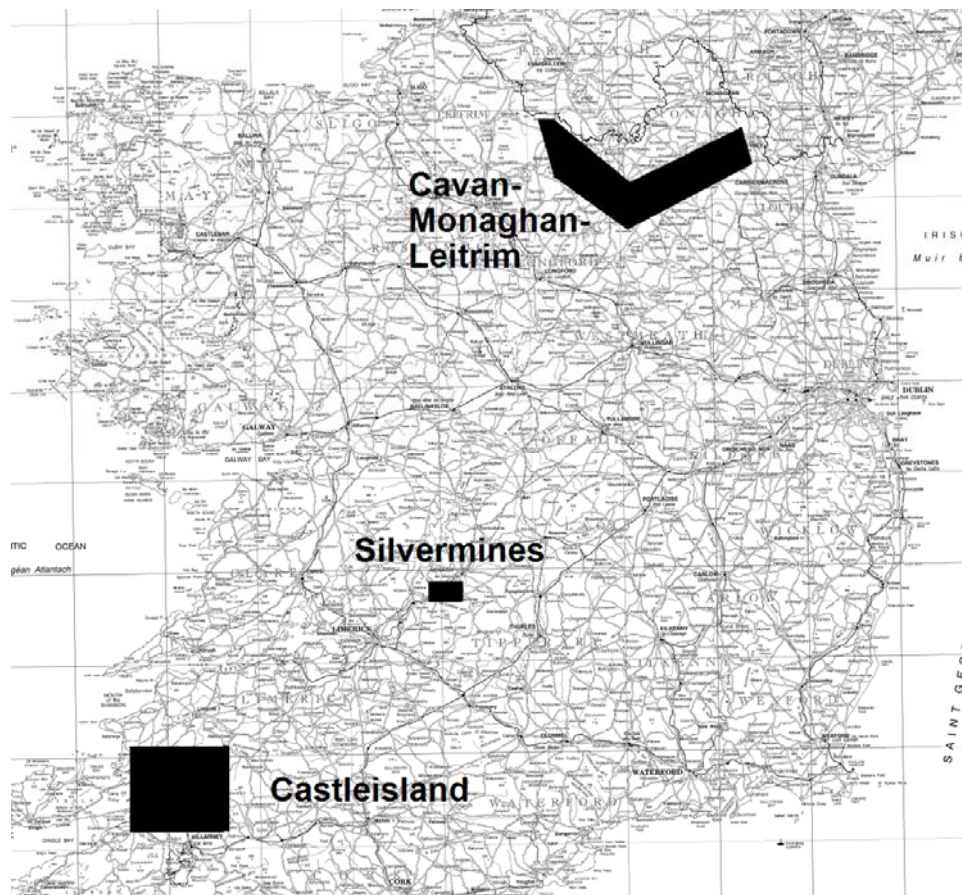


*Table 1. Summary of flight lines and survey line-km.*

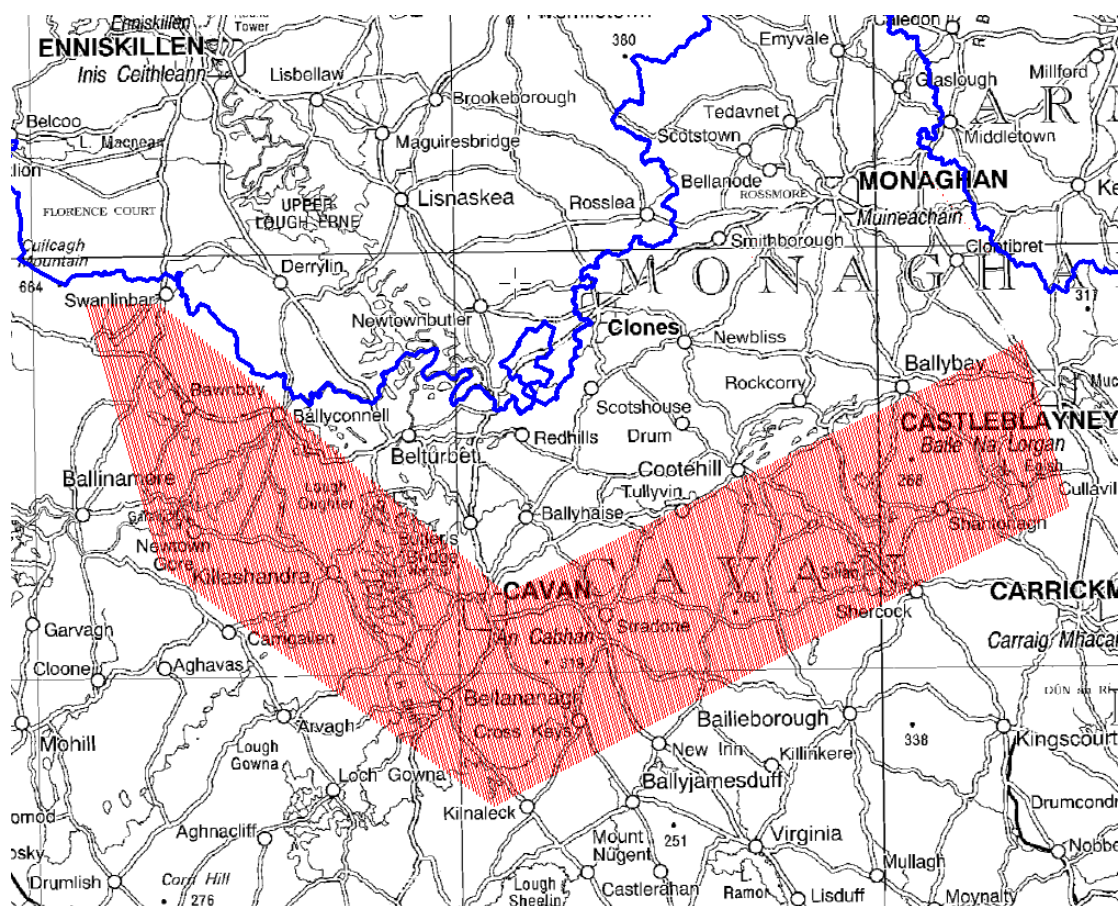
Site	Direction	Line separation	Number of lines	Line-km
Cavan	345	200	317	5077
Castleisland	360	200	164	4583
Silvermines	360	100	111	722

### 1.1.1 Cavan-Monaghan-Leitrim survey

The specifications used for the Northern Ireland Tellus survey were used as a basis for the Cavan-Monaghan-Leitrim survey due to the close vicinity of the NI border.

The flight line direction of 345 degrees geographic was originally set by Geological Survey of Northern Ireland on the basis of geological trends. Flight line spacing was set at an interval of 200 m.

*Figure 2. Flight line plan for Cavan-Monaghan-Leitrim survey. Blue line shows the border with Northern Ireland.*



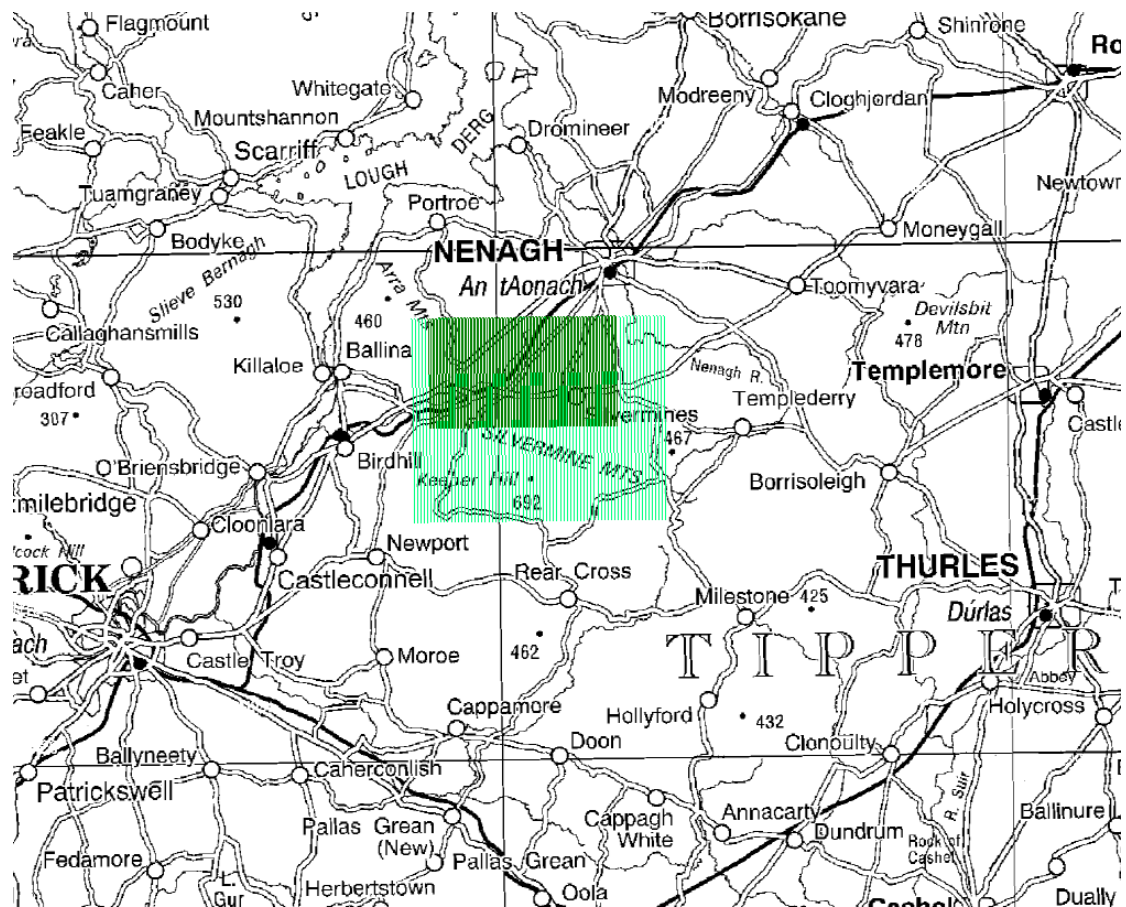
### 1.1.2 Castleisland and Silvermines surveys

A flight line direction of 360 degrees was set for the Castleisland and Silvermines sites by GSI.

Both of the areas were originally to be surveyed with a 200-meter line spacing. Later the Silvermines survey plan was modified and the flight line separation was set at 100 m. At the same time the number of lines was slightly reduced. The final flight plans for Castleisland and Silvermines areas are shown in Figure 3 and Figure 4, respectively.



Figure 4. Flight plan for the Silvermines survey. Lighter colour indicate the old flight plan with 200-meter line spacing, darker colour the new plan with 100-meter line spacing.



## 1.2 COORDINATE SYSTEM

The local geographical grid system used for the data is the IRISH GRID 1975 used as a national reference system by both The Republic of Ireland and Northern Ireland. Details of the system can be found on the Ordnance Survey of Northern Ireland Web site. Table 3 provides a main summary.

Table 2. Summary parameters for the IRISH GRID (1975) that define the local grid coordinates (Easting and Northing) used in the survey.

Projection	Transverse Mercator (Gauss Conformal)
True Origin	Lat. 53° 30' North, 8° 00' West of Greenwich
False Origin	200,000 m W, 250,000 m S, of true origin
Scale factor on central meridian	1.000035
Reference Ellipsoid	Airy (modified)
Semi-major axis (a)	6 377 340.189 m
Eccentricity ( $e^2$ )	0.0006 670 540

### **1.3 REFLIGHT SPECIFICATIONS**

Conditions for reflights were agreed in the survey specifications. The conditions were as follows:

- i. Where flight line spacing is greater than 130% of the nominal spacing over a distance of 2 kilometres or more or over any distance where flight line spacing is greater than 150% of the nominal spacing (except where ground conditions dictate otherwise, for example to avoid radio-masts etc).
- ii. Where terrain clearance exceeds  $\pm 20$  metres from the nominal survey height for more than 5 continuous kilometres or  $\pm 50\%$  of nominal survey height at any time on any line.
- iii. Where the nominal survey flying speed (210 kph) is exceeded by more than 30% (i.e. survey flying is faster than 270kph) for more than 5 continuous kilometres.
- iv. Where the noise envelope of the magnetic records exceeds 0.1nT as determined by the normalised fourth difference.
- v. If, during data acquisition, magnetic variations recorded at the local base magnetometer exceed 12 nT over any 3 minute chord or exceed 2 nT over any 30 second chord, on flight lines or tie lines. These limits may be revised by agreement in the light of experience gained during the first few weeks of data acquisition. The base magnetometer must be fully operational during all on-line data collection.
- vi. Where the average line gamma spectra for any line fails to meet acceptable standards or otherwise appears anomalous by comparison with neighbouring data, as demonstrated by the JAC proprietary software SPEKTNT, then the data of that line will be investigated in detail and re-flown if necessary.
- vii. If the in-flight EM signal/calibration check on phase orthogonality, at each measured frequency, indicates non-orthogonality or incorrect amplitude.

Conditions i, ii and iii above may be exceeded without reflight where such constraints would breach air regulations, or in the opinion of the pilot, put the aircraft and crew at risk.

### **1.4 SURVEY OPERATIONS**

#### **1.4.1 Survey Duration**

The survey data acquisition was conducted between 06 June 2005 and 27 June 2006. In order to minimise ferry flights, two airfields were used as operational bases, Enniskillen to fly Cavan-Monaghan-Leitrim and Kerry to fly Castleisland and Silvermines. The survey used Enniskillen airport (formerly St. Angelo) during the period 06 June to 15 June. The survey base transferred to Kerry Airport on 15 June and continued from that base until the termination of data acquisition on 27 June.

Operationally, a target of two 4-hour sorties each day was specified. The typical times were 08:00 to 12:00 and 15:00 to 19:00. Flight operations occupied a six-day week with Sunday designated a rest day. The operational chronology of data acquisition is provided in Table 3. The table summarises the dates, the time duration and the number of lines flown for each sortie. The survey comprised 33 operational flights with Flight/Material numbers from 084 to 114.

*Table 3. Survey duration.*

Flight number	Date	Survey area	Number of lines	Base	Off (UTC)	On (UTC)	Flight time
84	06-Jun	Cavan	0	Enn	07:51	08:08	00:17
84	06-Jun	Cavan	26	Enn	09:04	12:48	03:44
85	06-Jun	Cavan	24	Enn	14:16	18:06	03:50
86	07-Jun	Cavan	0	Enn	07:32	08:11	00:39
86	07-Jun	Cavan	26	Enn	10:55	14:51	03:56
87	07-Jun	Cavan	14	Enn	16:00	18:08	02:08
88	08-Jun	Cavan	30	Enn	10:22	14:04	03:42
89	08-Jun	Cavan	23	Enn	15:14	18:21	03:07
90	09-Jun	comp	0	Enn	07:22	08:19	00:57
91	09-Jun	Cavan	31	Enn	09:54	13:49	03:55
92	09-Jun	Cavan	24	Enn	15:00	18:08	03:08
93	10-Jun	Cavan	28	Enn	07:24	11:24	04:00
94	10-Jun	Cavan	26	Enn	12:57	16:55	03:58
95	13-Jun	Cavan	22	Enn	11:21	15:17	03:56
96	14-Jun	Cavan	26	Enn	08:24	12:47	04:23
97	14-Jun	Cavan	24	Enn	15:16	19:07	03:51
98	15-Jun	Cavan	15	Enn	07:29	10:29	03:00
99	15-Jun	ferry	0		12:36	13:13	00:37
100	16-Jun	comp	0	Kerry	15:26	16:09	00:43
101	17-Jun	comp	0	Kerry	08:16	09:22	01:06
102	17-Jun	comp	0	Kerry	11:53	12:41	00:48
103	17-Jun	comp	0	Kerry	14:32	15:40	01:08
104	19-Jun	Castle	15	Kerry	15:39	18:15	02:36
105	21-Jun	Castle	11	Kerry	07:44	10:02	02:18
106	22-Jun	Castle	27	Kerry	07:24	11:50	04:26
107	22-Jun	Castle	25	Kerry	14:05	18:11	04:06
108	23-Jun	Castle	26	Kerry	07:16	11:31	04:15
109	23-Jun	Castle	24	Kerry	14:00	17:58	03:58

Flight number	Date	Survey area	Number of lines	Base	Off (UTC)	On (UTC)	Flight time
110	24-Jun	Castle	22	Kerry	12:09	15:52	03:43
111	26-Jun	Castle	23	Kerry	08:15	12:25	04:10
112	26-Jun	Castle	14	Kerry	14:38	17:30	02:52
113	27-Jun	Silver	68	Kerry	09:45	13:55	04:10
114	27-Jun	Silver	54	Kerry	14:43	18:13	03:30

#### 1.4.2 Personnel

A list of personnel involved in the ROI survey is provided in Table 4.

*Table 4. List of project personnel.*

Position	Name	Affiliation
JAC Manager/Party Chief	Ms Maija Kurimo	GTK
Party Chief/Geophysicist	Ms Mari Lahti	BGS
Party Chief/Geophysicist	Ms Hanna Leväniemi	GTK
Electronics engineer/Operator	Mr Veli Leinonen	GTK
Operator	Mr Olli Halonen	GTK
Operator	Mr Ed Haslam	BGS
Operator	Mr Andy Hulbert	BGS
Operator	Mr Kai Nyman	GTK
Operator	Ms Helen Taylor	BGS
Captain	Capt Raimo Loukkola	FAA
Captain	Capt Raimo Vartiainen	FAA
Pilot	Mr Mika Kanto	FAA
Pilot	Mr Hannu Laitinen	FAA
Pilot	Mr Mika Raivonen	FAA
Navigator	Mr Esa Tiainen	FAA
Navigator	Mr Veikko Wetterstrand	FAA
FAA a/c Engineer	Mr Sami Jänis	FAA
Data Processing	Mr D Beamish	BGS
Data Processing	Mr R Cuss	BGS
Data Processing	Mr H Hautaniemi	GTK
Data Processing	Ms M Lahti	BGS
Data Processing	Ms H Leväniemi	GTK

Figure 5. Mr G. Stanley and Ms E. Doyle (on the right) of GSI and Ms O. Cahill of Aurum Exploration with Ms H. Leväniemi of GTK (on the left) at Kerry airport field office.



### 1.4.3 Exceptions to Specifications

Maps in Figure 6, Figure 7 and Figure 8 show the areas where the flight altitude exceeded the 50% limit. As these maps show, the exceptions are due to difficult terrain or urban areas and could not be avoided because of safety issues and flight regulations.

Figure 6. In the Cavan area high flight altitudes are mainly due to urban areas.

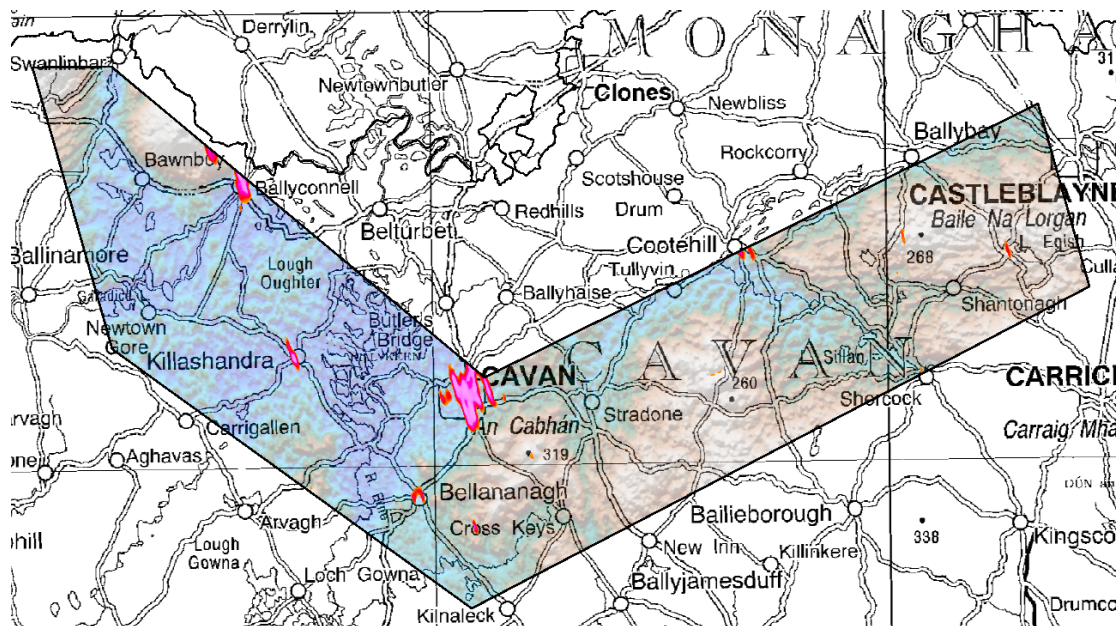


Figure 7. In the Castleisland area the fly-highs are caused by urban areas and high hills.

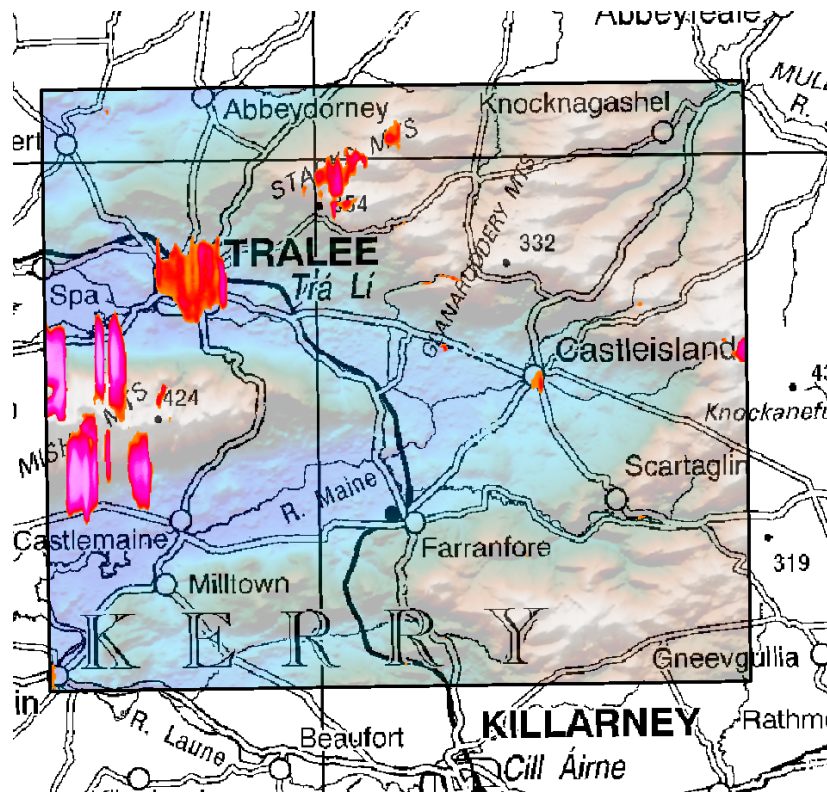
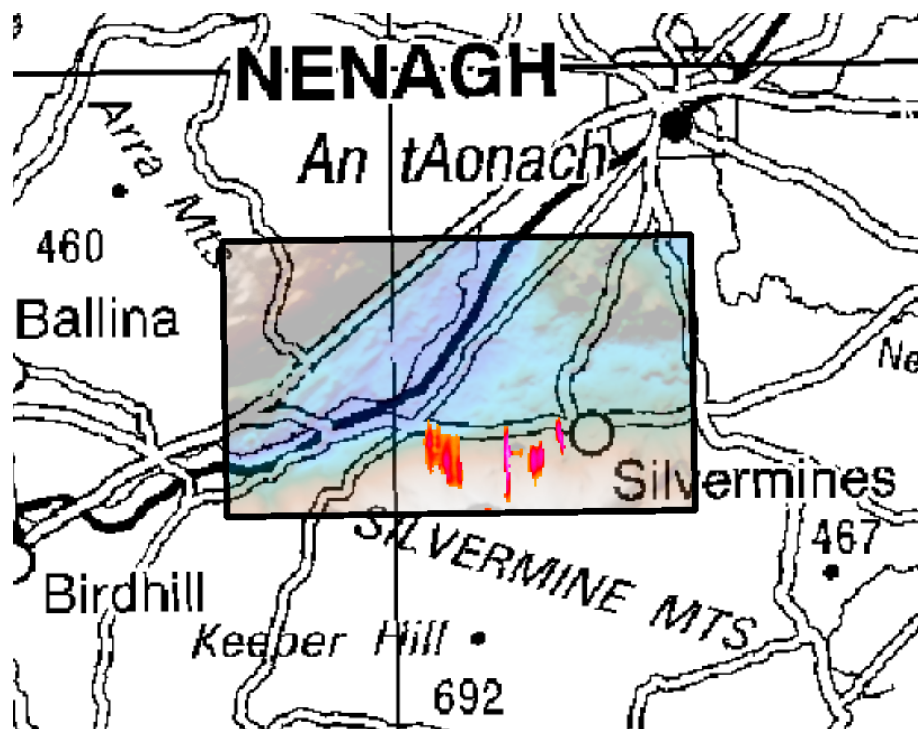


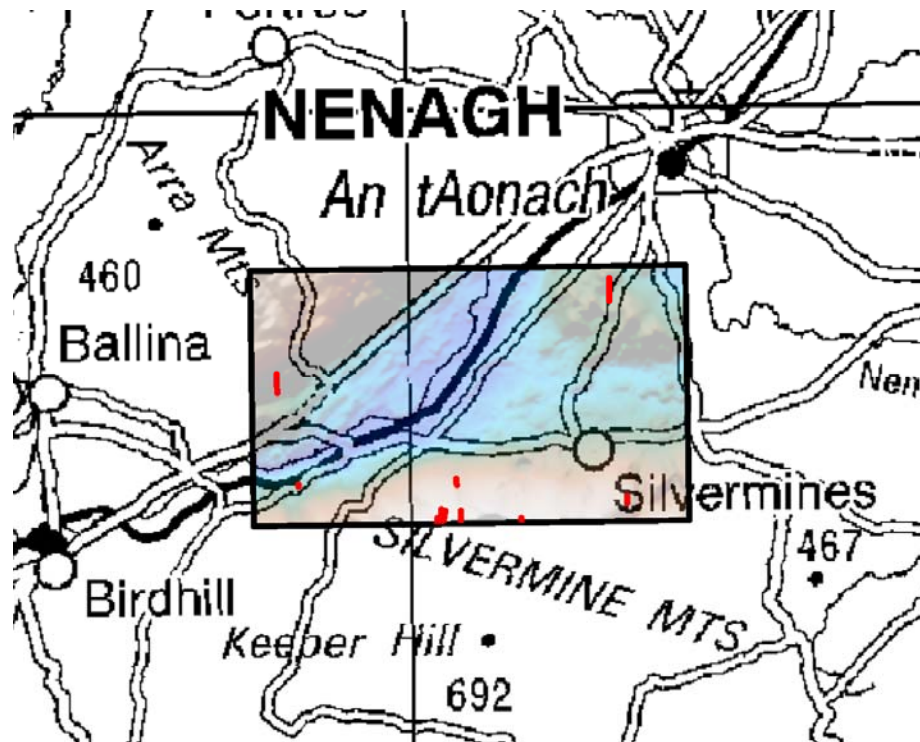
Figure 8. In the Silvermines area high altitudes are caused by the Silvermines Mountains.



In the Silvermines area, the short lines and rough terrain caused some higher deviations from the flight path. These were due to hilly areas, especially on the slopes

of the Silvermines Mountains. Not all of these we re-flown as the result was unlikely to improve because of the difficult flying conditions caused by the steep hillsides.

*Figure 9. Distance deviation exceeding the specifications in the Silvermines area.*



## 2 Equipment

The airborne survey equipment used on the survey comprises a geophysically equipped De Havilland Twin-Otter aircraft (OH-KOG). The details of the aircraft are provided in Appendix 1.

The aircraft is owned by the NERC/BGS and the geophysical equipment is owned by the JAC/GTK. The BGS and GTK undertake airborne geophysical survey work in a partnership venture known as the Joint Airborne geoscience Capability (JAC). The aircraft is operated by the Finnish Aviation Academy (FAA) who are based in Pori, Finland.

A background to the development of the geophysical equipment used by the JAC is given by Hautaniemi et al., (2005). The main components of the geophysical measurement system are summarised in Table 5.

*Table 5. Outline specification of the main geophysical systems.*

Electromagnetic system	GTK AEM2005 four frequency
Aircraft Magnetometer	2 Scintrex CS-2 caesium vapour sensors, located at the left wingtip and nose stinger
Magnetic Compensator	RMS Instruments Automatic Aeromagnetic Digital Compensator (AADCII)
Gamma-ray spectrometer	Exploranium GR-820/3 gamma-ray spectrometer 256-channels, self-calibrating
Altimeter	Collins radar altimeter
Navigation/data location system	Real time DGPS based on Ashtech GG-24 GPS+GLONASS receiver, when RDS signal available
Data acquisition system	GTK proprietary: control unit including server, power unit, alarm box, Local Area Network

Standard ancillary equipment includes an external temperature sensor and barometric height sensor and a power-line (50/60 Hz) sensor (housed in the nose of the aircraft). Details of these devices are included in Appendix 1.

*Figure 10. Twin Otter ready for take-off at Kerry airport.*



## **2.1 GROUND-BASED EQUIPMENT**

Ground-based equipment comprises two identical base magnetometer/GPS stations. One of the stations is termed the primary base station and records magnetic and GPS data prior to, during, and after each flight. The data from this station are used to post process the airborne data. The base magnetic data are used to correct diurnal variations of the airborne magnetic field records. The base GPS records are used to perform differential processing of the airborne GPS recordings. The second base station is termed the secondary base station and is operated in parallel with the primary base station. The secondary base station acts as a backup in the case of malfunction/noise of the primary base station data.

The magnetic data are logged at 1-second intervals and displayed on a base station laptop that controls data acquisition. The continuous display of the base station data (rolling screen) provides a capability for monitoring the magnetic disturbance conditions that would lead to a reflight condition.

*Figure 11. Base station. Magnetometer, GPS unit and control PC inside a tent. Magnetometer sensor, GPS sensor in the field. Photo: Kai Nyman.*



### **2.1.1 Base station at Enniskillen airport**

The primary and secondary base stations were located within the perimeter of Enniskillen Airport. The primary base station was located behind the airport hangar away from any roads or possible noise sources as shown in Figure 12. A grid of magnetic total field values was measured around the area in order to verify low magnetic gradients around the base station sensor.

Complete base station operations and precise locations are summarised in Table 6. An example of primary magnetic base station data acquired during the survey is shown in Figure 13.

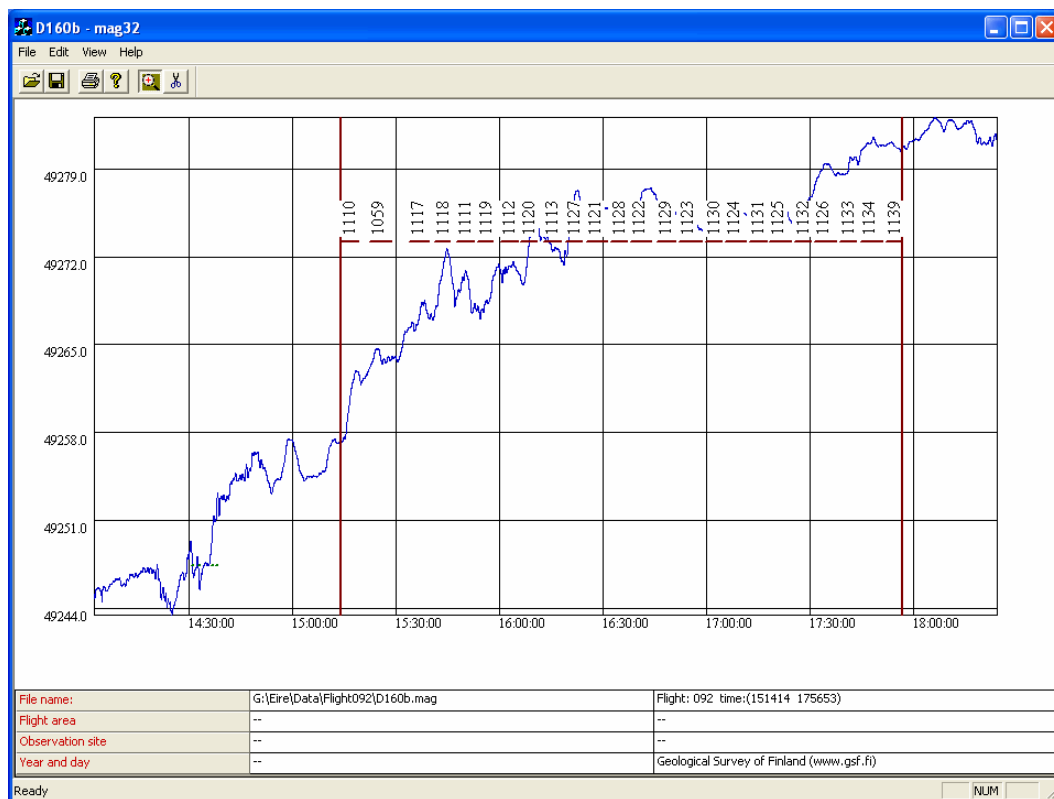
*Table 6. Summary of primary base station used during the Cavan-Monaghan-Leitrim survey.*

Primary Base Station	Enniskillen
Start Date (Julian Day)	06 June 2006 (157)
End date (Julian Day)	15 June 2006 (166)
Geographic latitude	54° 23' 32.90050"
Geographic Longitude	07° 38' 58.03622"
Elevation (m)	102.6381

Figure 12. The primary magnetic base station in its final location.



Figure 13. Example of magnetic base station recording (flight 092).



### 2.1.2 Base station at Kerry airport

Kerry base station was used for the surveys in the Castleisland and Silvermines areas.

At Kerry airport the primary and secondary base stations (both magnetic and GPS) were located at a short distance from each other on a field far away from any noise sources at the edge of the airfield area as shown in Figure 14.

The distance between the sensors was approximately eight meters and as the comparison of the sensor recordings in Figure 15 shows, the difference between the two sensors is some 10 nT meaning low-gradient location.

Base station operations are summarized in Table 7.

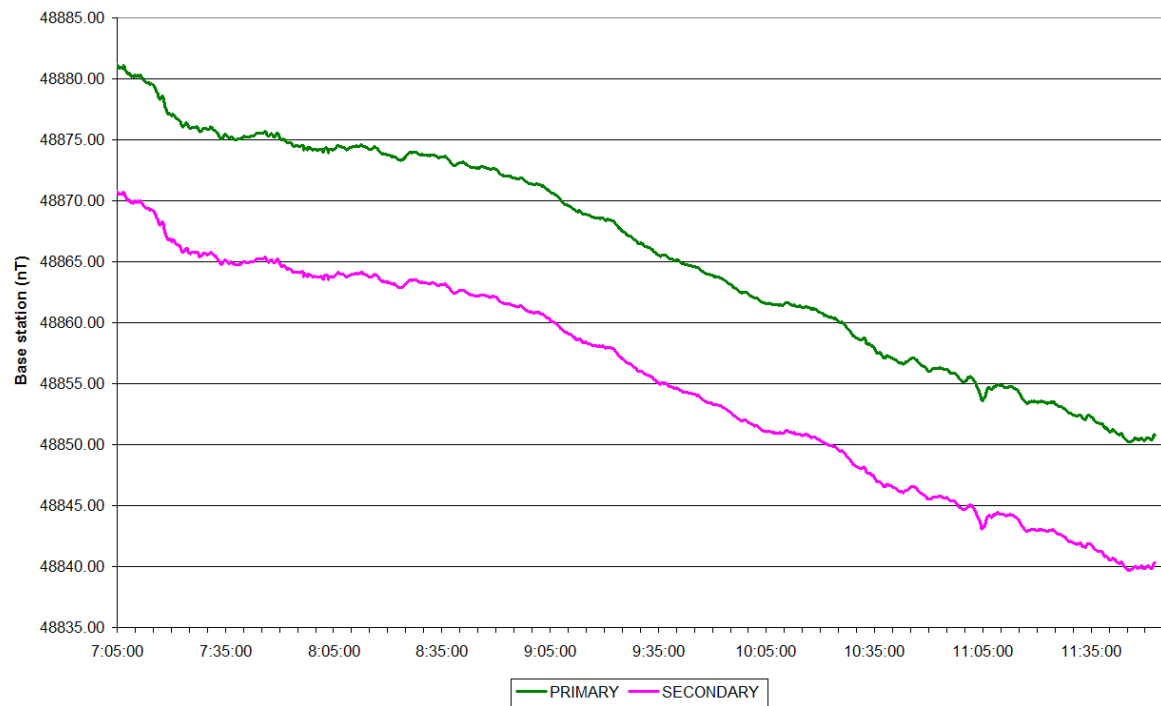
*Table 7. Summary of primary base station used during Castleisland and Silvermines surveys.*

Primary Base Station	Kerry
Start Date (Julian Day)	16 June 2006 (167)
End Date (Julian Day)	27 June 2006 (178)
Geographic Latitude	52° 10' 57.50376''
Geographic Longitude	09° 31' 55.92110''
Elevation (m)	83.9841

*Figure 14. Primary (at the back) and secondary (in front) magnetic base station sensors. The runway seen in the picture was not in use.*



Figure 15. Comparison of base station sensor recordings at Kerry airport on June 22, 2006 (Julian day 173).



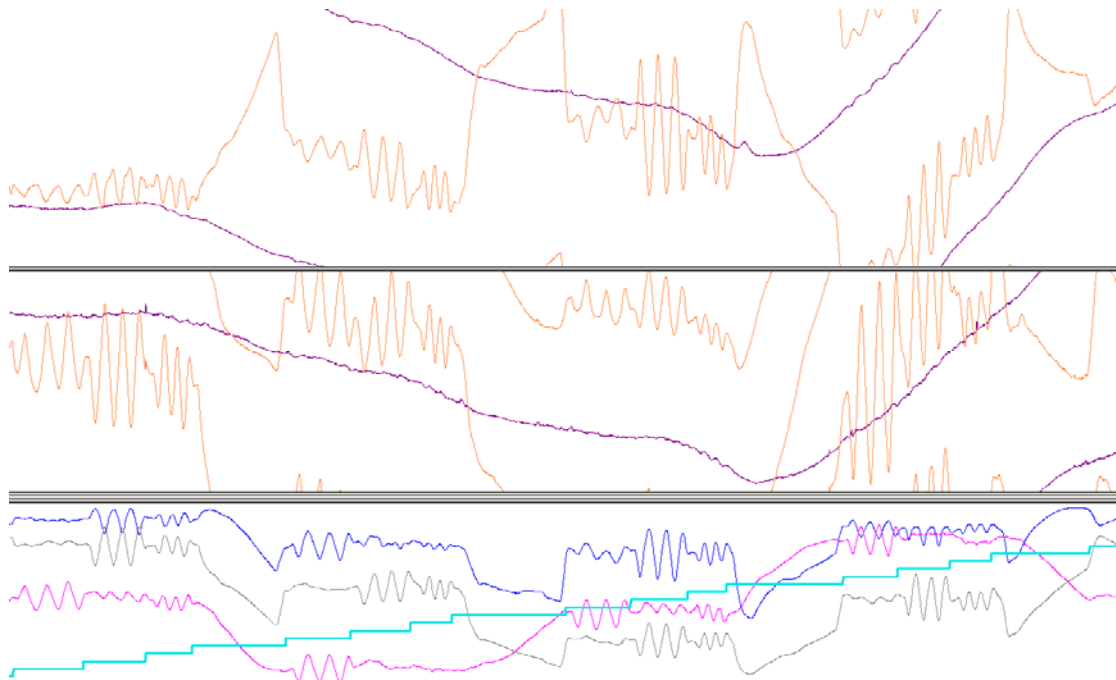
## 3 Calibration Data

### 3.1 MAGNETIC COMPENSATION

The effect caused by the movements of the aircraft is removed/diminished automatically during the flight by use of the compensation data. During the compensation flight the aircraft flies at 3 km altitude in the two flight line directions and the directions perpendicular to those and performs pitch ( $\pm 5^\circ$ ), roll ( $\pm 10^\circ$ ) and yaw ( $\pm 5^\circ$ ) manoeuvres along each direction. After recording the magnetic effects of all twelve movements, the AADCII compensator (RMS Instruments) computes the compensation coefficients, and stores the results to provide real-time corrections during the actual survey.

The effectiveness of the compensation is verified by a Figure-Of-Merit (FOM) survey immediately after the compensation during the same flight. The same movements are repeated and the new compensation parameter file is utilized. All three compensated movement effects are summarized in all four directions, and the FOM parameter is thus the sum of these 12 peak-to-peak anomaly values of the compensated magnetic field.

*Figure 16. The profiles of magnetometer compensation flight for Castleisland and Silvermines areas (see Chapter 3.1.2). Panels 1 and 2: uncompensated (orange) and compensated (magenta) left wingtip and nose stinger sensor, Panel 3: the three flux-gate magnetometer readings with fixpoint steps.*



### 3.1.1 Compensations for Cavan-Monaghan-Leitrim area

The first compensation flight was made over the sea near Newtonards in the end of April during the Northern Ireland Tellus flights. The FOM parameter was 1.8 nT for the left magnetometer and 2.5 nT for the right magnetometer. The survey direction of the Cavan-Monaghan-Leitrim area was the same as for Tellus survey so there was no need to repeat the compensation.

However, during the first survey week the effectiveness of the compensation was checked by a second compensation. The need for the check raised when the survey area showed very weak magnetic signature and the importance of good compensation became enhanced. The second compensation flight was carried out over Londonderry. The result showed improvement in compensation so the new compensation slot was used for the rest of the Cavan-Monaghan-Leitrim survey. The FOM parameters were 2.0 nT for left magnetometer and 2.3 for the nose magnetometer.

The FOM parameters of each direction and each movement are summarised in Table 8.

*Table 8. Figure of merit calculations for Cavan-Monaghan-Leitrim data.*

#### **Compensation 29<sup>th</sup> April 2006**

<b>Left sensor</b>				
Dir	Pitch	Roll	Yaw	Total
165	0.39	0.09	0.05	0.53
90	0.20	0.11	0.04	0.35
345	0.13	0.21	0.13	0.47
270	0.18	0.20	0.10	0.48
Total	0.90	0.61	0.32	<b>1.83</b>
<b>Nose sensor</b>				
Dir	Pitch	Roll	Yaw	Total
165	0.32	0.18	0.20	0.70
90	0.27	0.21	0.2	0.68
345	0.31	0.18	0.21	0.70
270	0.18	0.21	0.06	0.45
Total	1.08	0.78	0.67	<b>2.53</b>

#### **Compensation 9<sup>th</sup> June 2006**

<b>Left sensor</b>				
Dir	Pitch	Roll	Yaw	Total
165	0.19	0.17	0.11	0.47
90	0.21	0.29	0.22	0.72

345	0.20	0.17	0.05	0.42
270	0.14	0.17	0.09	0.4
Total	0.74	0.80	0.47	<b>2.01</b>
<b>Nose sensor</b>				
Dir	Pitch	Roll	Yaw	Total
165	0.14	0.22	0.21	0.57
90	0.19	0.20	0.20	0.59
345	0.10	0.25	0.36	0.71
270	0.16	0.12	0.12	0.40
Total	0.59	0.79	0.89	<b>2.27</b>

### 3.1.2 Compensation for Castleisland and Silvermines areas

After transferring the operation to Kerry airport a new compensation was needed for the Castleisland and Silvermines area as the flight direction changed from that of the Cavan-Monaghan-Leitrim area. The compensation flight was carried out north of the town of Tralee and Castleisland survey area.

After some unsuccessful compensation trials (the result of which didn't meet the quality criteria) adjustments were made to the aircraft hardware. After modifications the calibration worked well resulting in a good FOM seen in Table 9.

*Table 9. Figure of merit calculations for Castleisland and Silvermines areas.*

#### Compensation 17<sup>th</sup> June 2006

<b>Left sensor</b>				
Dir	Pitch	Roll	Yaw	Total
W	0.07	0.08	0.15	0.30
S	0.08	0.10	0.10	0.28
E	0.14	0.18	0.18	0.50
N	0.28	0.10	0.10	0.48
Total	0.57	0.46	0.53	<b>1.56</b>
<b>Nose sensor</b>				
Dir	Pitch	Roll	Yaw	Total
W	0.13	0.27	0.25	0.65
S	0.25	0.17	0.25	0.67
E	0.16	0.14	0.35	0.65
N	0.28	0.30	0.21	0.79
Total	0.82	0.88	1.06	<b>2.76</b>

## 3.2 RADIOMETRIC CALIBRATION DATA

As noted previously the radiometric instrument employed is the Exploranium GR-820 with 256-channels. The commonly adopted standard in carrying out airborne gamma-ray measurements is to calibrate and process the data in a manner presented in AGSO and IEAE reference manuals (Grasty and Minty, 1995; IAEA, 1991). The radiometric system was calibrated prior to the survey using locations and calibration ranges in Finland that have been used for over 25 years. The following sections summarise the calibrations that were performed for this survey.

### 3.2.1 Cosmic and background coefficients

To determine the aircraft and cosmic background, a test flight was carried out over the sea near the airport of Newtownards on March 29, 2006, at flight surfaces from 5000 to 10000 ft. Linear regression from the mean counts in each channel and equivalent cosmic channel count rate provide the constant and linear coefficients. The constant represents the background radiation from the aircraft and the linear coefficient is used to calculate the varying part of background radiation because of cosmic radiation.

The cosmic coefficients were found to be:

cos_tot	131.0 (0.810)	Total counts
cos_kal	10.4 (0.037)	Potassium
cos_ura	3.1 (0.029)	Uranium
cos_tho	0.0 (0.041)	Thorium
cos_Ur	0.5 (0.007)	Uranium upward

The numbers in parentheses are the linear coefficients.

### 3.2.2 Stripping ratios

The stripping ratios were determined using 4 transportable calibration pads (1m x 1m x 0.3m) on July 6, 2006 in Pori, Finland. Each pad was measured for 10 minutes and the stripping ratios were calculated using the Padwin program provided by the manufacturer of the pads. The calculated values are very close to the manufacturer's and IAEA's ideal values.

The results are listed here:

TH INTO U (ALPHA = $A_{23}/A_{33}$ )	.2408 (.0629)
TH INTO K (BETA = $A_{13}/A_{33}$ )	.4071 (.1330)
U INTO K (GAMMA = $A_{12}/A_{22}$ )	.7327 (.1760)
U INTO TH (A = $A_{32}/A_{22}$ )	.0453 (.0638)
K INTO TH (B = $A_{31}/A_{11}$ )	-.0031 (.0342)
K INTO U (G = $A_{21}/A_{11}$ )	.0032 (.0335)

The numbers in parentheses are estimated standard deviations.

### 3.2.3 Height attenuation

For determining height attenuation, a series of heights from 100 to 800 ft was used to take measurements on July 6, 2006 near Porvoo, Finland. This test line has been used for more than 25 years. Background and strip corrections were applied and the attenuation was calculated using the logarithmic values of corrected Tot, K, U and Th, and flight altitude.

The attenuation coefficients were calculated as:

K	-0.0091
U	-0.0089
Th	-0.0073
Total counts	-0.0078

### 3.2.4 Concentration coefficients

The same Porvoo test line was used to determine the system sensitivities. This same line has been measured for more than 25 years from the air with OH-KOG. The sensitivity parameters have been applied yearly to the radiometric data measured. Comparisons have been made also between different areas measured during different years to find out the possible variations. The variations are mostly due to different methods used earlier for sensitivity determining, e.g. pads, runaway. For the last few years the sensitivity parameters have been varied by just a few percent.

All the corrections were made to the radiometric test flight data and the concentrations were compared to earlier measurements and new sensitivity parameters were calculated as:

K	0.0072	%K/(pulses/s)
U	0.0713	ppm eU/(pulses/s)
Th	0.1128	ppm eTh/(pulses/s)

Dose rate: whole spectra technique, approved by SGU 2003.

### 3.2.5 Resolution of the spectrometer

The Spectrometer resolution was measured with a Cs-137 source on the July 6, 2006 in Pori, Finland. Background was also measured and after a background correction, the Cs peak was measured and the FWHM determined. The FWHM is across 5.0 channels, each with an energy of 12.1 keV, which makes 60.5 keV. Thus we obtain a spectrometer resolution of

$$R = 100 \cdot 60.5 \text{ keV} / 662 \text{ keV} = 9.14 \%$$

Individual crystals were measured on July 6, 2006 at Helsinki-Vantaa airport. The downward looking spectra was stabilized using K-40 and the upward looking with Cs-137. The results are given as Crystal Number with %Resolution in parentheses:

D1(7.4%), D2(11.0%), D3(7.5%), D4(6.1%), D5(5.3%), D6(5.9%), D7(5.9%), D8(5.4%), U13(9.5%), U14(7.9%)

D refers to downward and U to upward.

### 3.3 ELECTROMAGNETIC CALIBRATIONS

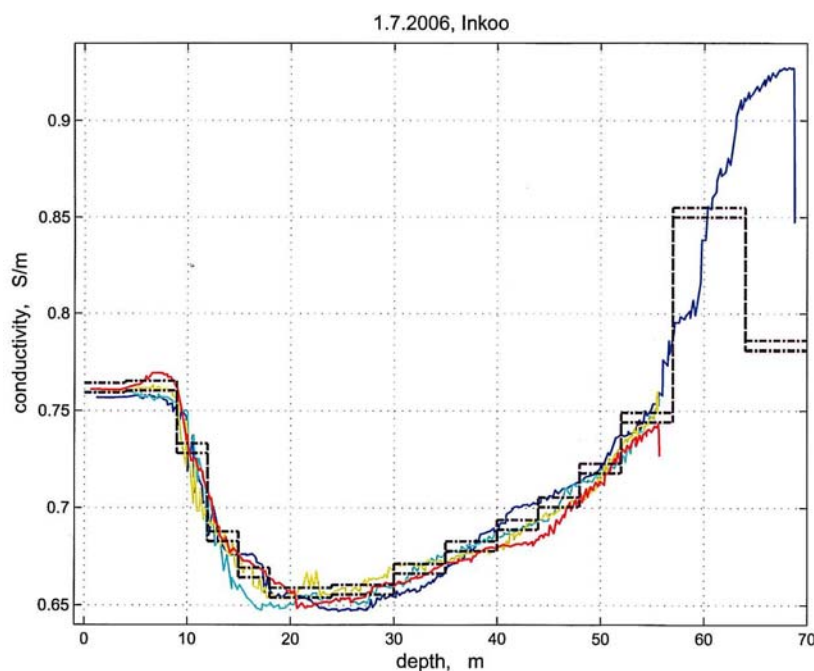
#### 3.3.1 Coefficient Calibration

The calibration of the JAC AEM-95 system used in the survey is described by Hautaniemi et al. (2005). The system specifications are also presented in more detail by Poikonen et al. (1998) and by Suppala et al. (2005).

The EM was calibrated by flying a test line over the sea (Gulf of Finland) on July 01, 2006 at different heights from 25 to 100 m. The conductivity of the sea was measured by a CTD sensor at 4 different points along the test line, from the surface to the sea bottom.

The conductivity of the sea was estimated by a model, which contains layers with a different conductivity for each layer. The results are displayed in Figure 17.

*Figure 17. The sea conductivity profiles recorded along the test line in the Gulf of Finland (coloured lines) and the layer model used in the model response calculation.*



The theoretical responses of the airborne EM to the model described above were calculated using the Leroi-air program developed by AMIRA. Non-linear optimization was used to obtain a best fit to a complex, scalar coefficient. The coefficients obtained at each frequency enables measured units to be converted to coupling ratios ( $H_s/H_p$ , meaning secondary over primary) in ppm (parts per million)

An example of the coefficient calculation is shown in Figure 18 and Figure 19.

Figure 18. EM optimisation results for the Real component calibration at 3005 Hz.

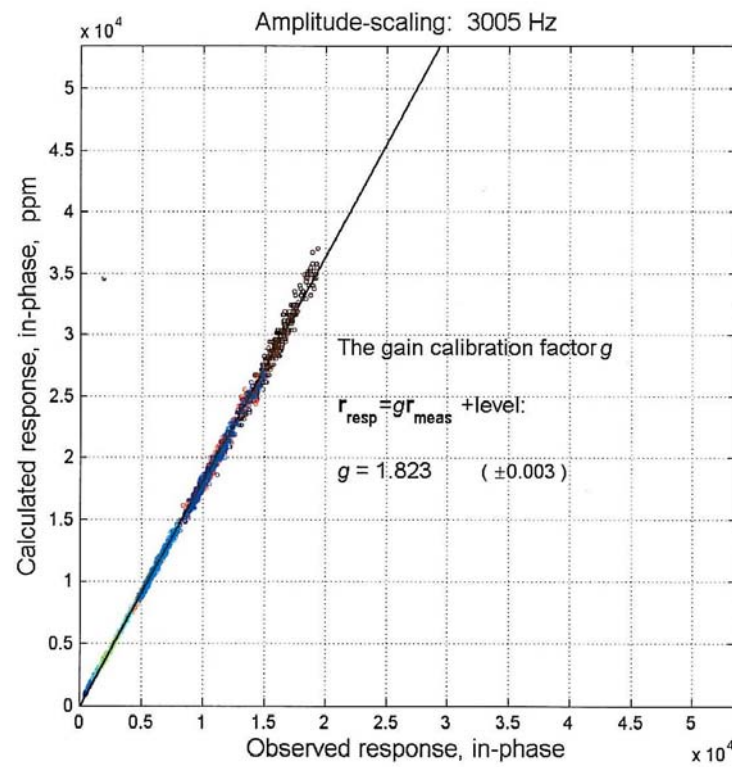
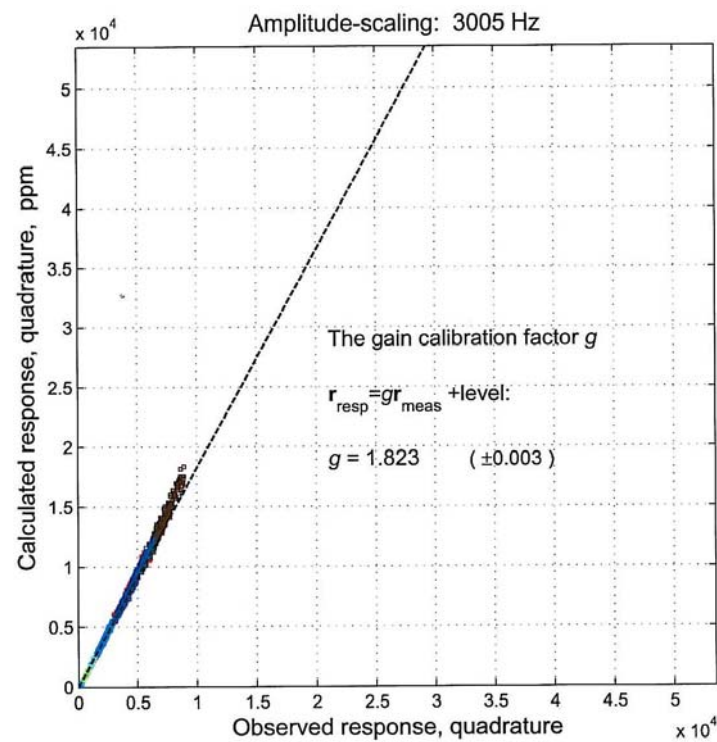


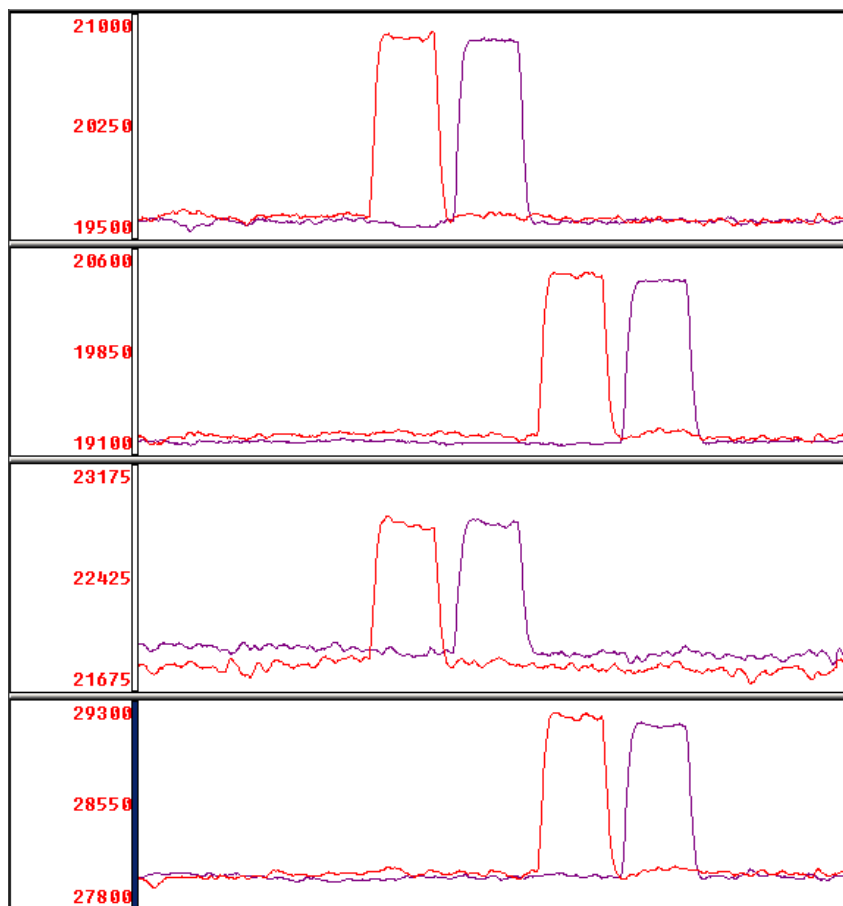
Figure 19. EM optimisation results for the Imaginary component calibration at 3005 Hz.



### 3.3.2 EM System orthogonality

The phase shift between in-phase (real) and quadrature (imaginary) components is checked and adjusted at the beginning and end of each survey flight. The test is undertaken at an ‘out-of-ground-effect’ elevation (e.g. 300 m). As the phase shift is 90 degrees, there should not be any trace in the quadrature component as an artificial signal is applied to in-phase component and vice versa. This procedure is done separately on each frequency to in-phase and quadrature components. At the end of each survey flight this same procedure is repeated to check for any possible phase drift during the flight. An example of the calibration pulses observed at the start of a flight is shown in Figure 20.

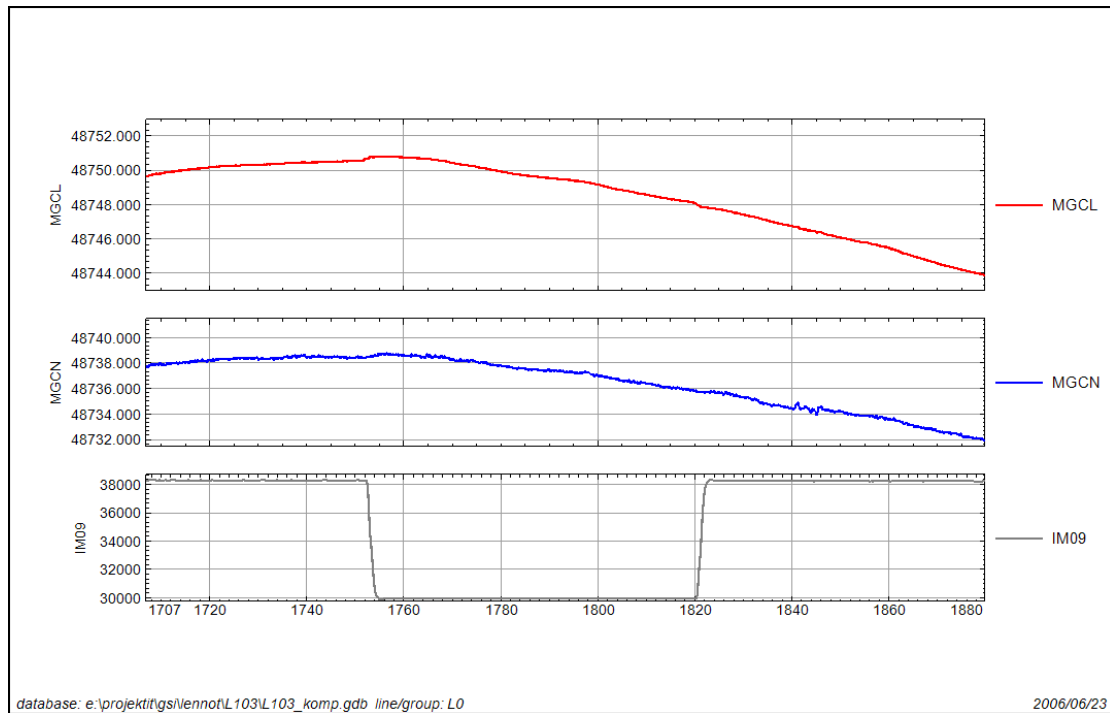
*Figure 20. The orthogonality test for Real and Imaginary components of the Twin Otter EM configuration at the end of Flight 094. Panels show the frequencies in increasing order from top to bottom with Real component in red and Imaginary component in magenta.*



### 3.3.3 EM Transmitter Effect on Magnetic Sensors

After magnetic calibration in Kerry (see Chapter 3.1.2), the EM transmitter was turned off and back on while flying straight and level at the calibration altitude. The transmitter was switched off for about one minute. The effect of the transmitter in both sensors is very small, less than one nT, as can be seen in Figure 21.

Figure 21. EM transmitter test. Panel 1: Left sensor, Panel 2: Nose sensor, Panel 3: IM09 showing where the transmitter has been switched off.



## 4 Data handling, QC procedures and Processing

The data handling and QC procedures used by the JAC are fully described by Hautaniemi et al., (2005).


The geophysical and avionic data acquired during each flight is monitored by a geophysical operator as shown in Figure 22. The geophysical operator monitors all the instruments and the data being acquired using a laptop computer. Each instrument is connected to a dedicated microprocessor. The microprocessor controls data transfer to a Local Area Network (LAN). A GPS-based synchronisation pulse is provided through the LAN at a frequency of 40 Hz.

*Figure 22. Geophysical operator and main instrument rack.*



The operator is responsible for maintaining the flight logs, which summarise all the required parameters for each survey flight. An example log from Flight 092 of the survey is shown in Figure 23. Noteworthy factors (e.g. urban fly-high conditions) and exceptions are digitally logged using a fixed-point (FP) number data channel that ties the operator's notes to the recorded data stream. Fixed points also define on-line and off-line conditions.

Figure 23. Example of a flight log from flight 092.

**JAC**  **OH-KOG**  
**SURVEY FLIGHT REPORT**

Joint Airborne-geoscience Capability  
Geological Survey of Finland/British Geological Survey

Report #	Material #	Line #	Dir	h	start min	h	end min	P	W	U	fp	M	fp	Other line notes
101	092	1	110	165	15:14	15:19	MS							
		2	1059	345	15:22	15:28								
Date	9 . G 2006 / 160	3	117	165	15:33	15:39								
		4	1178	345	15:41	15:48								
FAA crew	RL MK VW	Operator	AH	5	111	165	15:47	15:52						13 High start
		6	119	345	15:53	15:58								
Airbase	ENNISKILGI	7	112	165	16:00	16:05								18 High start
		8	120	345	16:06	16:10								
Survey area	CAVAN	9	113	165	16:12	16:17								24 High start
		10	127	345	16:19	16:24								
Magnetic stations	AIRPORT	11	121	165	16:25	16:31								
<input checked="" type="checkbox"/> Diurnal <input type="checkbox"/> GSM / Iridium		12	128	345	16:32	16:37								
		13	122	165	16:37	16:44								
TIME S		14	129	345	16:45	16:51	RL							
In	18:10	On	18:08	15	123	165	16:52	16:58						
Out	14:55	Off	15:00	16	130	345	16:59	17:04						40
Block	3:15	Total	3:08	17	124	165	17:05	17:11						46
		18	131	345	17:12	17:17								
<input checked="" type="checkbox"/> Server <input checked="" type="checkbox"/> Video <input checked="" type="checkbox"/> Laser		19	135	165	17:18	17:24								
<input checked="" type="checkbox"/> GPS <input checked="" type="checkbox"/> Memory cleared <input type="checkbox"/> RDS		20	132	345	17:25	17:30								
<input checked="" type="checkbox"/> MGM Compensation slot # 1		21	126	165	17:31	17:37								
<input checked="" type="checkbox"/> ADC <input checked="" type="checkbox"/> Signal Calib start <input type="checkbox"/> stop <input type="checkbox"/>		22	133	345	17:38	17:43								
<input checked="" type="checkbox"/> ADC QNH 1018 hPa Baro 260 m		23	134	165	17:44	17:51								
<input checked="" type="checkbox"/> GR-820 <input checked="" type="checkbox"/> Gains Calibration VCS		24	139	345	17:52	17:56								
Rec 1 start	15:09	stop	17:59	25	:	:								
Rec 2 start	:	stop	:	26	:	:								
		27	:	:	:	:								
		28	:	:	:	:								
		29	:	:	:	:								
		30	:	:	:	:								

Remarks

Continue ☐

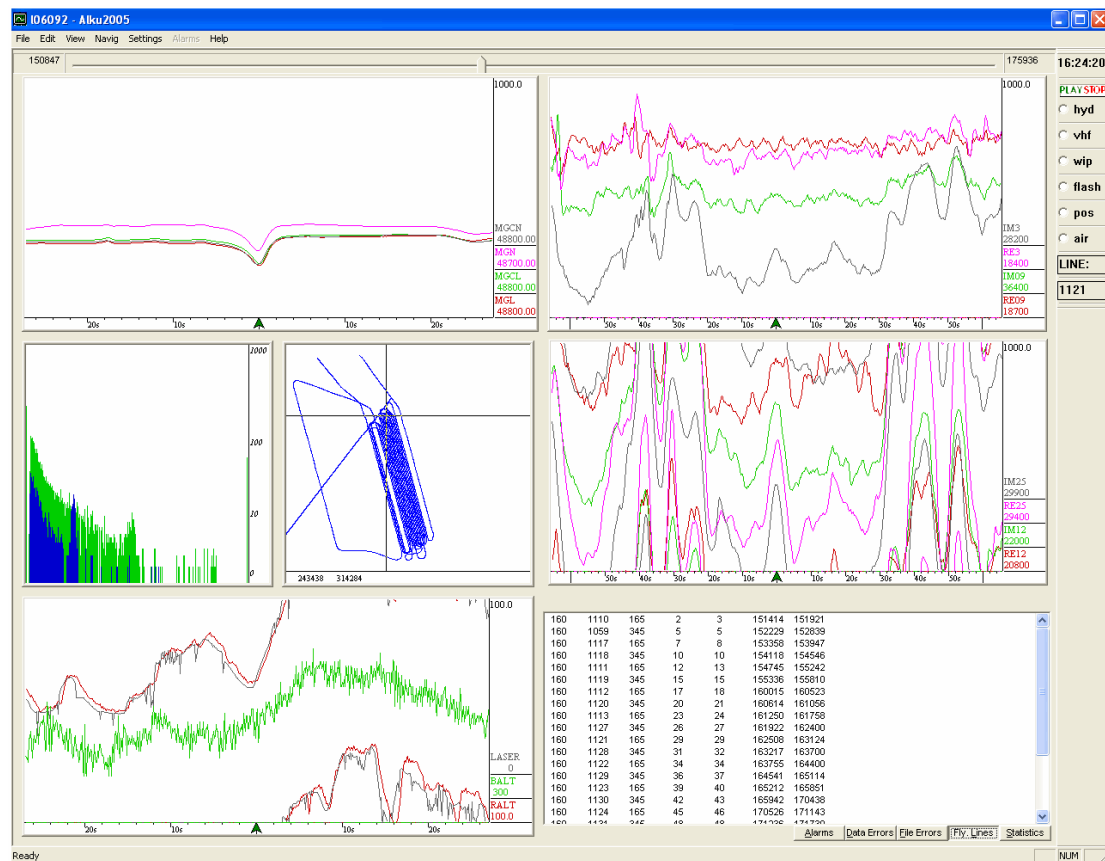
P=pilot W=weather: s=shower, r=rain, m=mist, f=fog, t=turbulence, w=strong wind U=urban area fix points M=maast fix points

## 4.1 QC AND FIELD PROCESSING

The basic processing of the recorded data is undertaken immediately after each flight and before the start of the next flight.

In the first stage the data is examined for any apparent errors such as file corruption or significant data errors. An example of this is shown in Figure 24. After this, the data profiles are examined more carefully. Standard processing and QC involves the use of fourth differences in the magnetic and electromagnetic channels. The appearance, quality and noise levels of all data components together with EM calibrations, drift levels and noise peaks are examined.

Figure 24. Example of the initial QC using ALKU2000



Base station magnetic and GPS data are also checked. For magnetic data this means comparing the recorded data against specification conditions for reflights. Any noise or features that can be regarded as 'local' are filtered by a combined median and averaging filter. The GPS data are checked for any recording gaps or low-quality data.

Although the final levelling of the EM data is performed after the whole area has been surveyed, preliminary levelling is carried out at this phase. This initial levelling step, carried out in the field, is important in that it allows for a greater degree of QC on the EM coupling ratios acquired.

After all these processing steps, further programs are then applied for the calibration and the application of methodological corrections to the geophysical data. These procedures provide an initial, but still preliminary, set of text files (termed .xyz) for each flight and for each of the three geophysical data sets. These data sets are finally assembled into a Geosoft database for further QC assessments according to those required by the survey specifications.

The outcome of the application of the procedures mentioned above, together with the DGPS corrections, result in flight-line by flight-line xyz text files for each geophysical parameter. These are transferred to Geosoft databases where further QC control is applied. Altitude deviation is checked statistically and also by plotting colour profiles. The line paths are compared to the specified line paths and the flight path deviation is analysed. Sampling intervals and survey speed are also checked.

Average radiometric spectra and the main energy windows are plotted for each line. This allows an assessment of any spectral drift. Spectral stability and overall functioning of the spectrometer is controlled during the survey in real-time (geophysical operator), together with the initial QC and line-based spectral inspection.

Processed data for each successive flight are appended to the survey area databases. Geophysical parameters, errors and noise levels of all measurements are examined on a line-by-line basis. Geophysical parameters are also interpolated to grids and examined. All these grids are preliminary but they form useful updated summaries of the behaviour of the survey data.

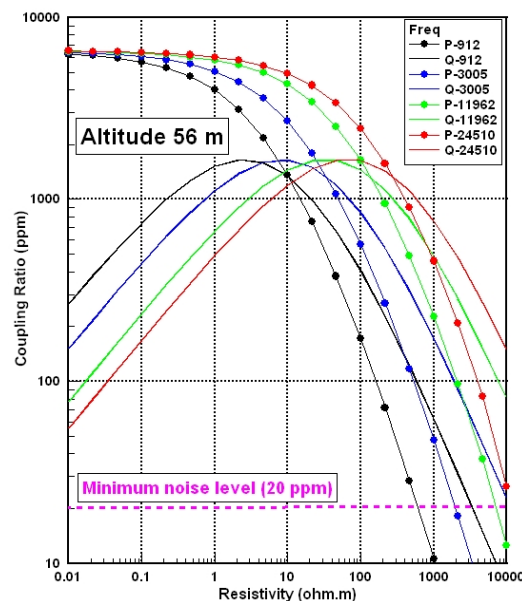
## 4.2 FINAL PROCESSING

The final processing was done at the office after the survey had been completed.

The flight-based zero level correction of EM made during the survey was rechecked and further defined. The levels were also checked line by line and adjusted if needed. A median filtering technique described in Hautaniemi et al. (2005) was applied to the EM data in order to remove remaining levelling errors. After standard corrections, the radiometric data was also filtered with the floating-window median filter.

The final levelled EM data were used to calculate apparent resistivity and depth according to a half-space model (Hautaniemi et al., 2005). Limit values and light median filtering were used to enhance the reliability of the calculations. The behaviour of the EM coupling ratios for a range of half-space resistivities is shown in Figure 25.

Figure 25. 4 frequency AEM-05 coupling ratios (in-phase= $P$ , quadrature= $Q$ ) across a range of half-space resistivities, at an elevation of 56 m.



A system noise level of 20 ppm is indicated. The actual survey noise levels in the EM channels may be higher. It can be seen that, particularly in resistive terrains, the lower frequency in-phase ( $P$ ) components may approach and descend into the noise level.

This behaviour limits our ability to obtain valid estimates of apparent resistivity and depth. In conditions of variable flight elevation, the levels of signal/noise may also vary (signal decreases with increasing elevation). Such effects decrease with increasing frequency and are thus most pronounced in the 912 Hz data.

Magnetic data is not calculated to IGRF values but the base value for the data is the base value of the survey time and place as shown in Table 10. IGRF data will be delivered later – as especially Cavan-Monaghan-Leitrim area is meant to be comparable to Northern Ireland Tellus data when it comes to data levels, it is best to wait for Tellus data to be tied to IGRF level first and then deliver the IGRF data for these survey areas after that.

Magnetic data was levelled using the JAC Virtual Tie Line approach which basically applies a constant level correction for each line if needed. The magnetic grid was further microlevelled using procedures available in Geosoft Oasis Montaj.

*Table 10. Magnetic base levels.*

<b>Survey area</b>	<b>Magnetic base level (nT)</b>
Cavan-Monaghan-Leitrim	49240
Castleisland	48870
Silvermines	48870

In Silvermines area use of VHF radio was necessary on some lines as required by Shannon ATC. This caused a short spike in magnetic data which has been manually removed.

For radiometrics standard window-technique processing is used. As is the case with IGRF corrected TMI data, the Cesium concentrations will be calculated in post-processing phase using a full-spectrum technique and delivered later.

## 5 Deliverables

### 5.1 XYZ FILES

The XYZ files delivered on the CD are text files conforming to the Geosoft XYZ file format. XYZ file content is described in Table 11 and file structures in **Error! Reference source not found.** - Table 15. In file and grid names 'xxx' refers to area name abbreviation – for example the EM data file for Castleisland is called *emcaslev.xyz* and shown in the tables as *em'xxx'.lev*.

*Table 11. XYZ file contents descriptions.*

File name	Contents	File structure
em'xxx'lev.xyz	EM measurement results and calculated apparent resistivities for all the frequencies	Described in Table 12
ml'xxx'lev.xyz (*)	Magnetic measurement results of the left wingtip sensor	Described in Table 13
mn'xxx'lev.xyz (*)	Magnetic measurement results of the nose stinger sensor	Described in Table 14
ra'xxx'lev.xyz (**)	Radiometric measurement results	Described in Table 15

(\*) Please note: Magnetic grids (see Table 16) are not produced by gridding the data above. The magnetic grids result from a further grid-based microlevelling procedure. Magnetic data is not yet IGRF corrected (see Chapter 4.2).

(\*\*) Please note: Cesium concentration will be delivered later after post-processing as explained in Chapter 4.2.

Table 12. Channel name descriptions for file *em'xxx'lev.xyz*.

Channel	Description	Unit
X	Easting coordinate (Irish Grid)	m
Y	Northing coordinate (Irish Grid)	m
LAT	WGS84 Latitude	deg
LON	WGS84 Longitude	deg
FID	Fiducial	-
FLIGHT	Flight number	-
DATE	Survey date	-
DAY	Julian day	-
TIME	Recording time in HHMMSS.SSS format	-
DIR	Flight direction (from North)	deg
RALT	Flight altitude	m
GPS_H	GPS altitude	m
DTM	Terrain model (elevation from WGS-84 ellipsoid surface)	m
PLM	Powerline monitor	-
RE09	Real component, 912 Hz	ppm
IM09	Imaginary component, 912 Hz	ppm
RE3	Real component, 3005 Hz	ppm
IM3	Imaginary component, 3005 Hz	ppm
RE12	Real component, 11962 Hz	ppm
IM12	Imaginary component, 11962 Hz	ppm
RE25	Real component, 24510 Hz	ppm
IM25	Imaginary component, 24510 Hz	ppm
AR09	Apparent resistivity, 912 Hz	$\Omega\text{m}$
AD09	Apparent depth of conductor, 912 Hz	m
AR3	Apparent resistivity, 3005 Hz	$\Omega\text{m}$
AD3	Apparent depth of conductor, 3005 Hz	m
AR12	Apparent resistivity, 11962 Hz	$\Omega\text{m}$
AD12	Apparent depth of conductor, 11962 Hz	m
AR25	Apparent resistivity, 24510 Hz	$\Omega\text{m}$
AD25	Apparent depth of conductor, 24510 Hz	m

Table 13. Channel name descriptions for file *ml'xxx'lev.xyz*.

Channel	Description	Unit
X	Easting coordinate (Irish Grid)	m
Y	Northing coordinate (Irish Grid)	m

Channel	Description	Unit
LAT	WGS84 Latitude	deg
LON	WGS84 Longitude	deg
FID	Fiducial	-
FLIGHT	Flight number	-
DATE	Survey date	-
DAY	Julian day	-
TIME	Recording time HHMMSS.SSS format	-
DIR	Flight direction	deg
RALT	Flight altitude	m
GPS_H	GPS altitude	m
DTM	Terrain model (elevation from WGS-84 ellipsoid surface)	m
ORIGL	TMI value for left wingtip sensor before base station correction	nT
MGCL	Corrected TMI value for left wingtip sensor	nT
BASE	TMI value recorded at the base station	nT

Table 14. Channel name descriptions for file mn'xxx'lev.xyz.

Channel	Description	Unit
X	Easting coordinate (Irish Grid)	m
Y	Northing coordinate (Irish Grid)	m
LAT	WGS84 Latitude	deg
LON	WGS84 Longitude	deg
FID	Fiducial	-
FLIGHT	Flight number	-
DATE	Survey date	-
DAY	Julian day	-
TIME	Recording time	-
DIR	Flight direction	deg
RALT	Flight altitude	m
GPS_H	GPS altitude	m
DTM	Terrain model (elevation from WGS-84 ellipsoid surface)	m
ORIGN	TMI value for nose stinger sensor before base station correction	nT
MGCN	Corrected TMI value for nose stinger sensor	nT
BASE	TMI value recorded at the base station	nT

Table 15. Channel name descriptions for file ra'xxx'lev.xyz.

Channel	Description	Unit
X	Easting coordinate (Irish Grid)	m
Y	Northing coordinate (Irish Grid)	m
LAT	WGS84 Latitude	deg
LON	WGS84 Longitude	deg
FID	Fiducial	-
FLIGHT	Flight number	-
DATE	Survey date	-
DAY	Julian day	-
TIME	Recording time HHMMSS.SSS format	-
DIR	Flight direction	deg
RALT	Flight altitude	m
BALT	Barometric altitude	m
TOUT	Temperature outside the aircraft	°C
GPS_H	GPS altitude	m
DTM	Terrain model (elevation from WGS-84 ellipsoid surface)	m
D_TOT_CPS	Total radiometric concentration	cps
D_TOT_NGY	Total radiometric concentration	nGy/h
D_KAL	Potassium concentration	%K
D_URA	Uranium concentration	eU ppm
D_THO	Thorium concentration	eTh ppm

## 5.2 GRID FILES

Grid files are described in Table 16. Images of the grids are shown in Appendix 2.

Table 16. Grid file descriptions.

Grid file name	Description	Unit
APD09'XXX'.grd	Apparent depth of conductor, 912 Hz	m
APD12'XXX'.grd	Apparent depth of conductor, 3005 Hz	m
APD25'XXX'.grd	Apparent depth of conductor, 11962 Hz	m
APD3'XXX'.grd	Apparent depth of conductor, 24510 Hz	m
APR09'XXX'.grd	Apparent resistivity, 912 Hz	$\Omega$ m
APR12'XXX'.grd	Apparent resistivity, 3005 Hz	$\Omega$ m
APR25'XXX'.grd	Apparent resistivity, 11962 Hz	$\Omega$ m
APR3'XXX'.grd	Apparent resistivity, 24510 Hz	$\Omega$ m

<b>Grid file name</b>	<b>Description</b>	<b>Unit</b>
DTM'XXX'.grd	Terrain model (elevation from WGS-84 ellipsoid surface)	m
IM09'XXX'.grd	Imaginary component, 912 Hz	ppm
IM12'XXX'.grd	Imaginary component, 3005 Hz	ppm
IM25'XXX'.grd	Imaginary component, 11962 Hz	ppm
IM3'XXX'.grd	Imaginary component, 24510 Hz	ppm
KAL'XXX'.grd	Potassium concentration	%K
MAG'XXX'.grd	Microlevelled magnetic TMI value	nT
RE09'XXX'.grd	Real component, 912 Hz	ppm
RE12'XXX'.grd	Real component, 3005 Hz	ppm
RE25'XXX'.grd	Real component, 11962 Hz	ppm
RE3'XXX'.grd	Real component, 24510 Hz	ppm
THO'XXX'.grd	Thorium concentration	eTh ppm
TOT_CPS'XXX'.grd	Total radiometric concentration	cps
TOT_NGY'XXX'.grd	Total radiometric concentration	nGy/h
URA'XXX'.grd	Uranium concentration	eU ppm

## 6 References

Grasty, R.L. and Minty, B.R.S., 1995. A guide to the technical specifications for airborne gamma-ray surveys. Australian Geological Survey Organisation, Record, 1995/20.

Hautaniemi, H., Kurimo, M., Multala, J., Leväniemi, H. and Vironmäki, J. 2005. The 'three in one' aerogeophysical concept of GTK in 2004. In: Airo, M-L. (ed.) Aerogeophysics in Finland 1972-2004: Methods, System Characteristics and Applications, Geological Survey of Finland, Special Paper 39, 21-74.

IAEA, 1991. Airborne gamma ray spectrometer surveying, International Atomic Energy Agency, Technical Report Series, No. 323.

Poikonen, A., Sulkanen, K., Oksama, M., & Suppala, I. 1998. Novel dual frequency fixed wing airborne EM system of Geological Survey of Finland (GTK). *Exploration Geophysics* 29, 46-51.

Suppala, I., Oksama, M. and Hongisto, H. 2005. GTK airborne EM system: characteristics and interpretation guidelines. In: Airo, M-L. (ed.) Aerogeophysics in Finland 1972-2004: Methods, System Characteristics and Applications, Geological Survey of Finland, Special paper 39, 103-118.

# Appendix 1: Survey Equipment

## Aircraft

The aircraft used in the survey is a fixed-wing, twin-engine DHC-6/300 Twin Otter (registration sign OH-KOG, registered in Finland). The aircraft is owned by Natural Environment Research Council / British Geological Survey (NERC / BGS). Flying and maintenance are operated by Finnish Aviation Academy (FAA) and the geophysical equipment monitoring on flights is operated by Geological Survey of Finland (GTK) together with BGS.

The specifications of the aircraft are presented in Appendix 2: Table 1.

*Appendix 2: Table 1. OH-KOG specifications.*

Normal flight speed	220 km/h
Flight speed on survey flights	160 – 220 km/h (50 – 60 m/s)
Rate of climb	7.5 m/s
Total flight hours	About 16000 hours to date
Landings	About 8000 landings to date

This aircraft was build in Canada in 1979 and has been in use since 1980 for aerogeophysical measurements. During the manufacturing of the Twin Otter several modifications were made to its electrical systems in order to reduce the electrical noise levels. Condition of the aircraft is good.

The aircraft offers several major advantages in terms of utility and cost, including excellent performance reserves, low-speed handling characteristics and operational flexibility allowing the use of unsupervised and unpaved air strips. The twin Otter was selected for the measuring platform as the most suitable fixed-wing aircraft for low altitude STOL (short take-off and landing) operations.

## Geophysical Equipment

The components of the geophysical equipment installed in the Twin Otter are connected to each other by a local area network (LAN).

### Magnetics

- Two Scintrex CS-2 Caesium magnetometers, one at the left wingtip and one at the nose stinger
- Automatic compensation unig RMS AADCII
- Sampling rate of 10 Hz

### Time-domain electromagnetic four-frequency unit

- Model AEM-05, vertical-coplanar coil configuration
- Frequencies in use: 912 Hz, 3005 Hz, 11962 Hz and 24510 Hz

- Coil separation 21.4 meters
- Sampling rate of 4 Hz

#### Gamma-ray spectrometer

- Exploranium GR-820/3
- Two sets of NaI crystals, each containing four downward looking and one upward looking package
- Total volume 42 litres
- Sampling rate of 1 Hz

#### Navigation system:

- Ashtech GG24 (24-channel GPS + Glonass receiver)
- Accuracy 7 m / 16 m (50% / 95 %)
- Real time DGPS when differential signal available
- Sampling rate 1 Hz

#### Altitude

- Collins radar altimeter
- Resolution 0.1 m, accuracy 0.5 m
- Sampling rate of 10 Hz

#### Auxiliary equipment

- Digital camera
- Riegl laser altimeter
- Barometer, thermometer, accelerometer

#### Base station equipment

- Scintrex CS-2 sensor for magnetic recording
- Ashtech Ranger GPS receiver for DGPS correction
- Picodas MEP-7110 magnetometer

## Appendix 2: Maps of the Survey Area

The data images presented in this section were produced using the final delivered data. Data are presented for the Cavan, Castleisland and Silvermines survey areas in turn. For each area, the geophysical data sequence is magnetic (MAG), electromagnetic (EM) and radiometric (RAD).

### OVERVIEW

In overview, the magnetic data respond to both at-surface and concealed magnetic rocks at all depths (a wavelength dependence). The magnetic data shown here are Total Magnetic Intensity (TMI, in nT). The radiometric data respond to about 30 cm of the radiometric content of the surface material. The actual content might relate to either the soil material (e.g. mineralogy but also moisture content) and/or the parent geological material. Although, the 3 individual natural radionuclide elements Potassium (K-40), Thorium (Th-232) and Uranium (U-238) may be examined, our initial comments are provided by the images formed using Total Counts and/or the Ternary image formed by a tri-state arrangement of red-green-blue colours assigned to the 3 elements.

The basic EM data comprise coupling ratios that may be difficult to interpret in a simple fashion, due to both a dependence on sensor elevation and the fact that both in-phase and quadrature components are required to understand the response. The coupling ratios are converted to estimates of apparent resistivity and apparent depth as described previously. Apparent resistivity ( $\rho_a$ ) may also be converted to apparent conductivity ( $\sigma_a$ ) using the formula  $\sigma_a = 1000.0/\rho_a$ , where  $\rho_a$  is in ohm.m and  $\sigma_a$  is in mS/m. The half-space parameters form more convenient interpretation products but, as they derive from a uniform Earth assumption, they have limitations when geology/resistivity varies rapidly.

The depth of investigation of the JAC EM data may vary (typically) between 60 and 100 m. This is a simplification in that:

- i) sensitivity to resistivity variations is a maximum at the surface and decreases with depth
- ii) the statement only refers to the vertical distribution of resistivity

In broad terms, data at the lowest frequencies (0.9 and 3 kHz) may reveal deeper structure while data at the highest frequency (25 kHz) relates to the shallow subsurface. When a resistivity anomaly occurs at or near the surface, data at all frequencies may respond with the amplitude of the response decreasing with decreasing frequency.

### Signal/Noise features in the data

When data are acquired across populated areas, several issues are worth noting.

The first is that regulatory/safety high fly conditions (as discussed and illustrated in Section 1.4) result in zones of reduced or loss of geophysical signal. The spatial pattern of high-fly is imposed on the resulting images, and this 'spatial convolution' may be complex (see Section 1.4). Typically MAG retains a signal but at a reduced amplitude while RAD and EM may be 'out-of-ground' effect.

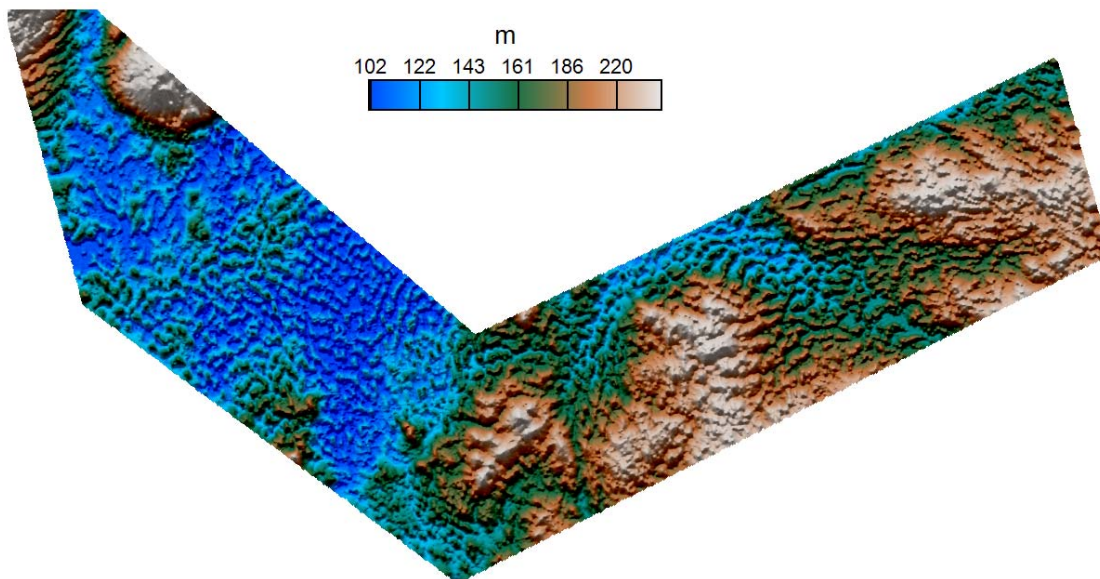
The geophysical data may respond to both geology and/or cultural features across any given survey area. Detailed interpretation of the geophysical responses ultimately requires an understanding on the non-geological responses e.g. topographic and other maps must be used in conjunction with the geophysical data.

MAG typically responds to buildings/structures with high metal content. The distortions are usually easily observed when examining detailed line-based data while in gridded images, the distortions appear as highly localised 'bulls-eyes' (closed contours).

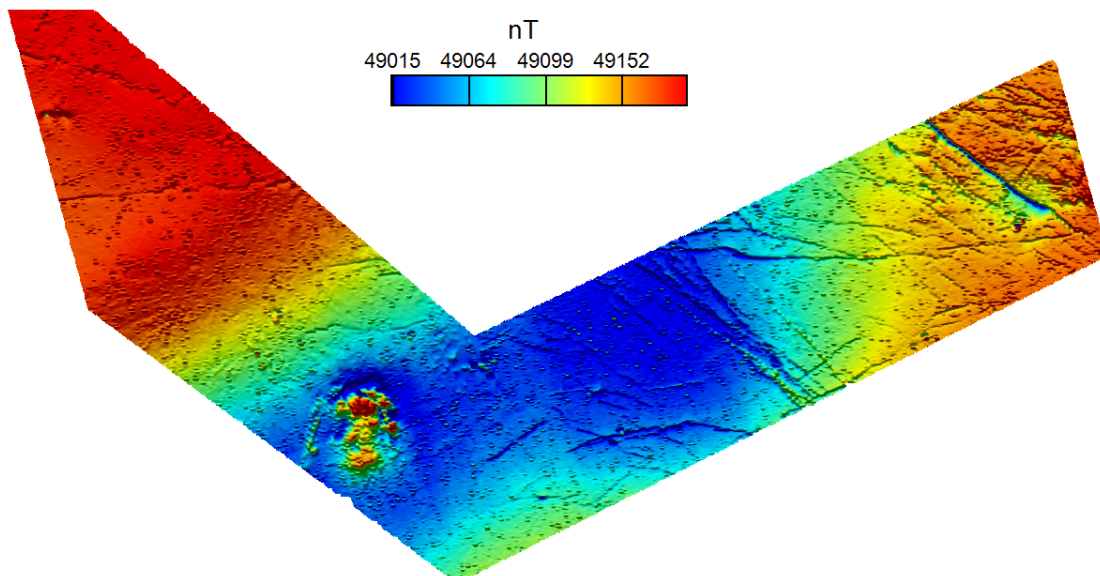
The RAD signal above made-ground and structures should reduce to zero (theoretically) however the footprint of the RAD response (height dependent) is typically so large that the response is averaged (smeared) across both geological and non-geological zones.

The EM data (being an active source measurement) is perhaps, most prone to man-made interference. Noise distortion is entirely survey area specific. For this reason, reference should be made to images of the power-line monitor (PLM). In addition, linear/quasi linear features observed in the EM images may also relate to roads; ('road-anomalies'). Such features may relate to road-side routing of services (e.g. electricity, gas, water).

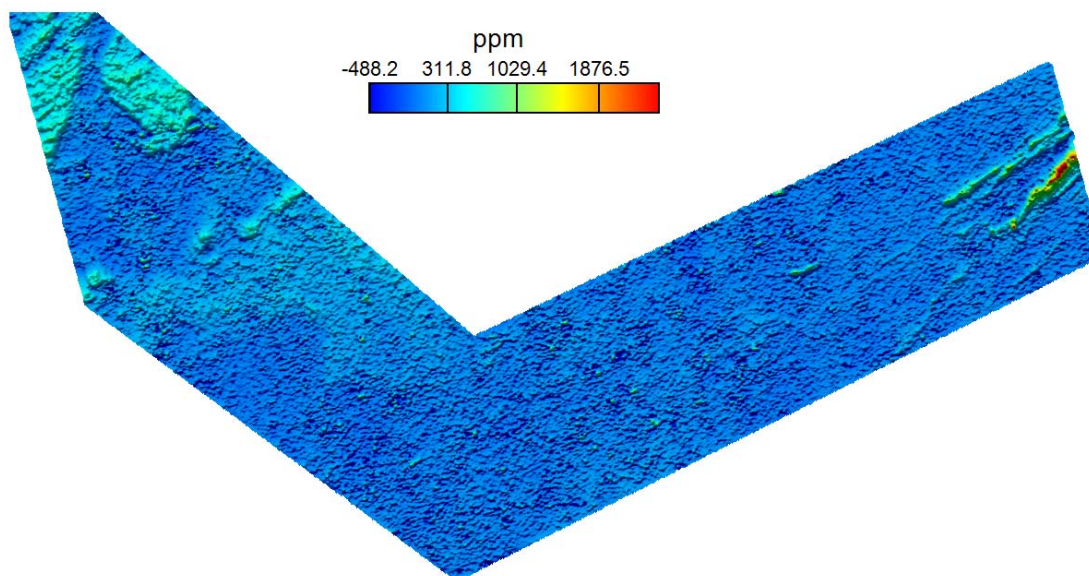
## CAVAN-MONAGHAN-LEITRIM



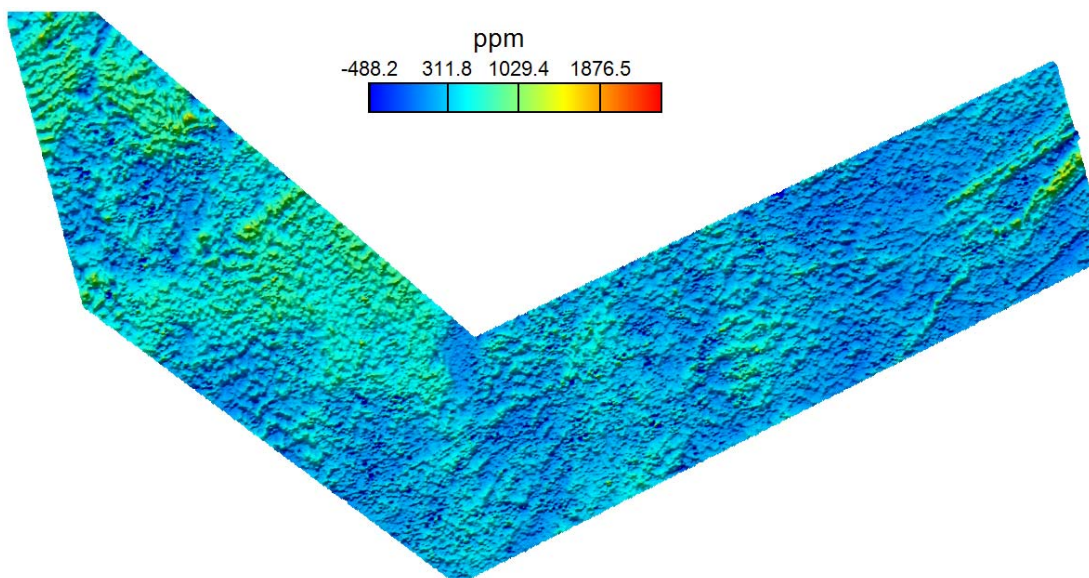
*Appendix 2: Figure 1. Cavan Monaghan-Leitrim: Digital terrain model*



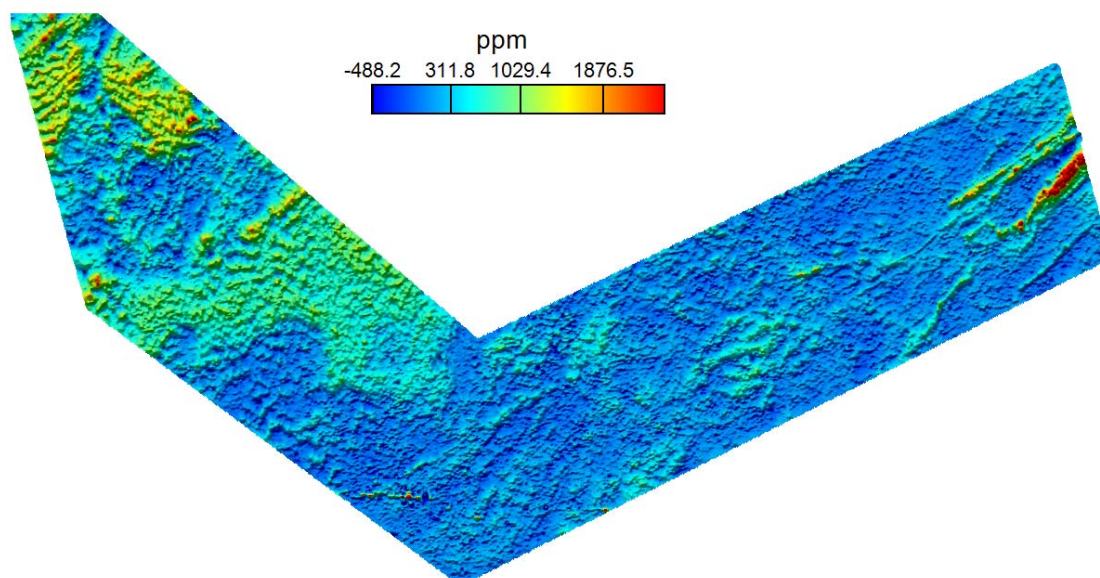
*Appendix 2: Figure 2. Cavan Monaghan-Leitrim: Total magnetic intensity*



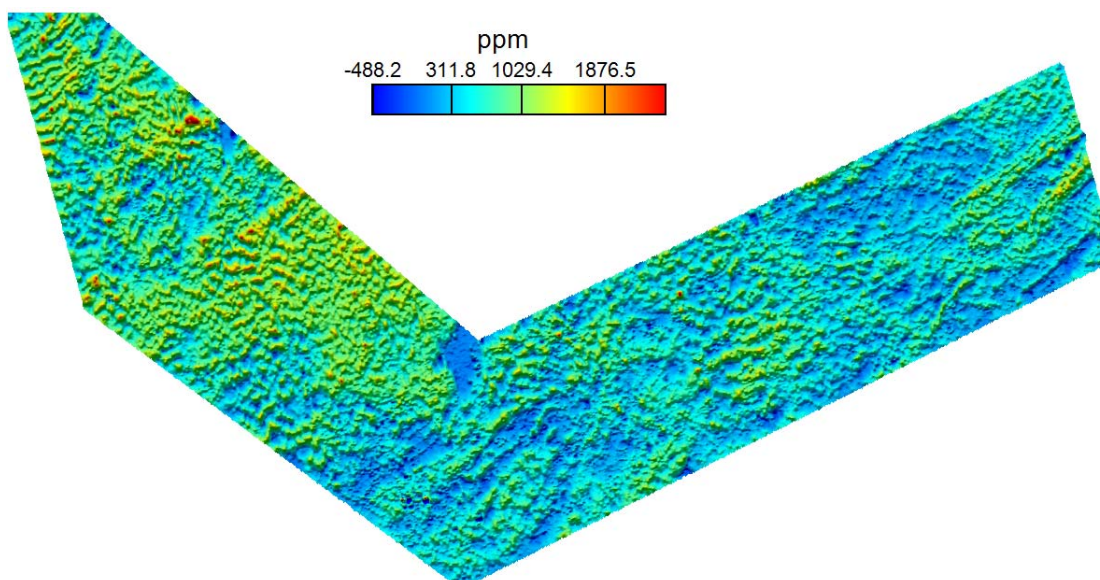
*Appendix 2: Figure 3. Cavan Monaghan-Leitrim:Real component, 0.9 kHz*



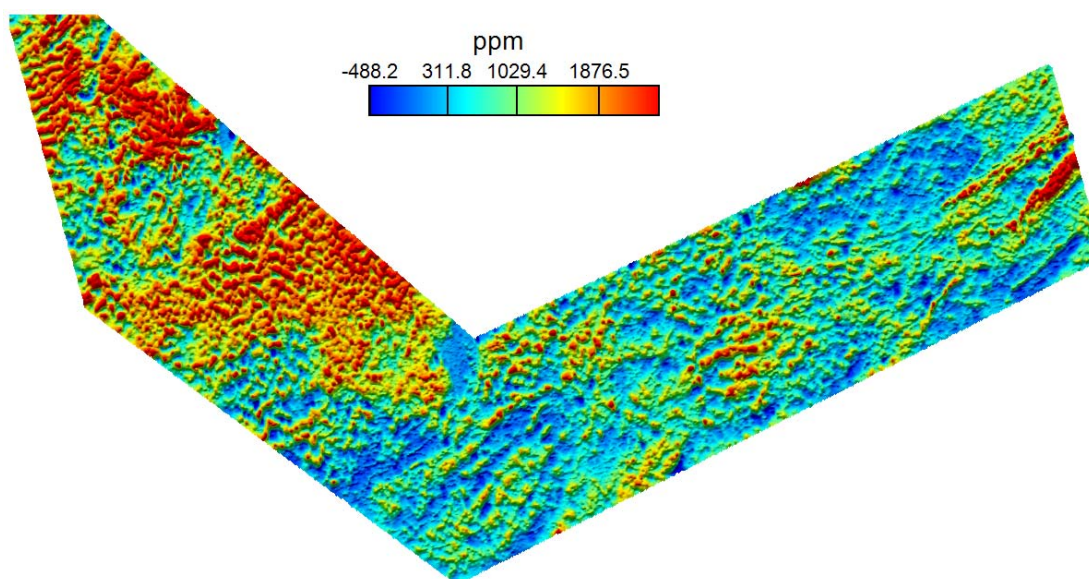
*Appendix 2: Figure 4. Cavan Monaghan-Leitrim:Imaginary component, 0.9 kHz*



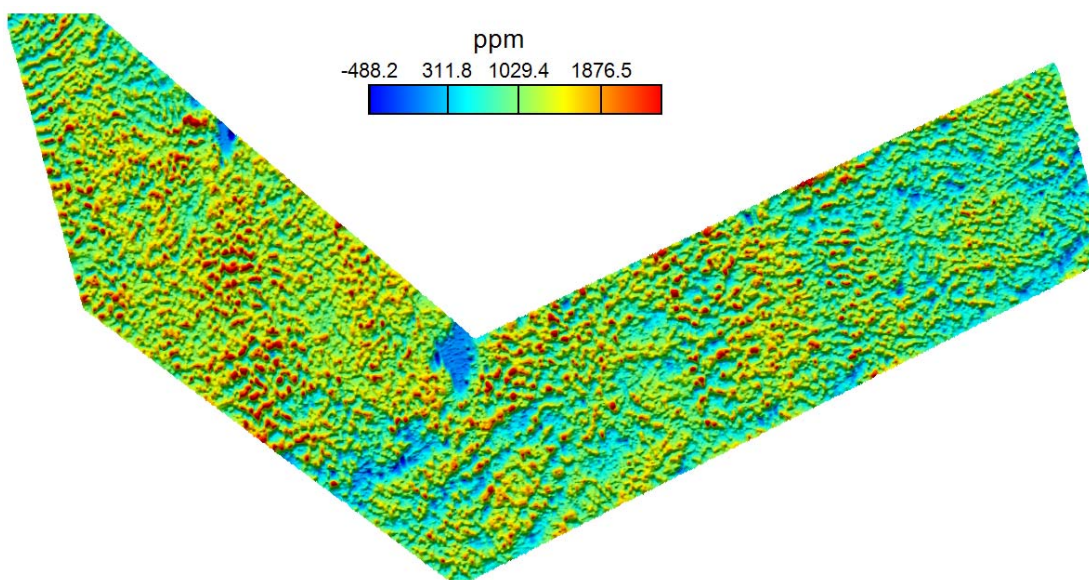
*Appendix 2: Figure 5. Cavan Monaghan-Leitrim: Real component, 3 kHz*



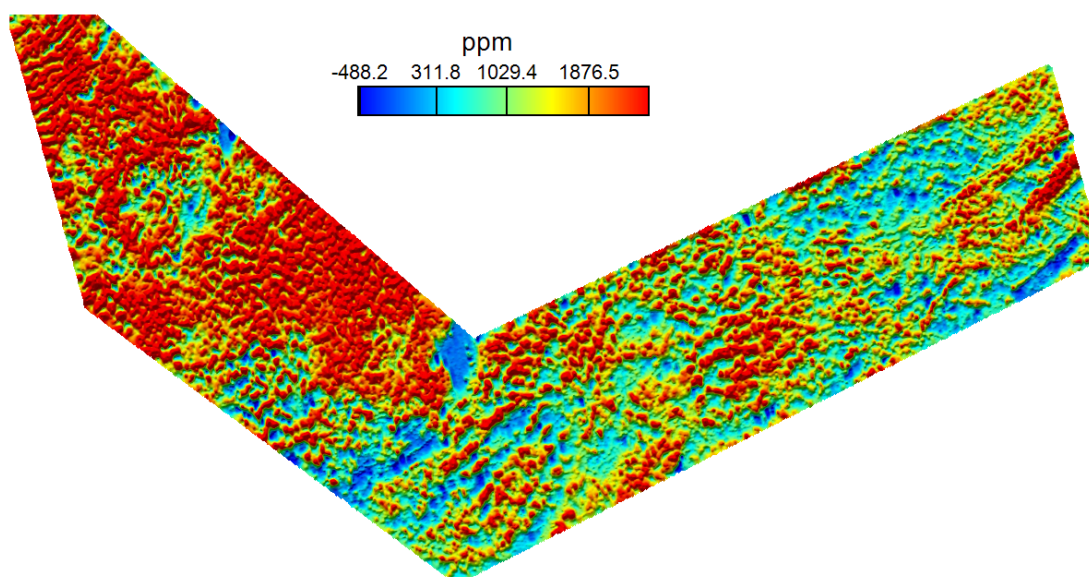
*Appendix 2: Figure 6. Cavan Monaghan-Leitrim: Imaginary component, 3 kHz*



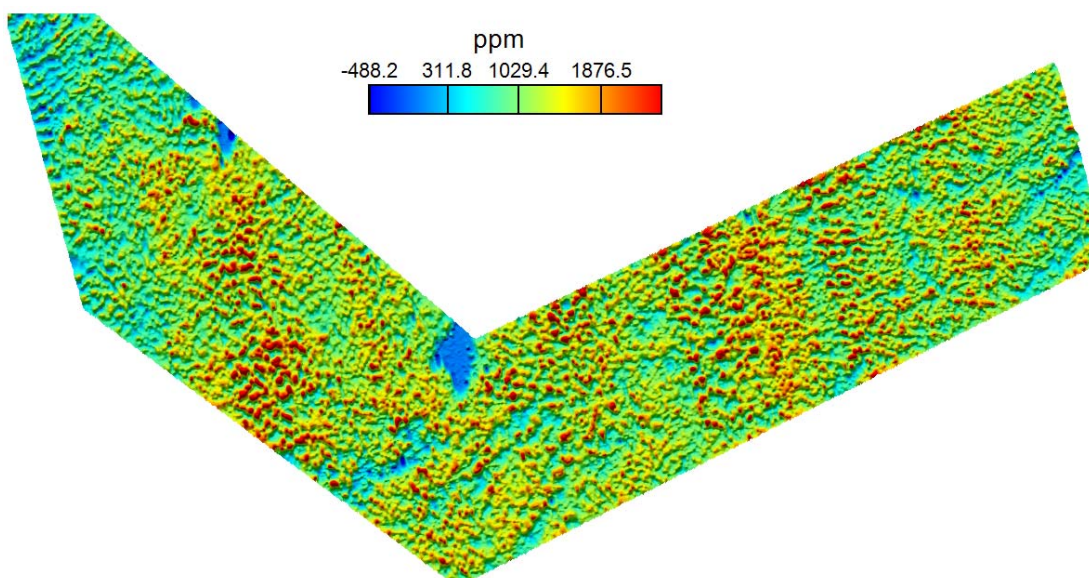
*Appendix 2: Figure 7. Cavan Monaghan-Leitrim: Real component, 12 kHz*



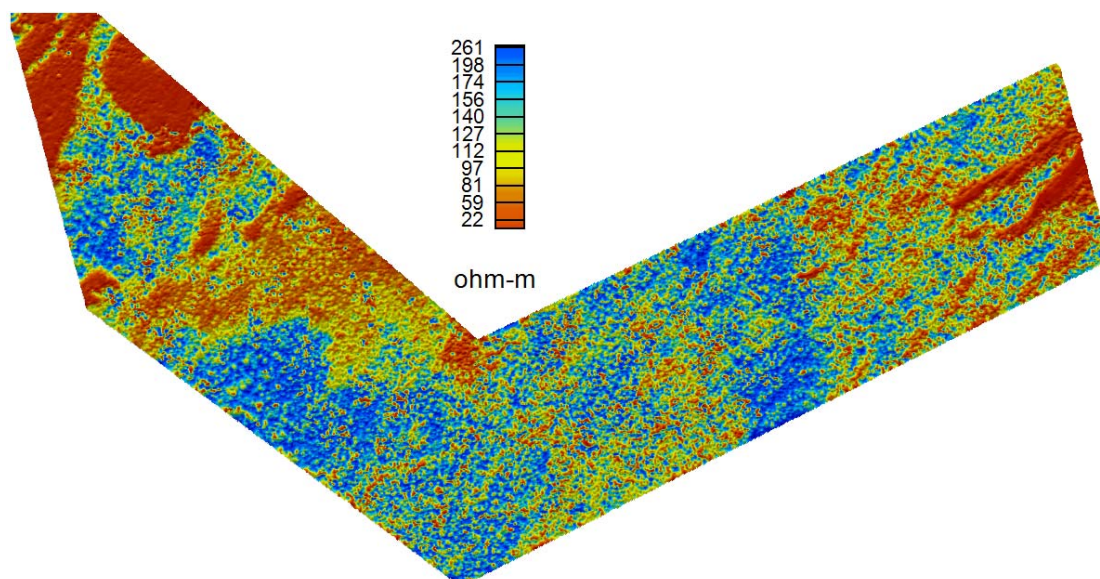
*Appendix 2: Figure 8. Cavan Monaghan-Leitrim: Imaginary component, 12 kHz*



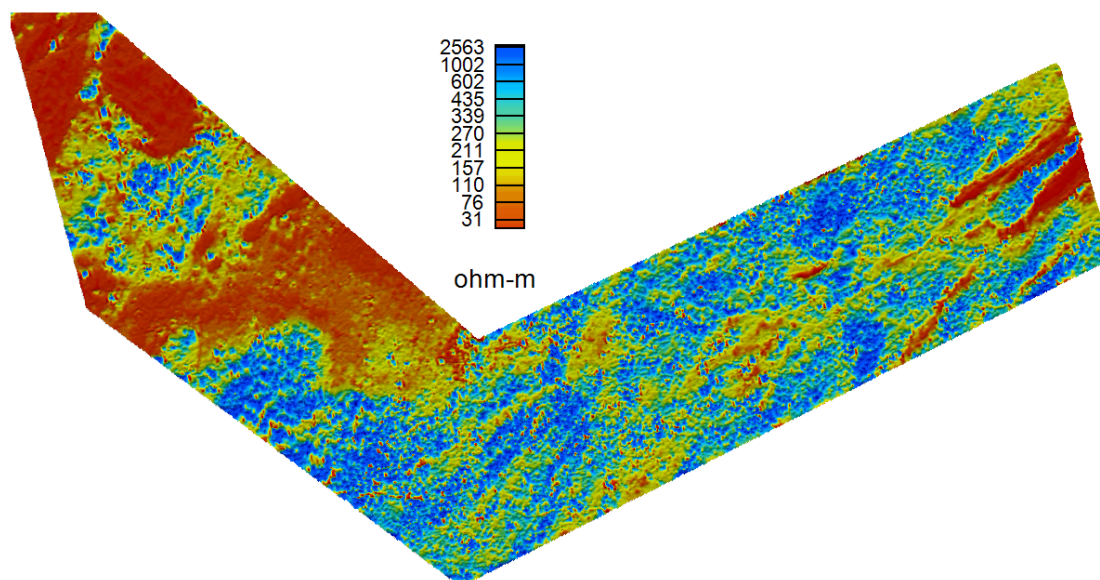
*Appendix 2: Figure 9. Cavan Monaghan-Leitrim: Real component, 24.5 kHz*



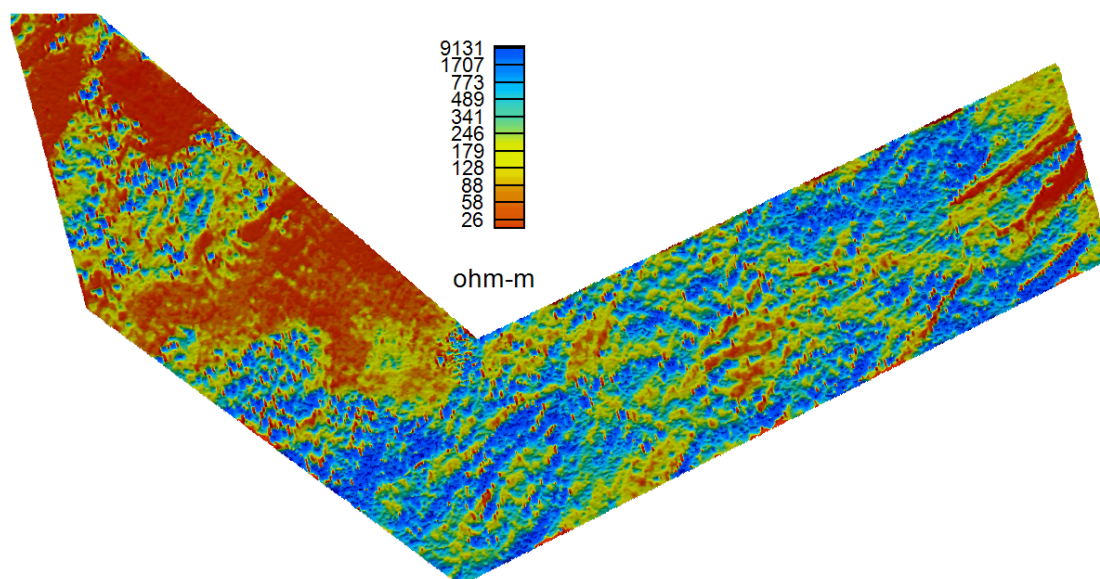
*Appendix 2: Figure 10. Cavan Monaghan-Leitrim: Imaginary component, 24.5 kHz*



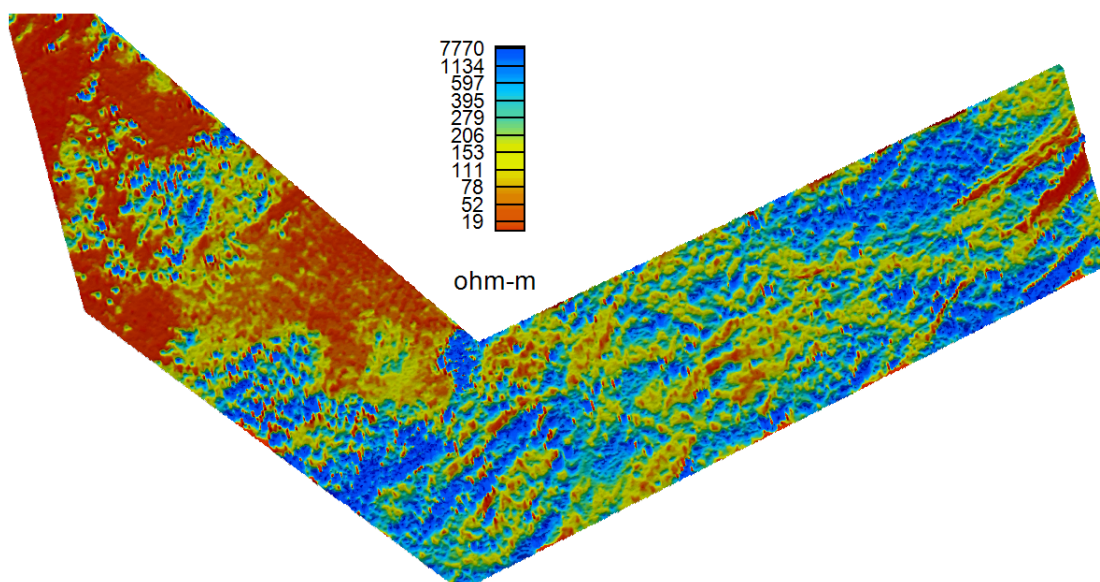
*Appendix 2: Figure 11. Cavan-Monaghan-Leitrim: Apparent resistivity, 0.9 kHz*



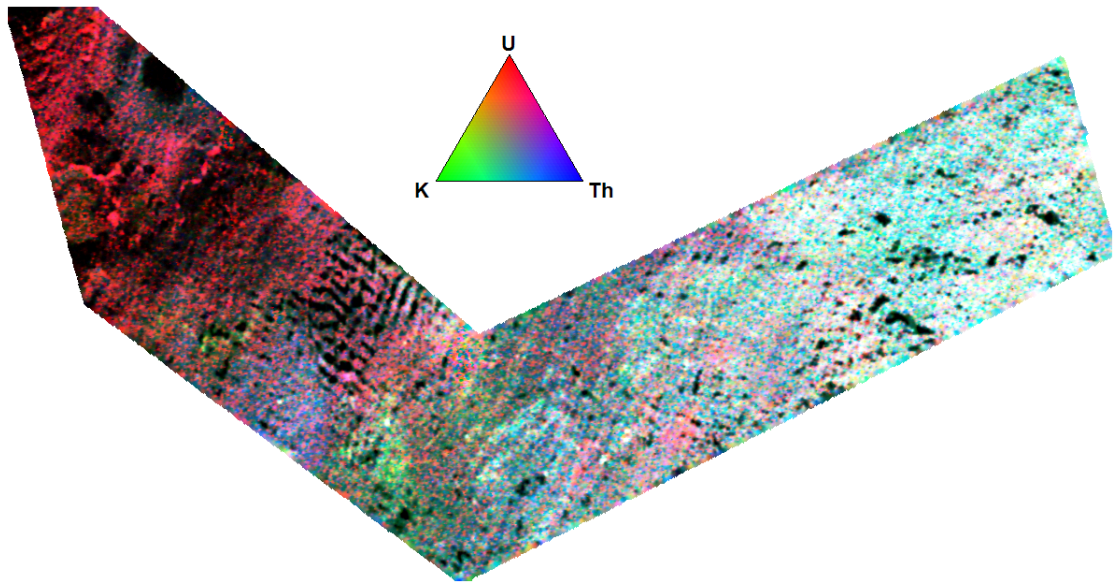
*Appendix 2: Figure 12. Cavan-Monaghan-Leitrim: Apparent resistivity, 3 kHz*



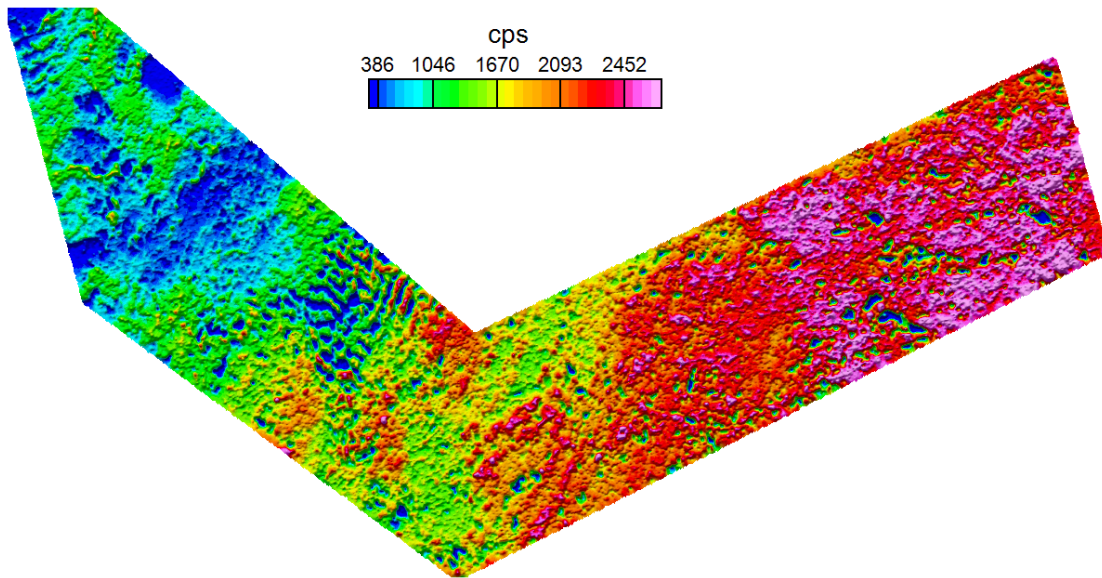
*Appendix 2: Figure 13. Cavan-Monaghan-Leitrim: Apparent resistivity, 12 kHz*



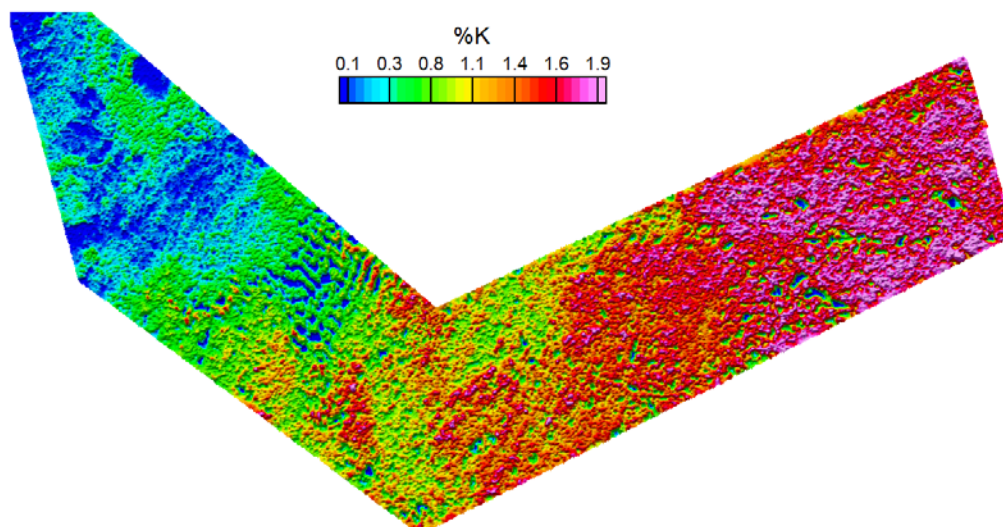
*Appendix 2: Figure 14. Cavan-Monaghan-Leitrim: Apparent resistivity, 24.5 kHz*



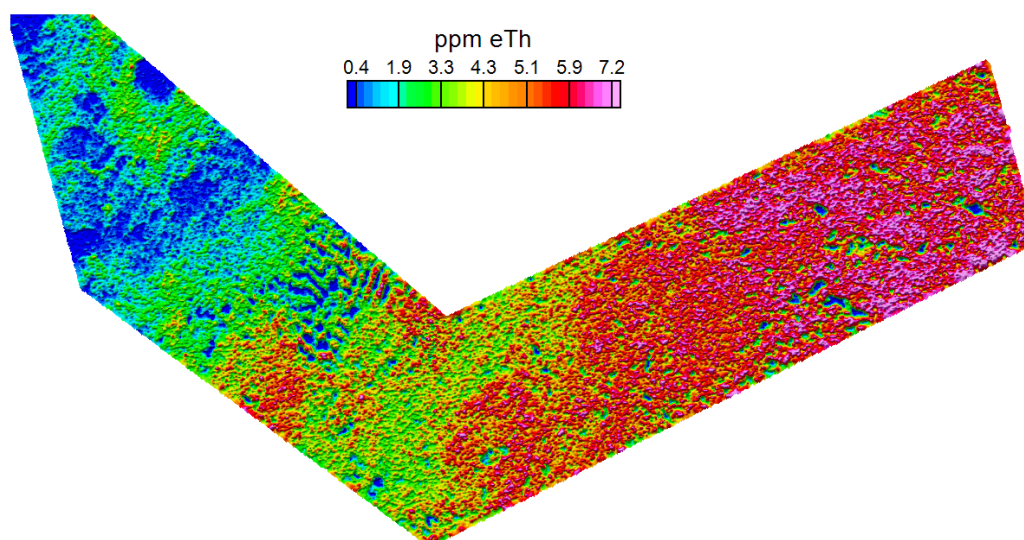
*Appendix 2: Figure 15. Cavan Monaghan-Leitrim: Rariometric ternary image*



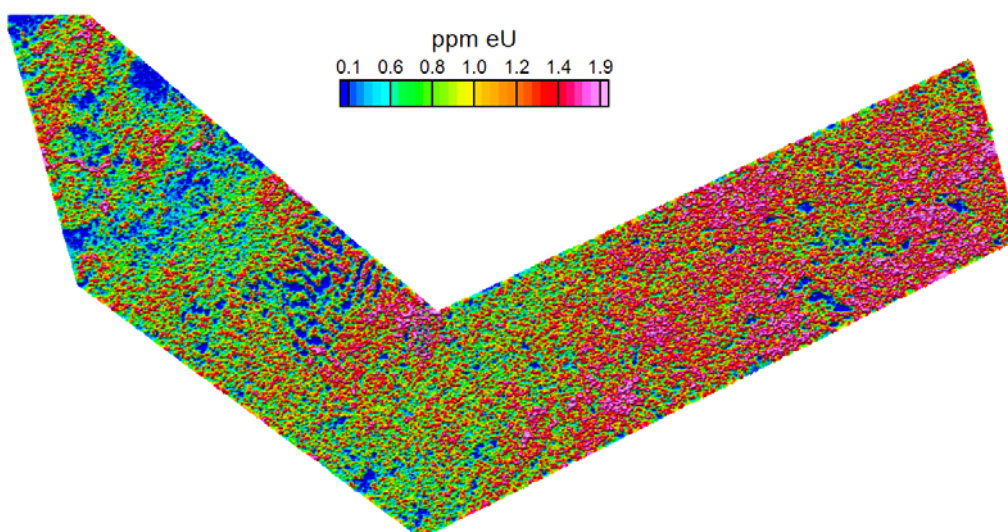
*Appendix 2: Figure 16. Cavan Monaghan-Leitrim: Total radiation*



Appendix 2: Figure 17. Cavan Monaghan-Leitrim: Potassium concentration



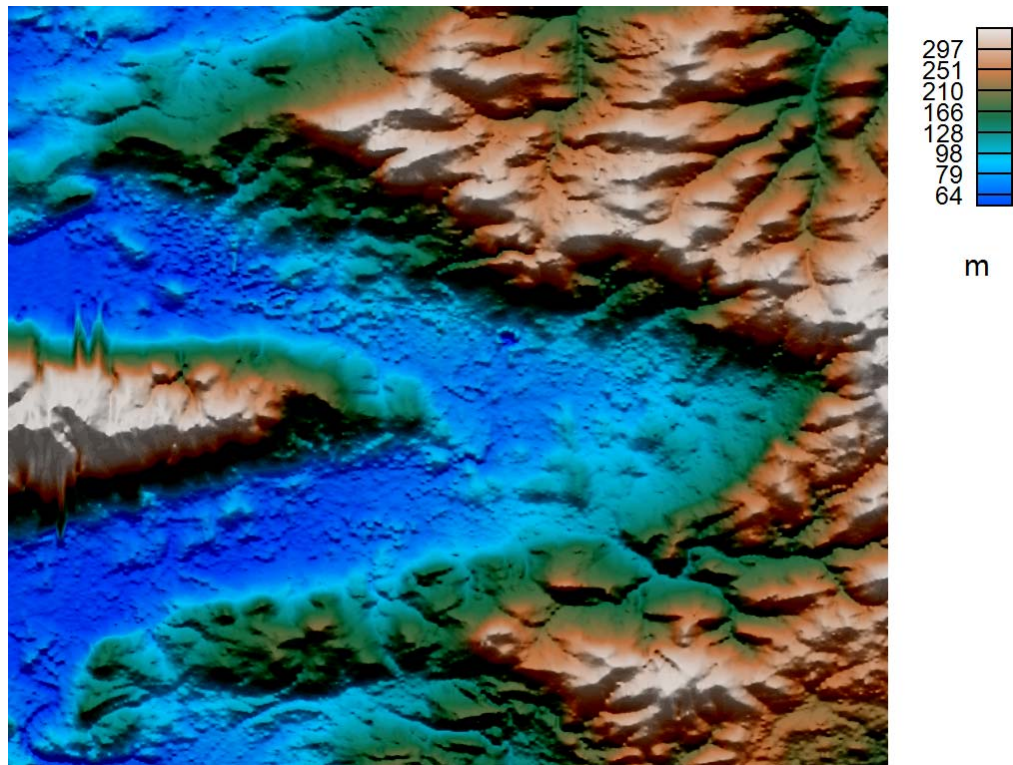
Appendix 2: Figure 18. Cavan Monaghan-Leitrim: Thorium concentration



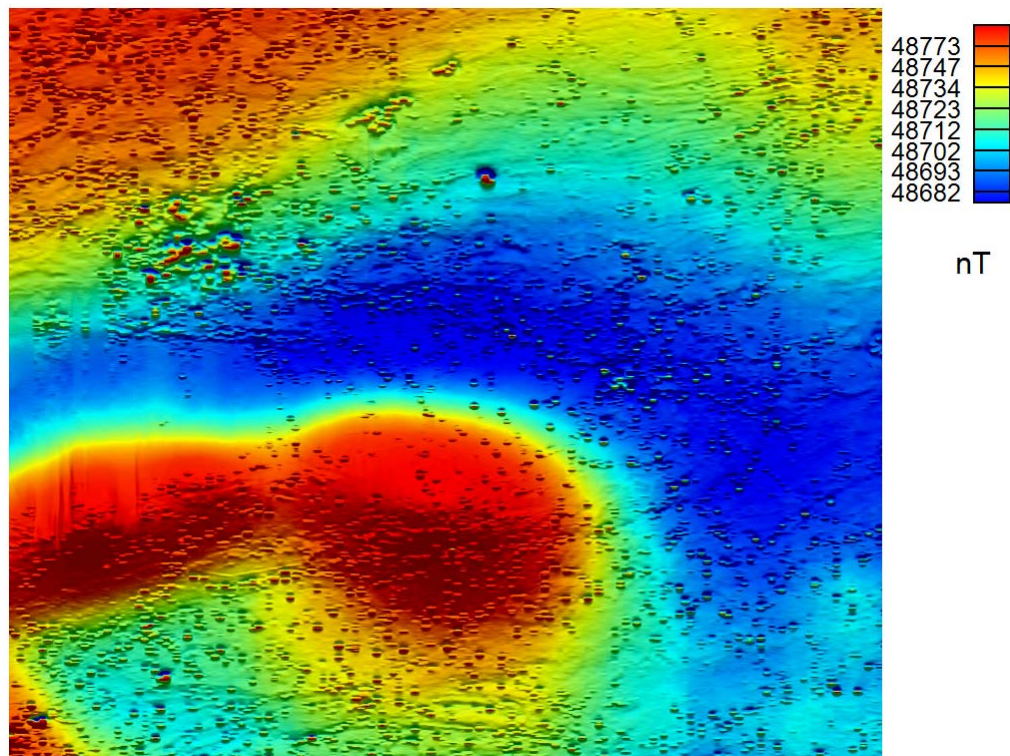
Appendix 2: Figure 19. Cavan Monaghan-Leitrim: Uranium concentration



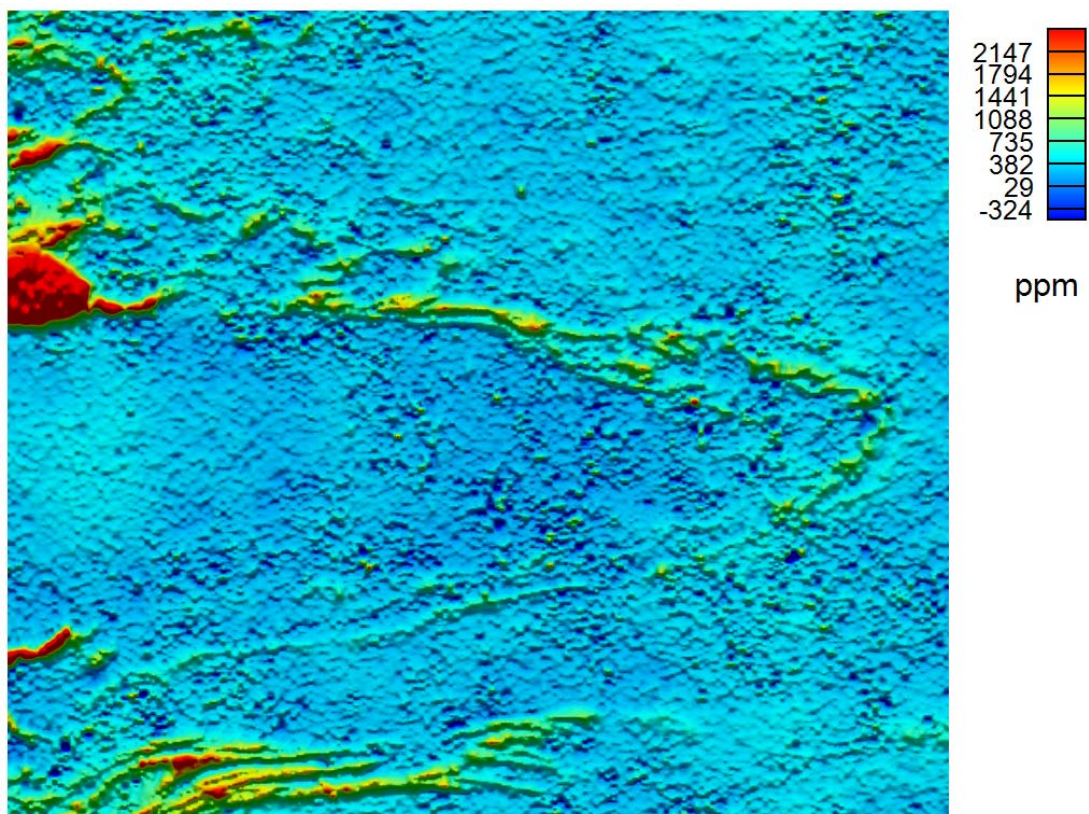
## CASTLEISLAND



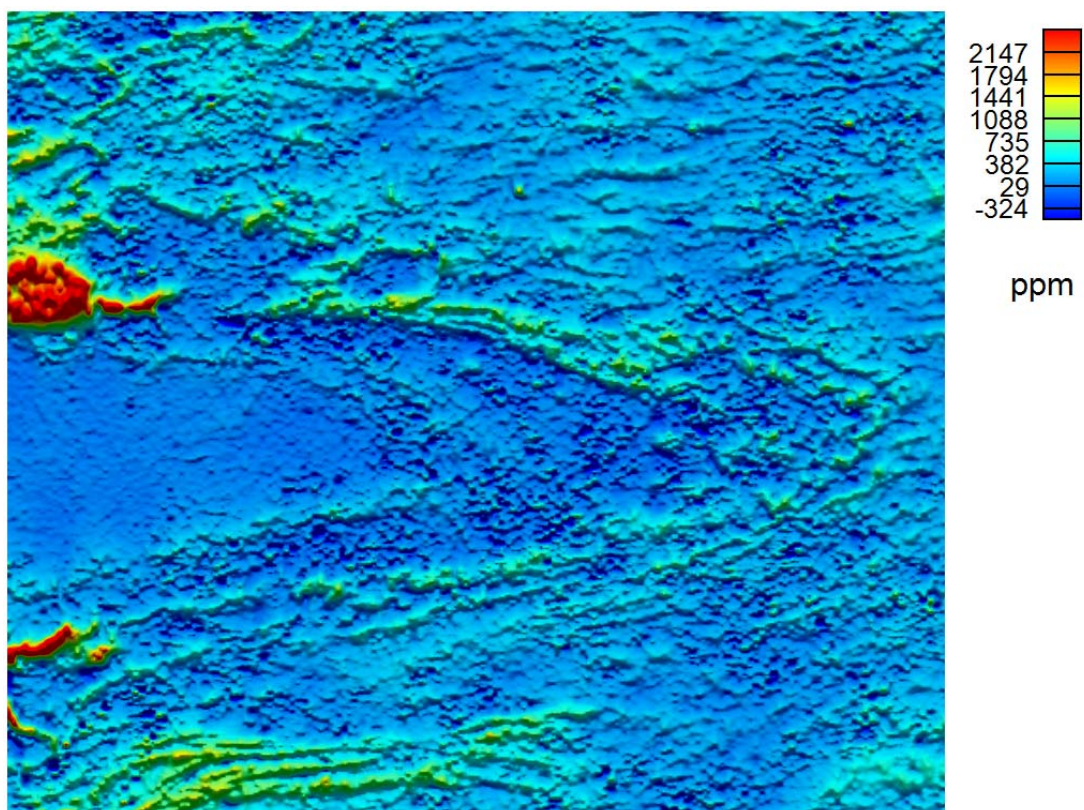
*Appendix 2: Figure 20. Castleisland: Digital terrain model*



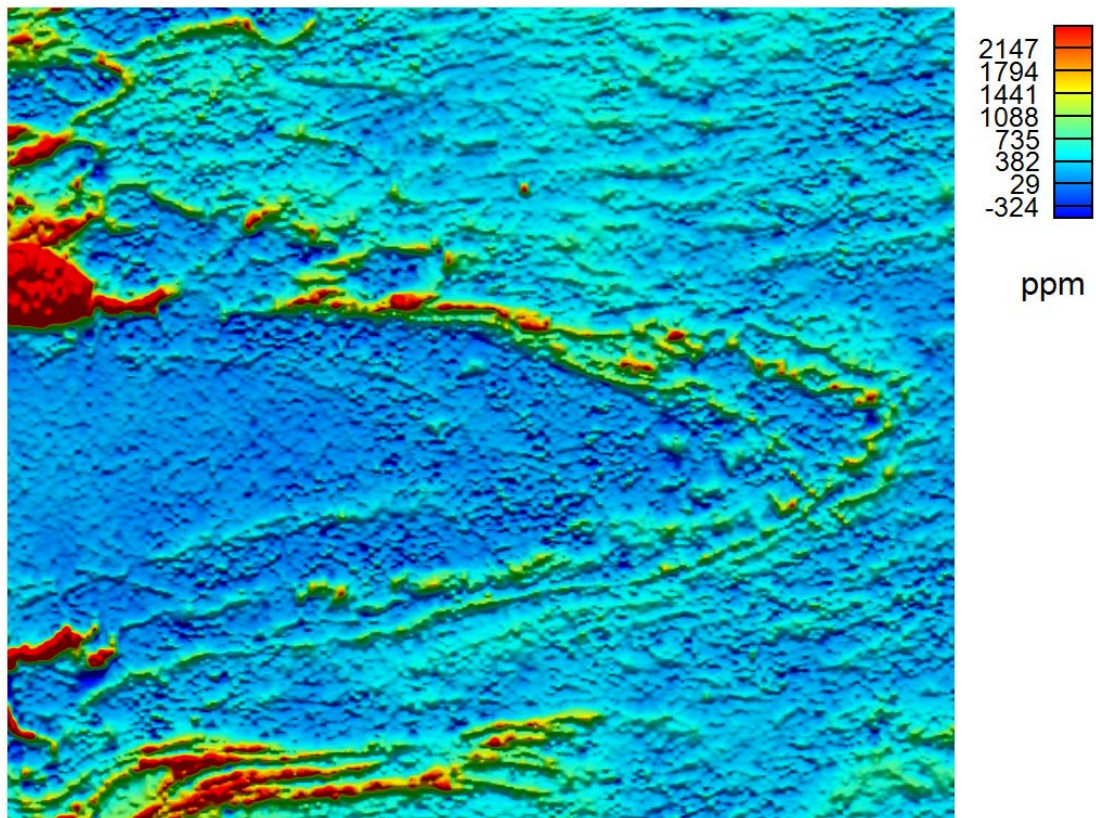
*Appendix 2: Figure 21. Castleisland: Total magnetic intensity*



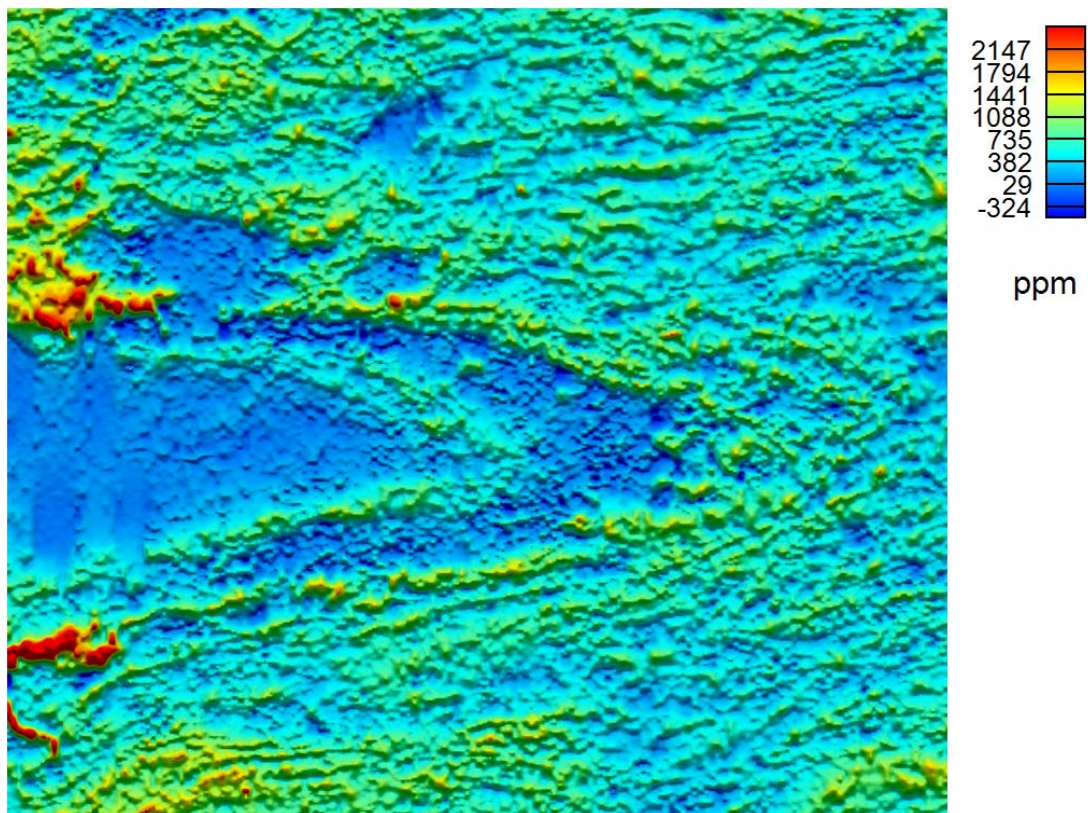
Appendix 2: Figure 22. Castleisland: Real component, 0.9 kHz



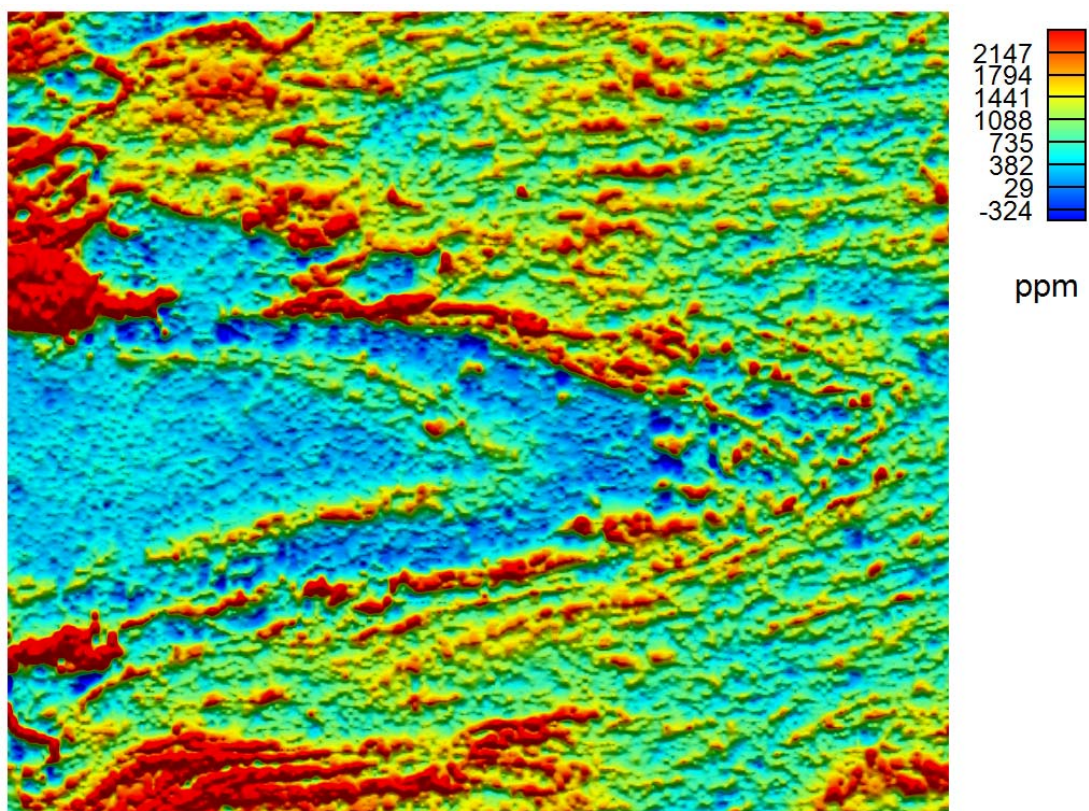
Appendix 2: Figure 23. Castleisland: Imaginary component, 0.9 kHz



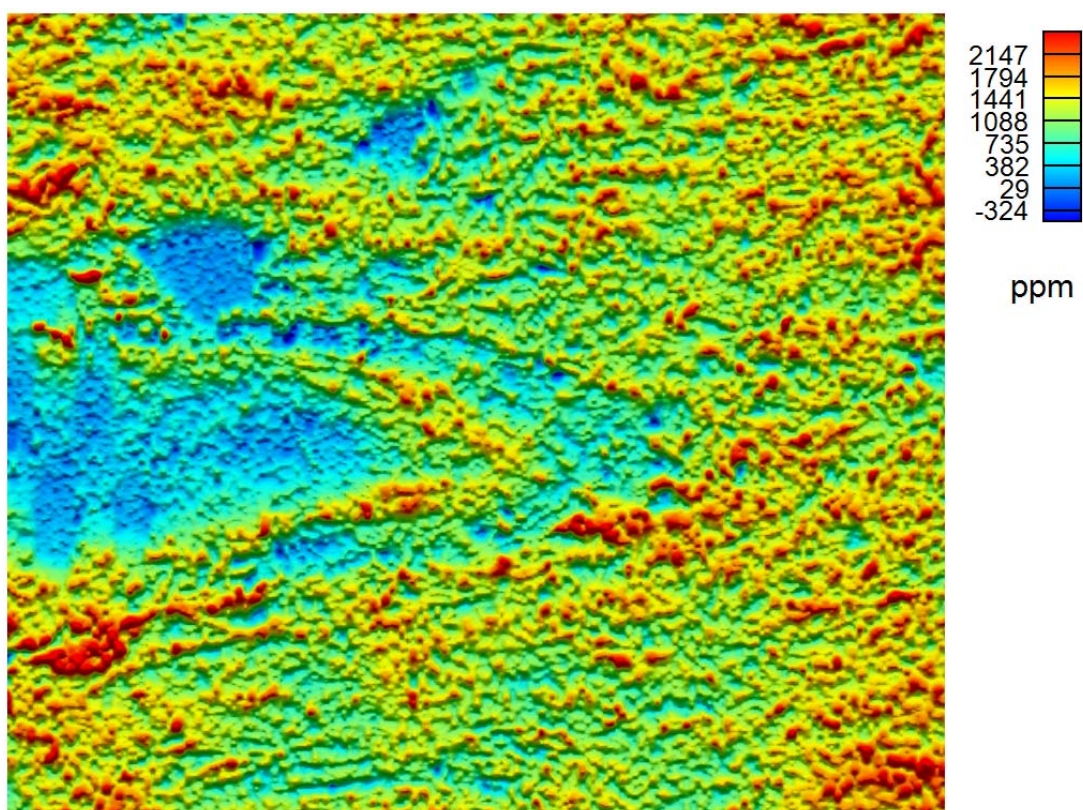
*Appendix 2: Figure 24. Castle Island: Real component, 3 kHz*



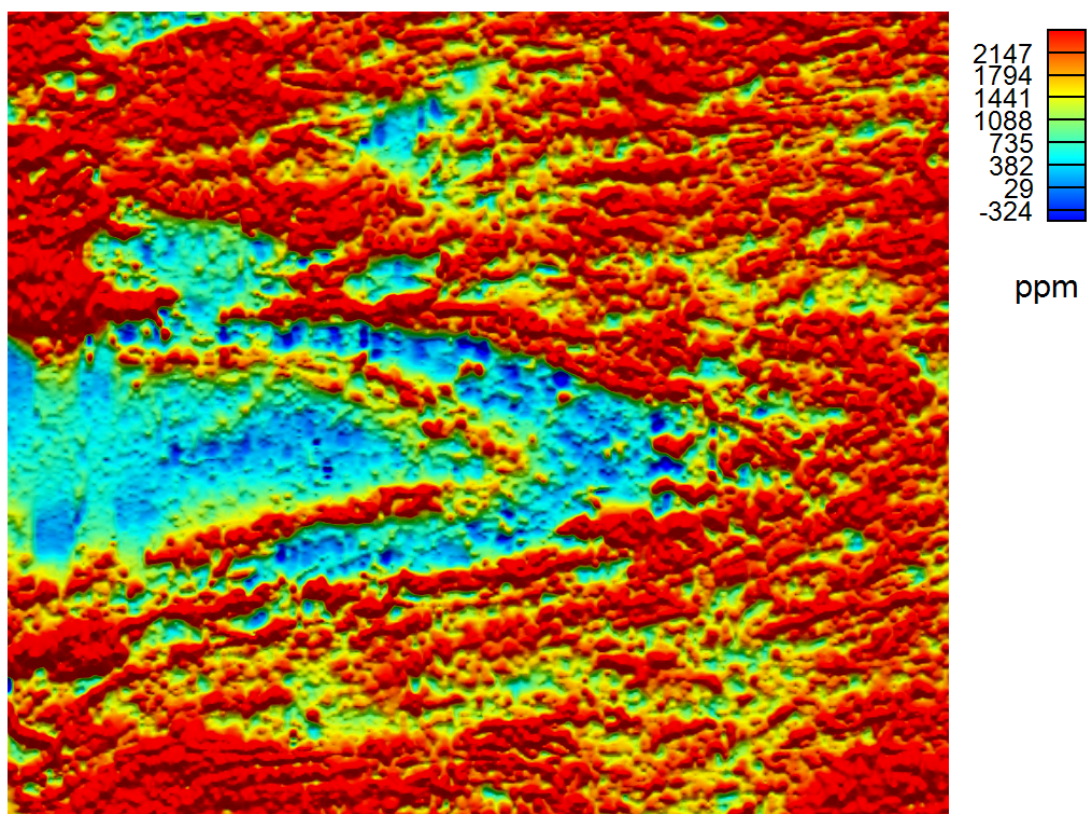
*Appendix 2: Figure 25. Castle Island: Imaginary component, 3 kHz*



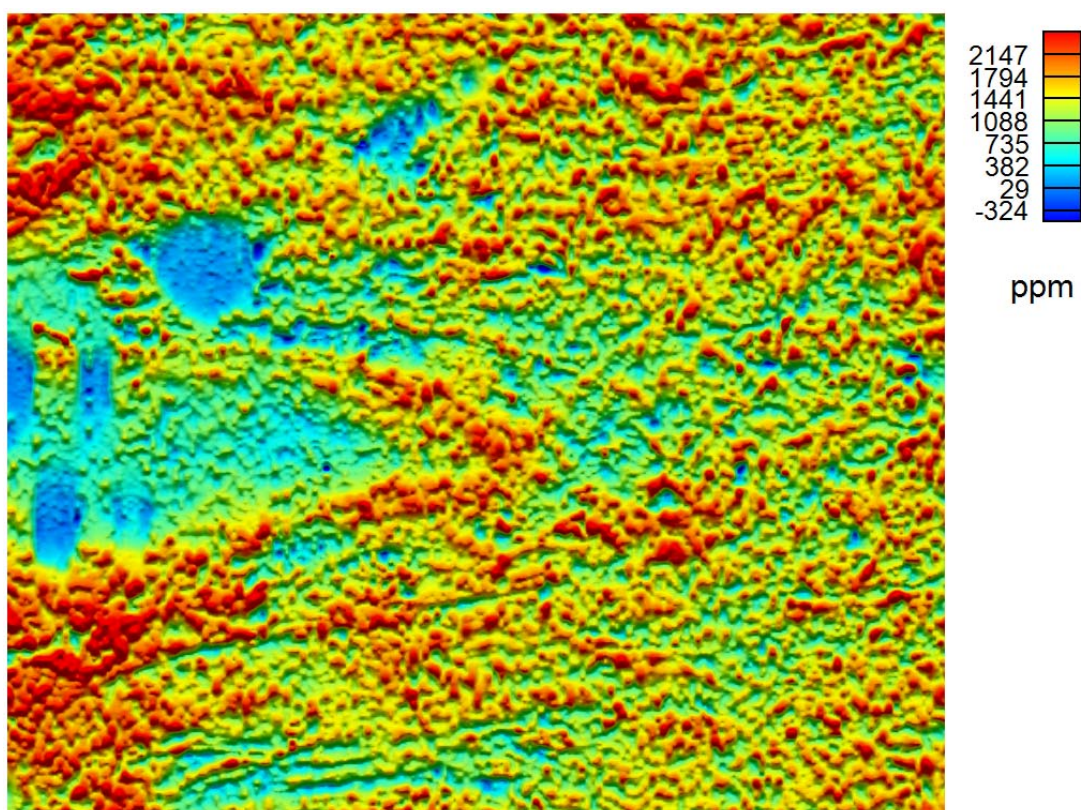
Appendix 2: Figure 26. Castleisland: Real component, 12 kHz



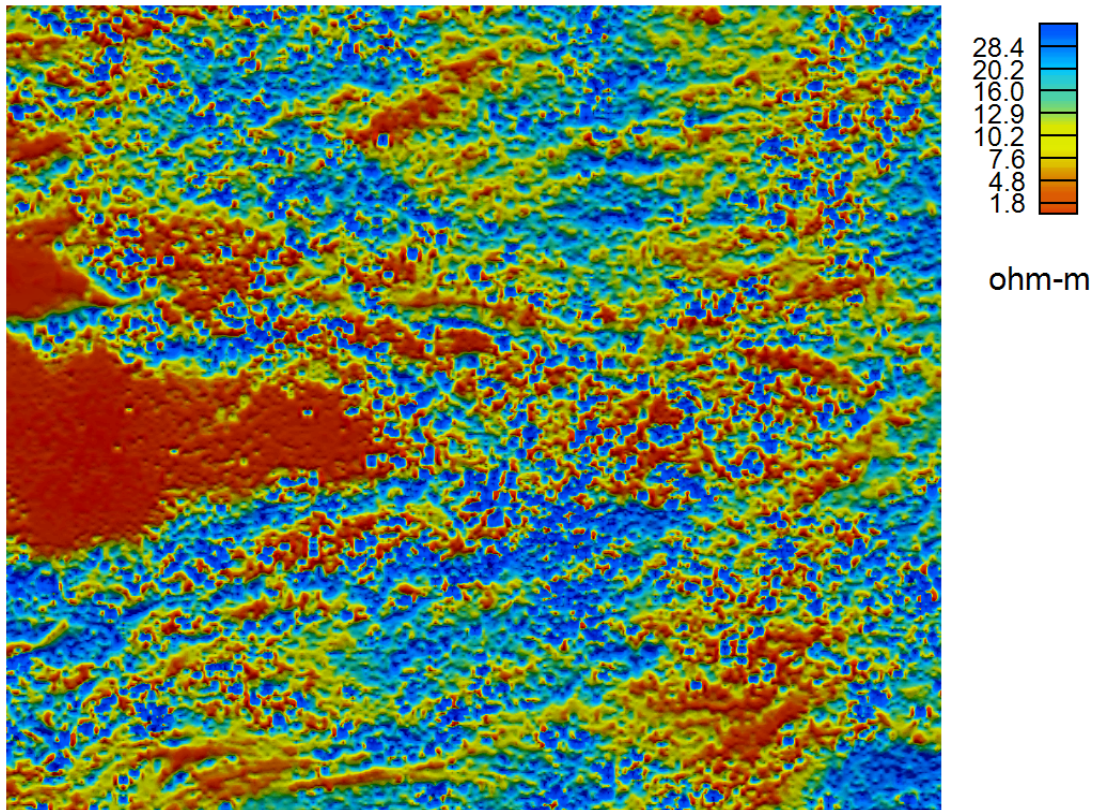
Appendix 2: Figure 27. Castleisland: Imaginary component, 12 kHz



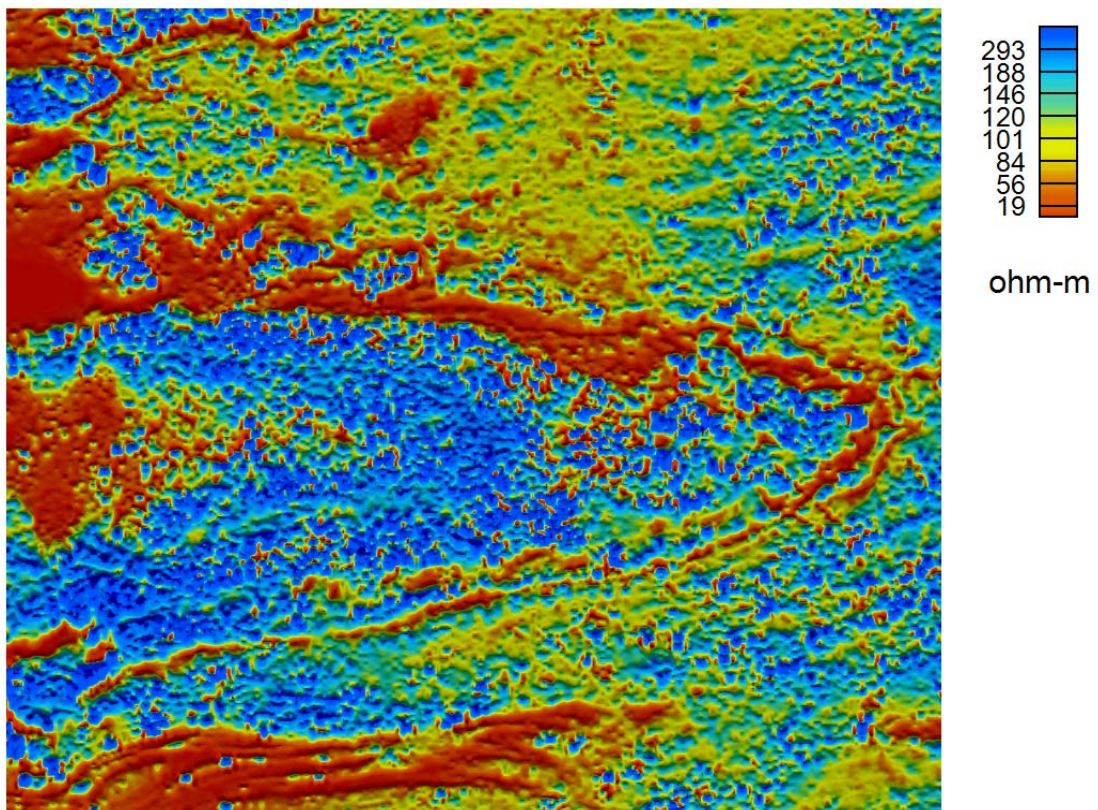
Appendix 2: Figure 28. Castle Island: Real component, 24.5 kHz



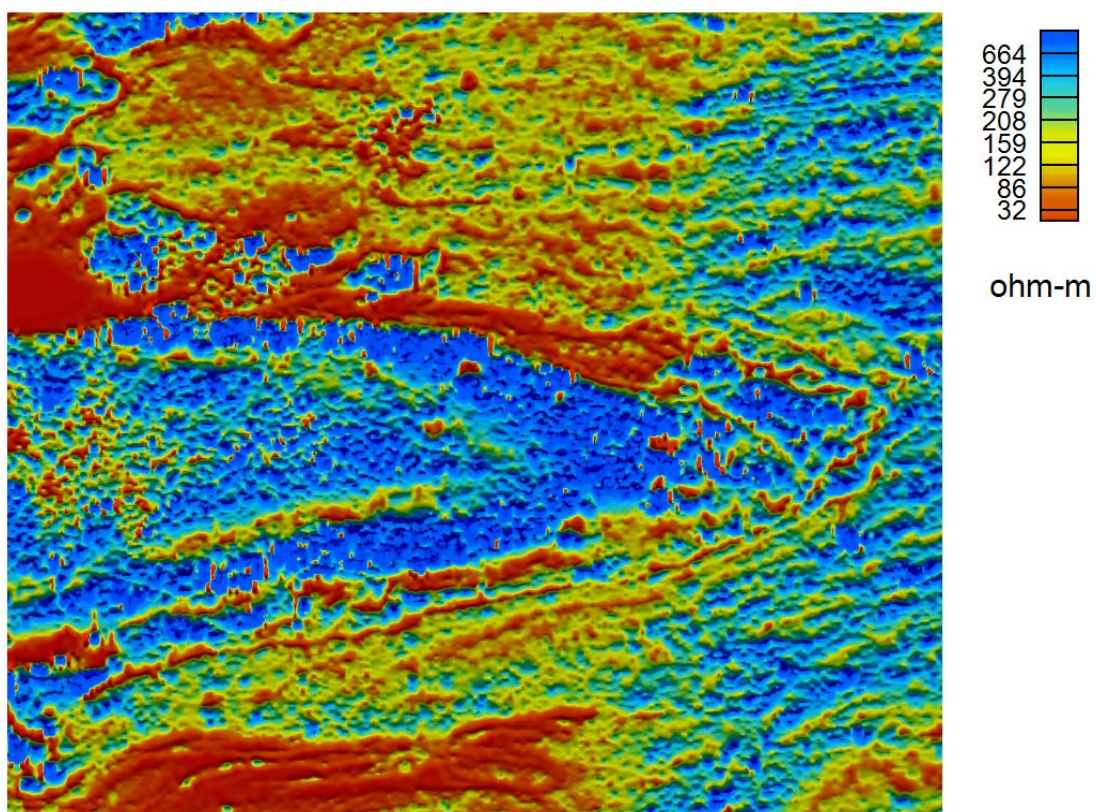
Appendix 2: Figure 29. Castle Island: Imaginary component, 24.5 kHz



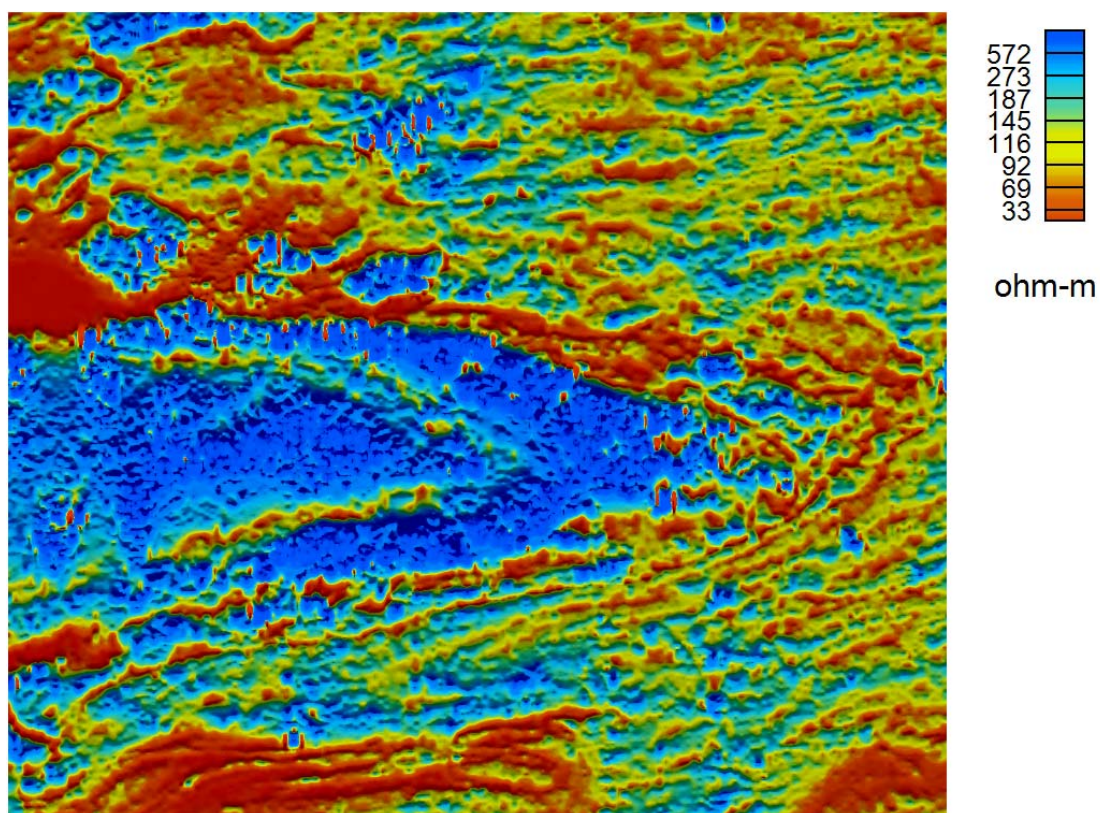
Appendix 2: Figure 30. Castleisland: Apparent resistivity, 0.9 kHz



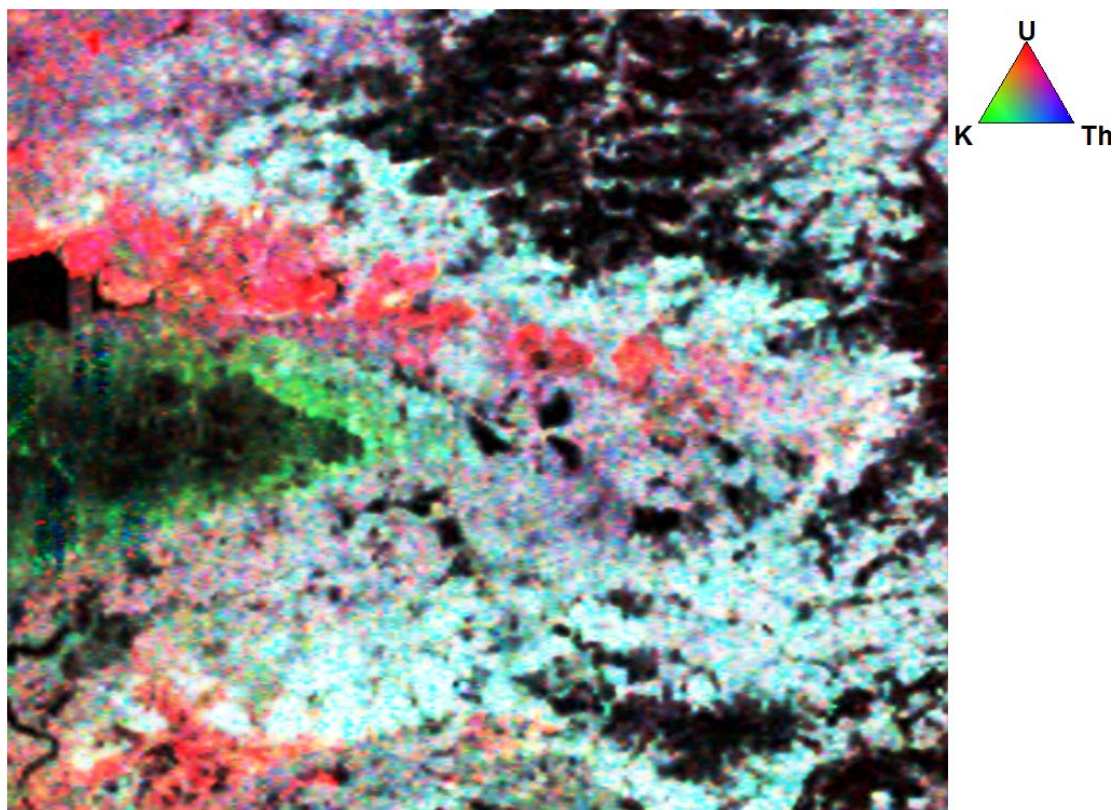
Appendix 2: Figure 31. Castleisland: Apparent resistivity, 3 kHz



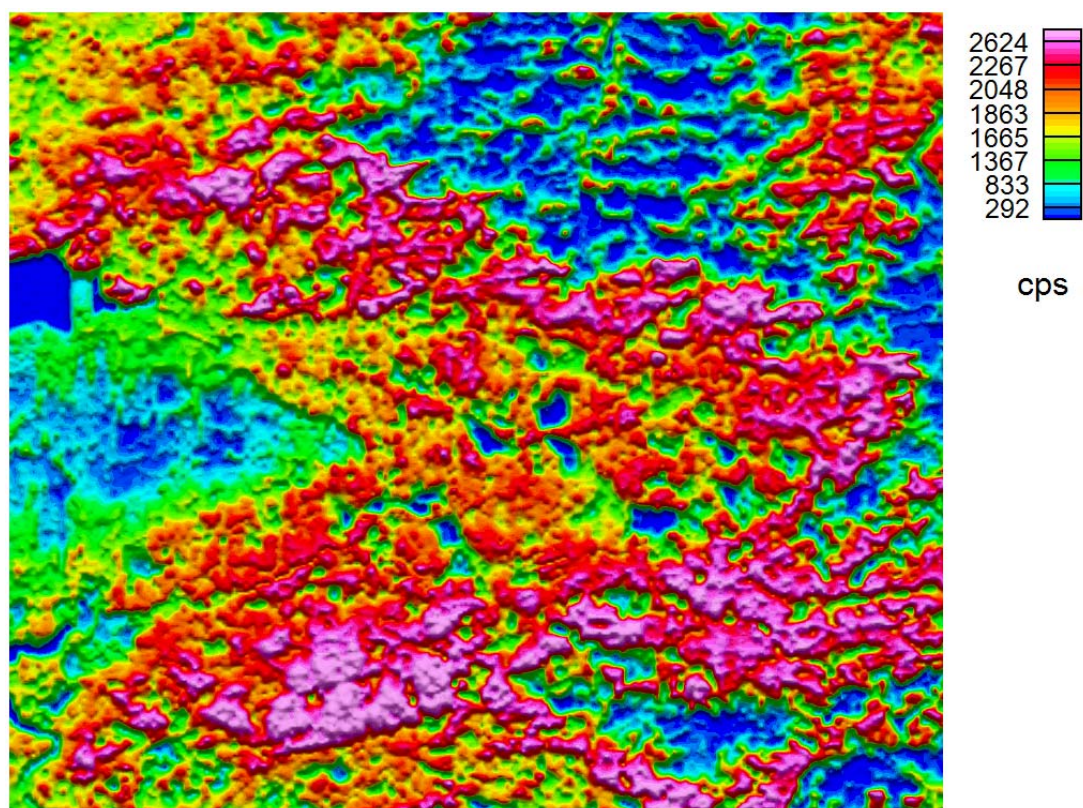
Appendix 2: Figure 32. Castle Island: Apparent resistivity, 12 kHz



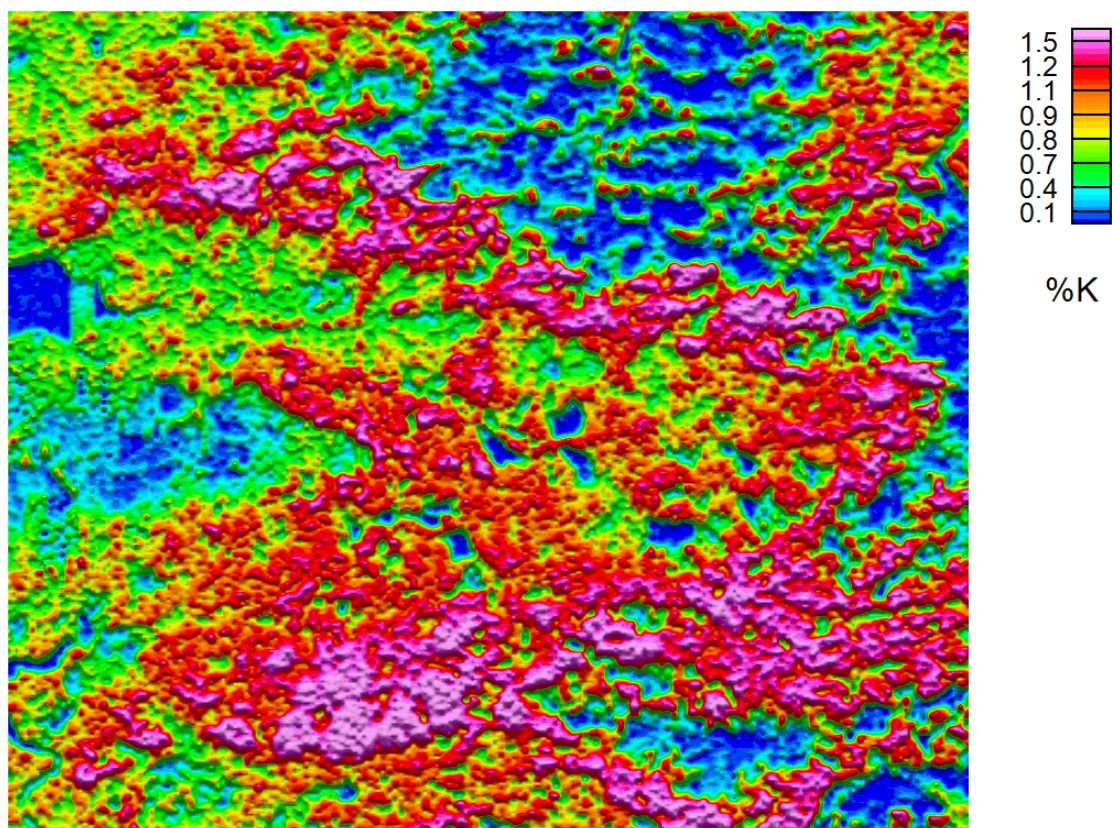
Appendix 2: Figure 33. Castle Island: Apparent resistivity, 24.5 kHz



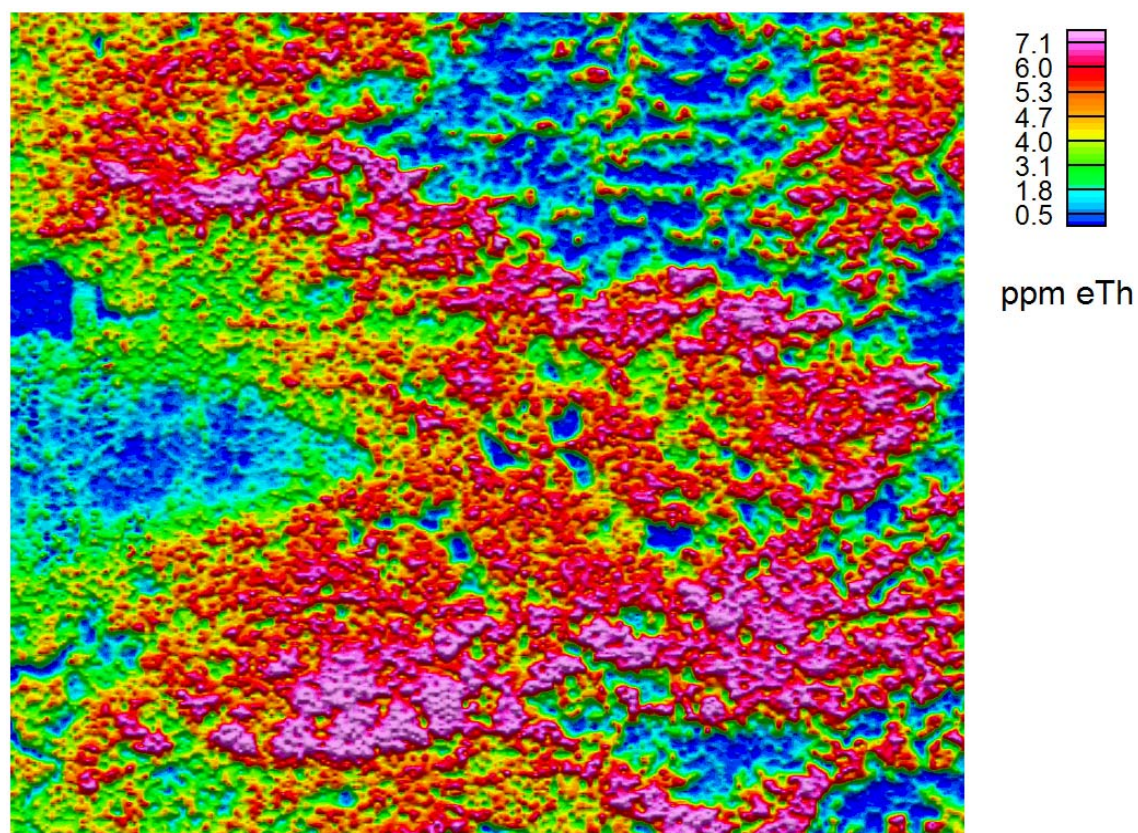
Appendix 2: Figure 34. Castleisland: Radiometric ternary image



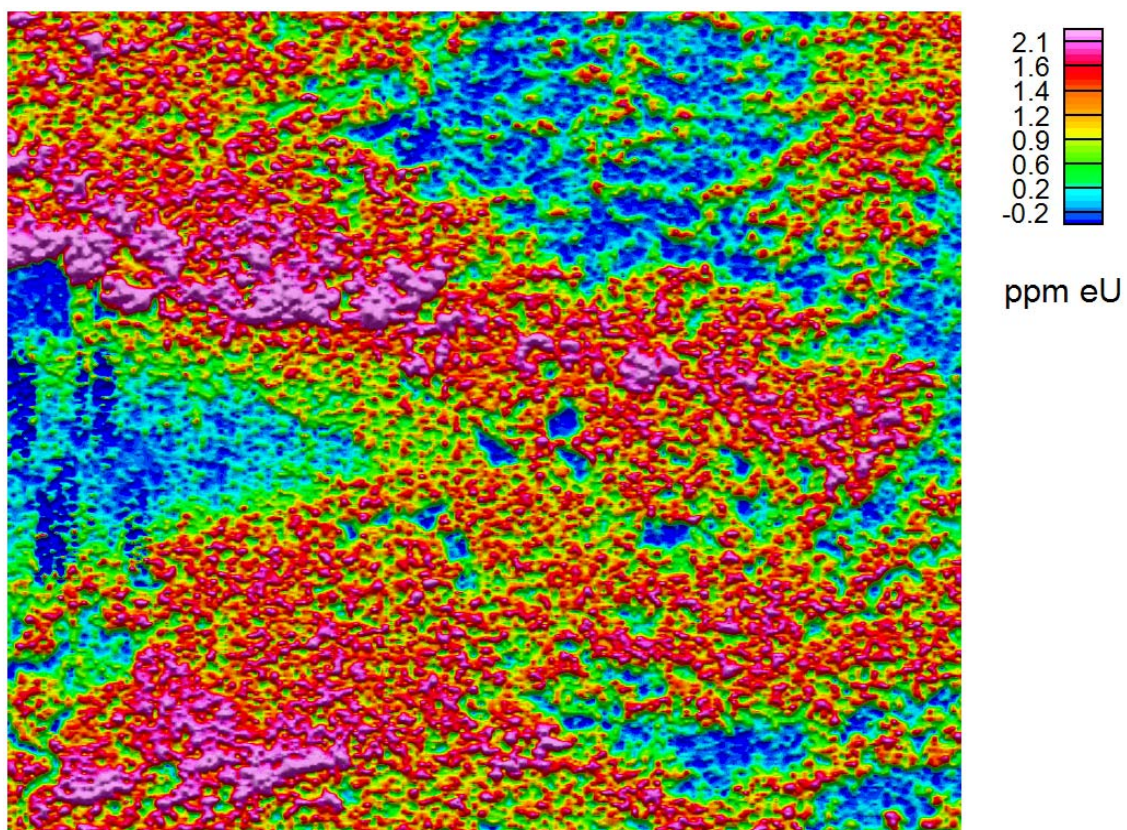
Appendix 2: Figure 35. Castleisland: Total radiation



Appendix 2: Figure 36. Castleisland: Potassium concentration

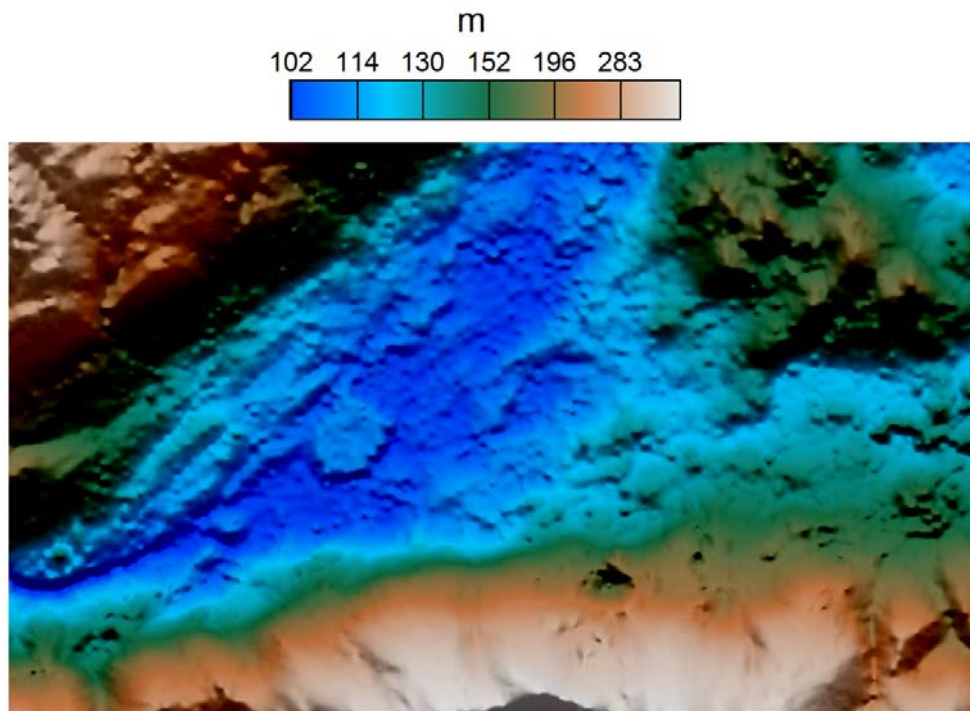


Appendix 2: Figure 37. Castleisland: Thorium concentration

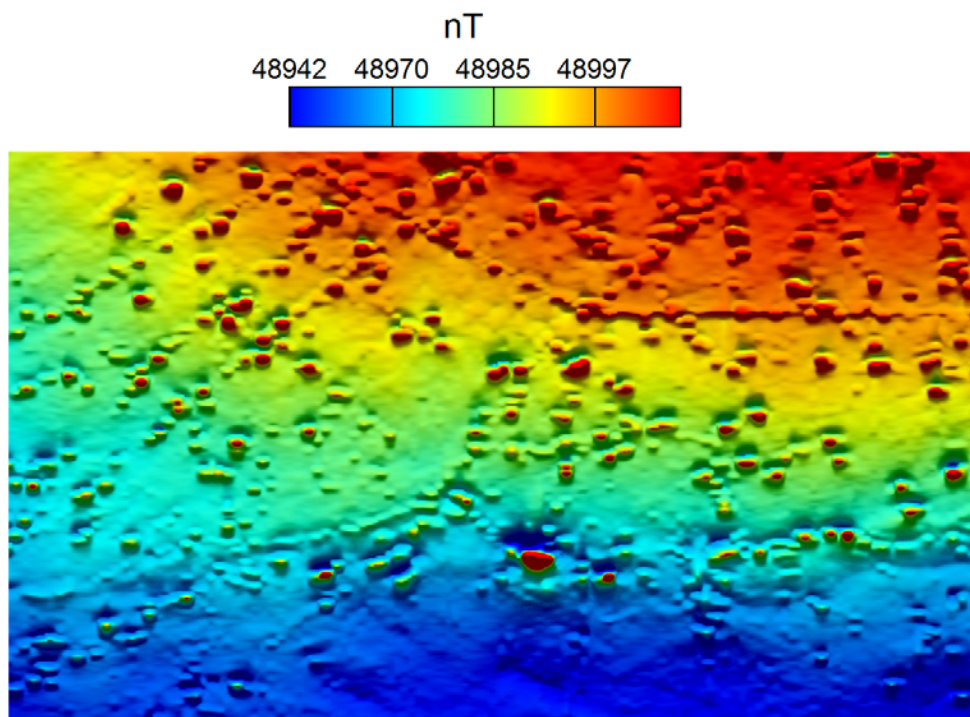


*Appendix 2: Figure 38. Castleisland: Uranium concentration*

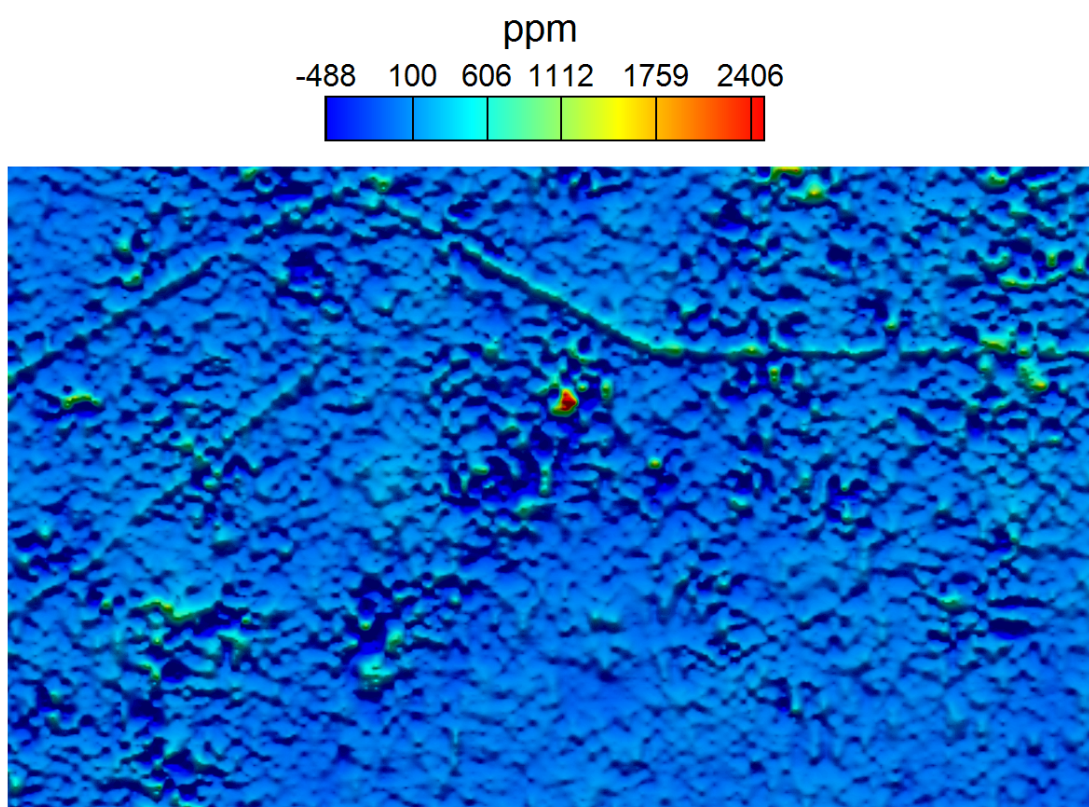
## SILVERMINES



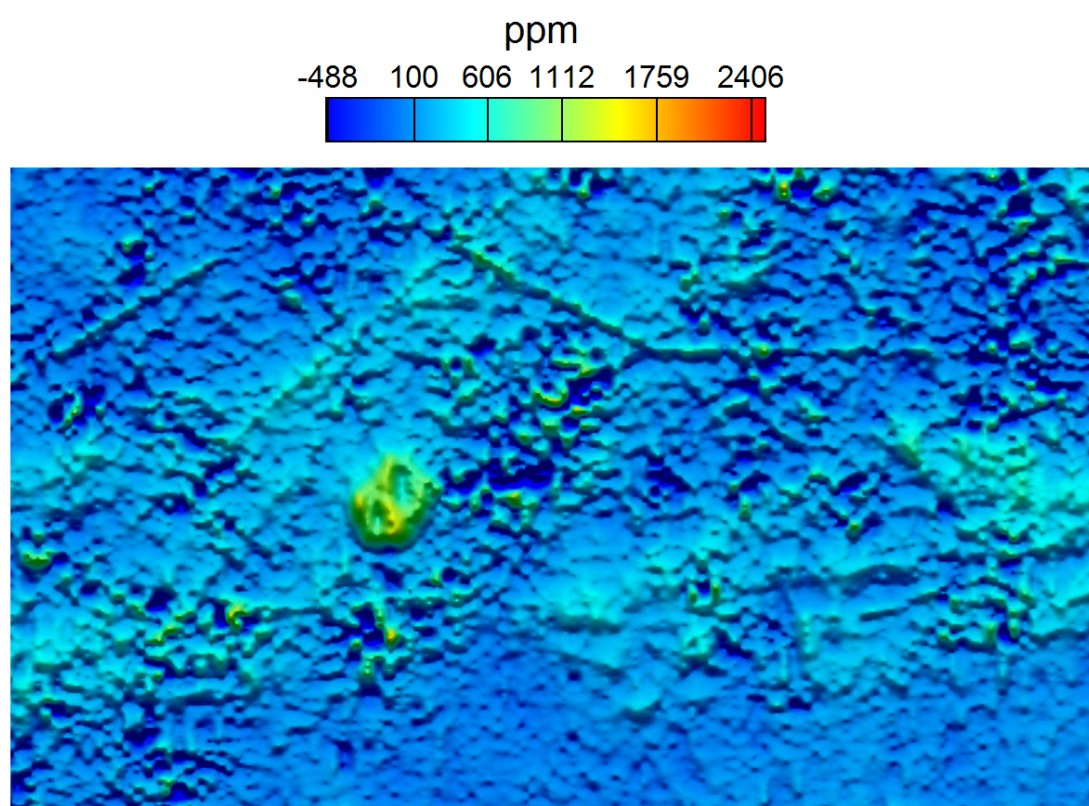
*Appendix 2: Figure 39. Silvermines: Digital terrain model*



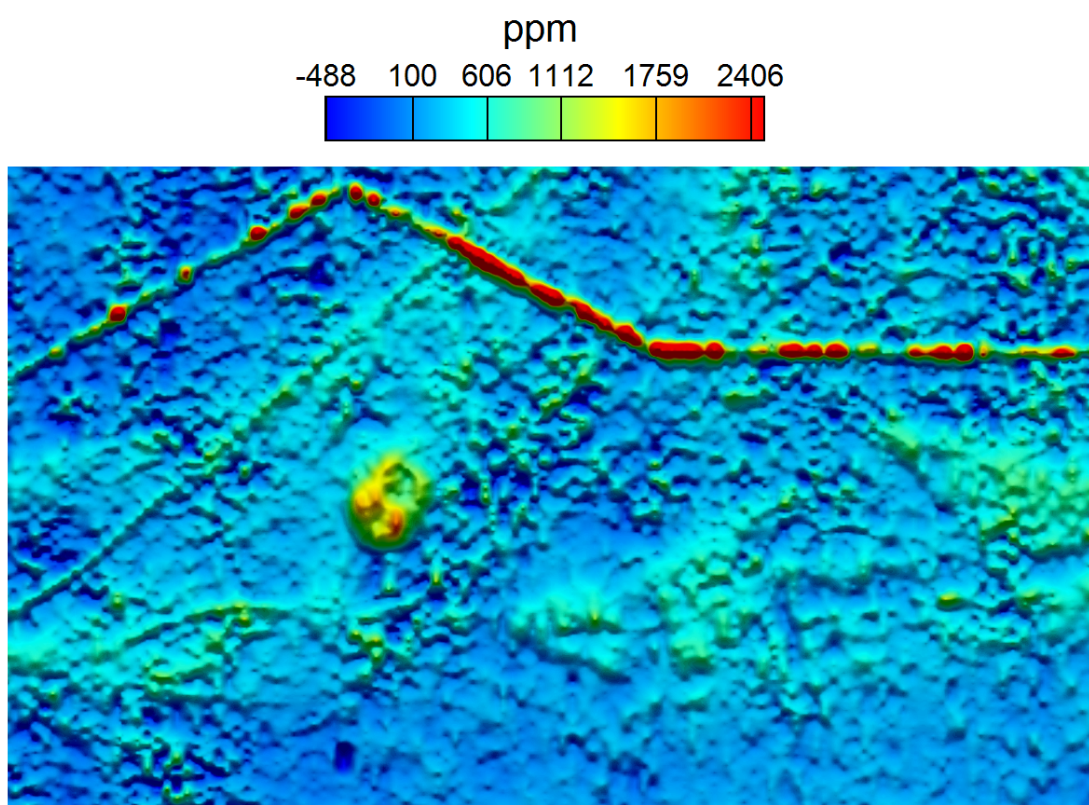
*Appendix 2: Figure 40. Silvermines: Total magnetic intensity*



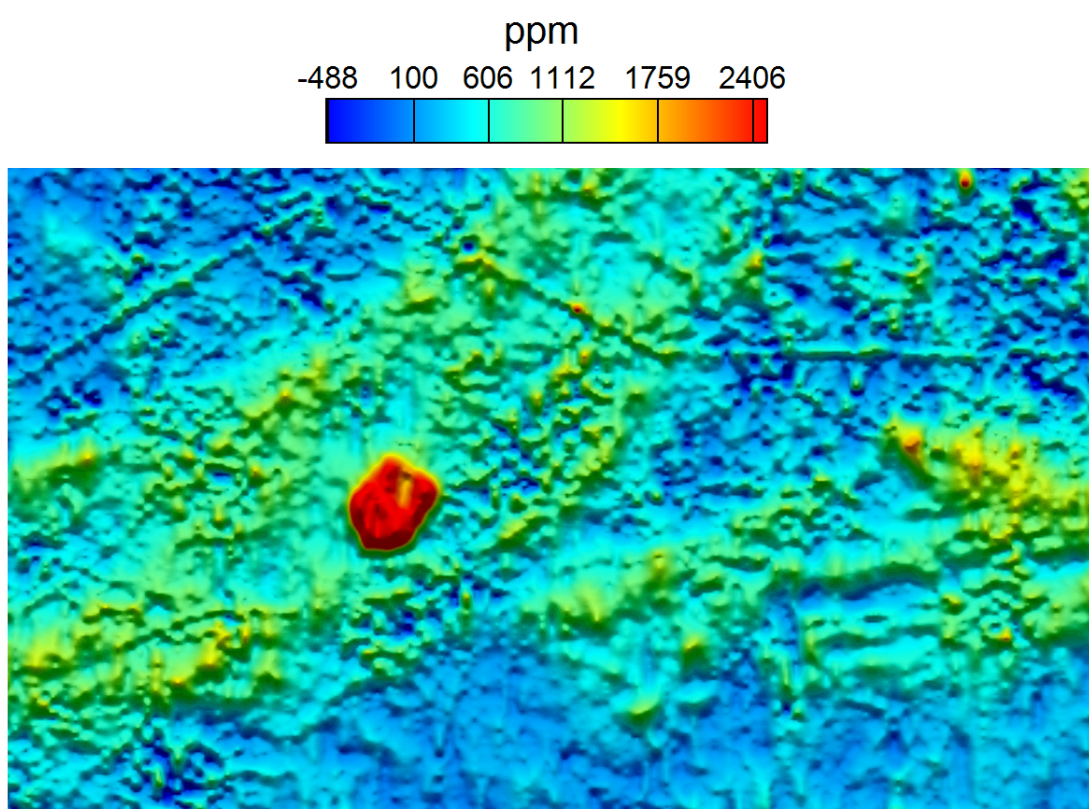
*Appendix 2: Figure 41. Silvermines: Real component, 0.9 kHz*



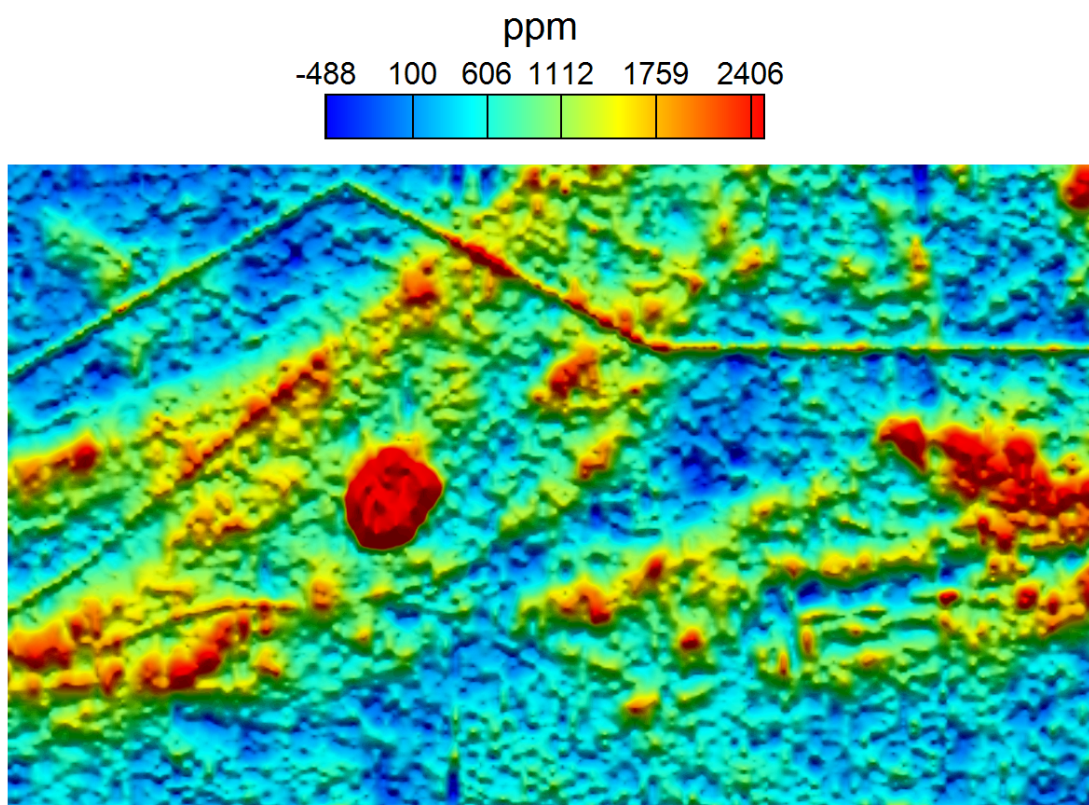
*Appendix 2: Figure 42. Silvermines: Imaginary component, 0.9 kHz*



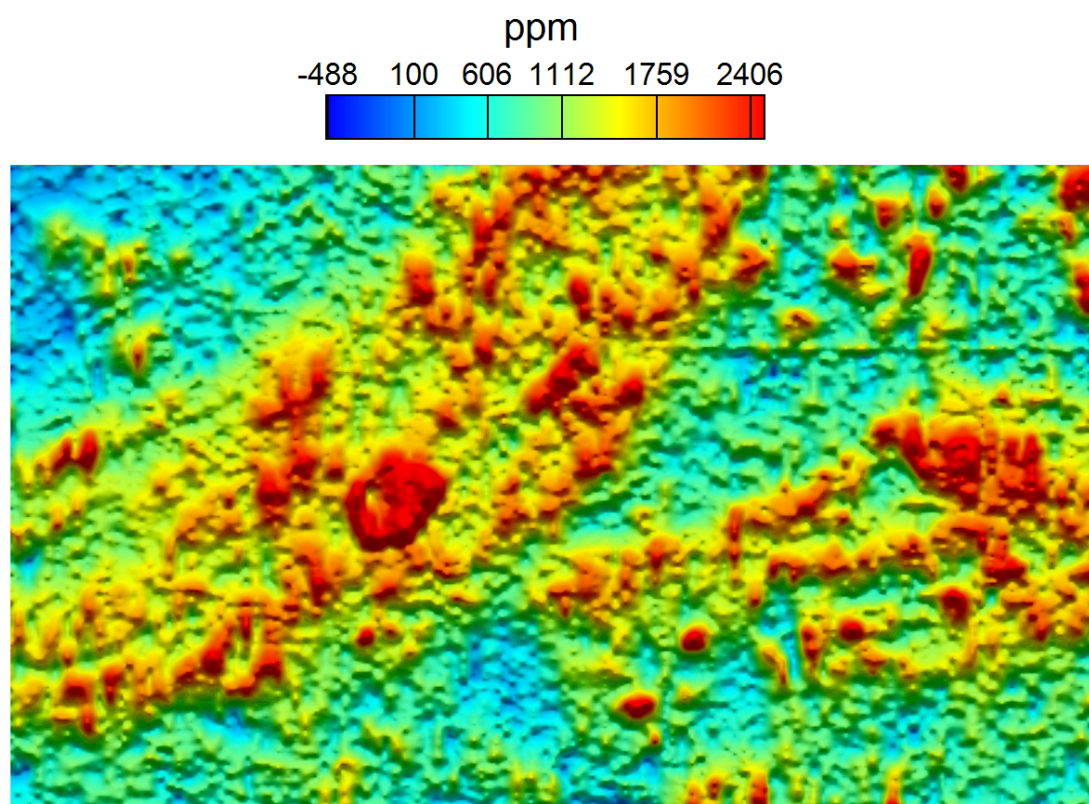
Appendix 2: Figure 43. Silvermines: Real component, 3 kHz



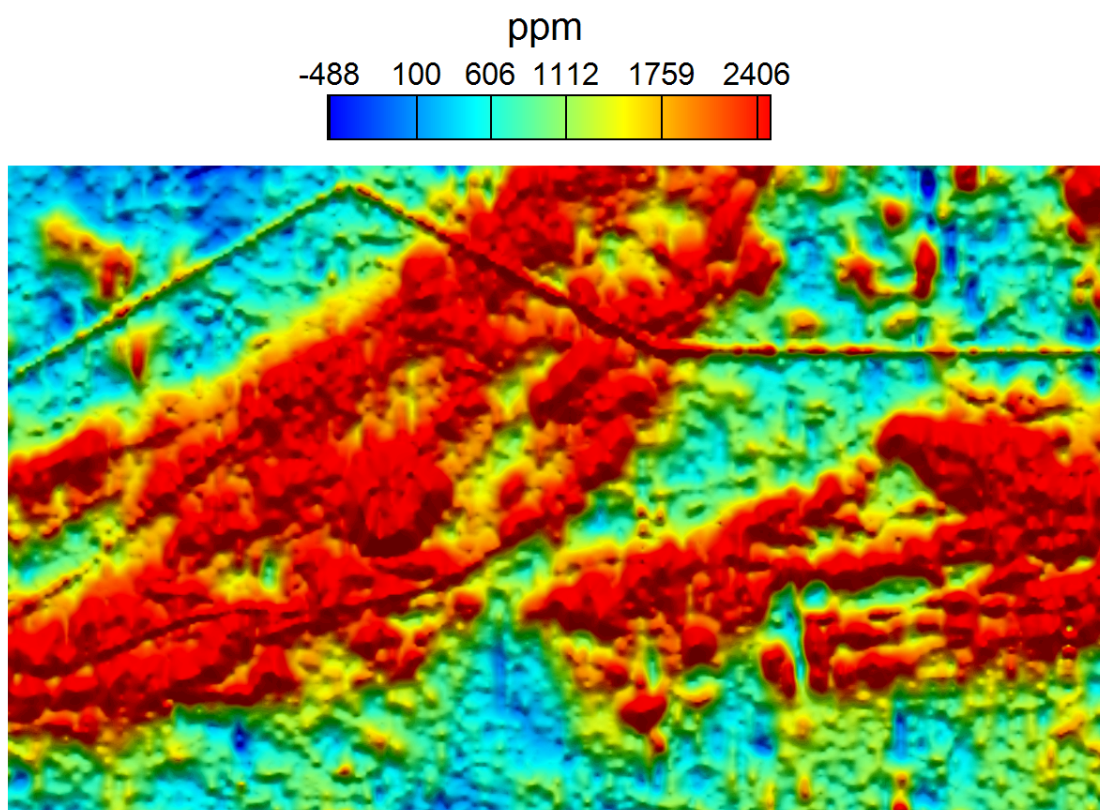
Appendix 2: Figure 44. Silvermines: Imaginary component, 3 kHz



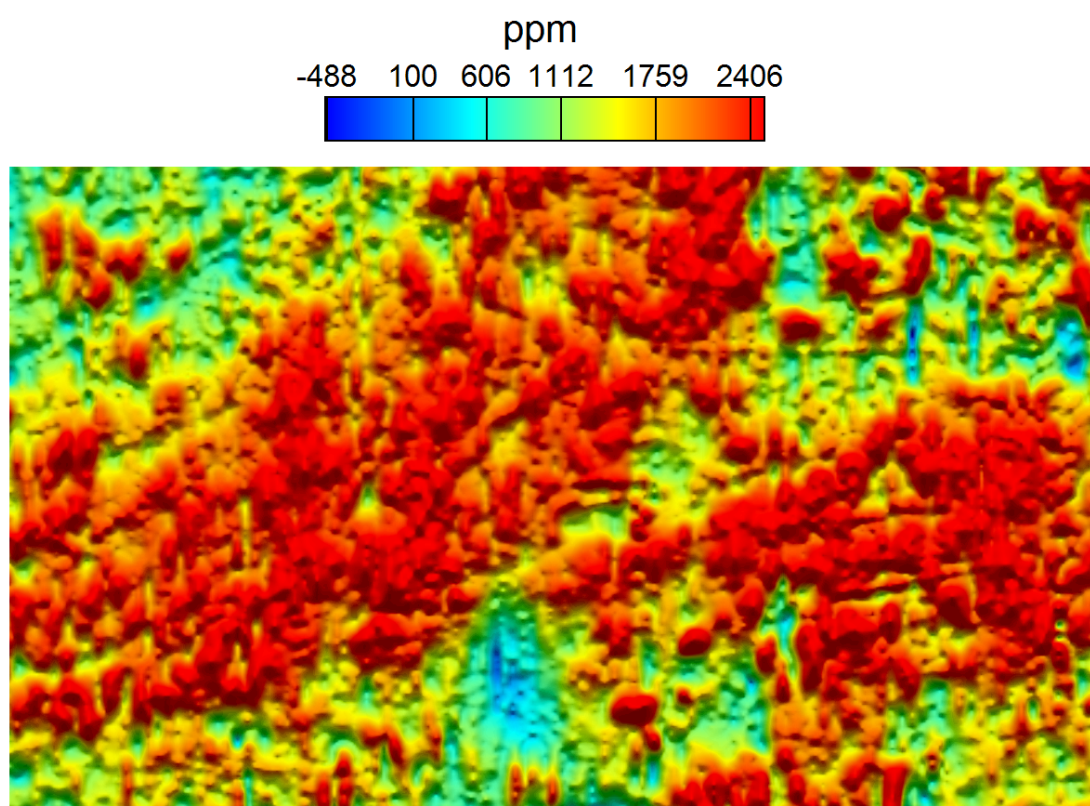
*Appendix 2: Figure 45. Silvermines: Real component, 12 kHz*



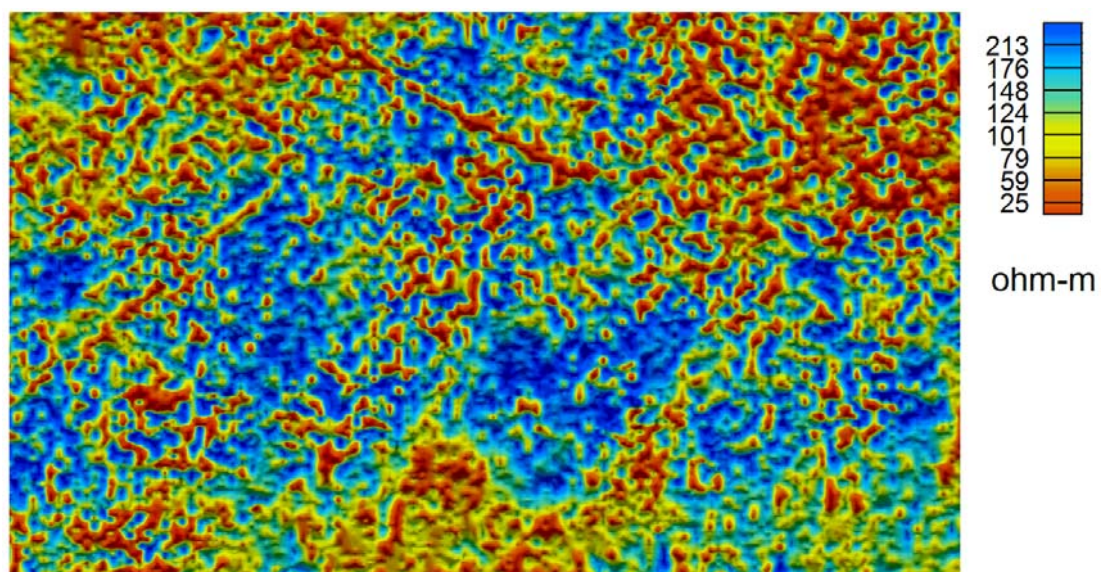
*Appendix 2: Figure 46. Silvermines: Imaginary component, 12 kHz*



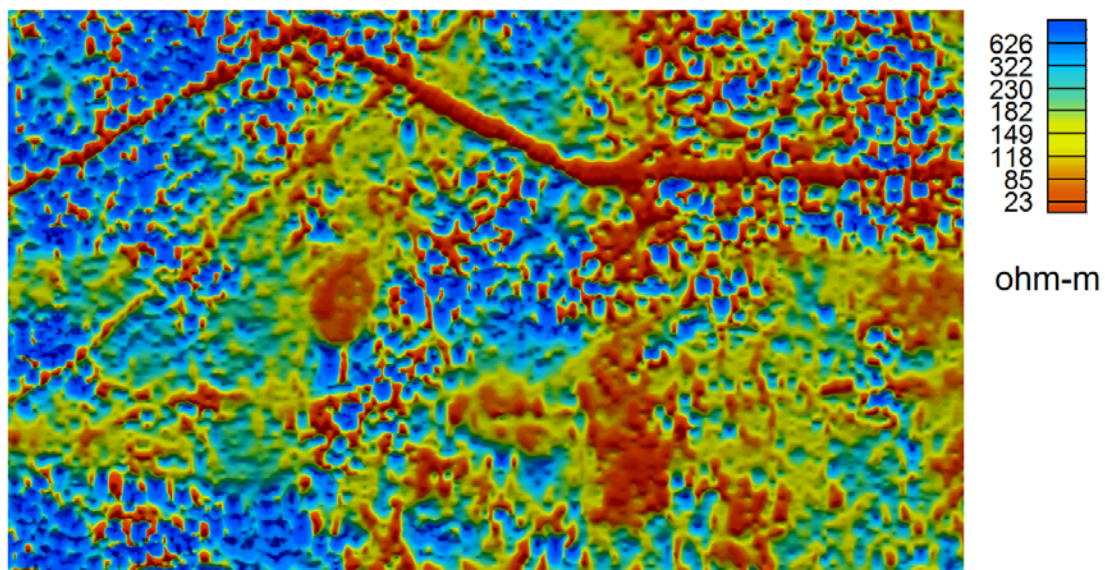
Appendix 2: Figure 47. Silvermines: Real component, 24.5 kHz



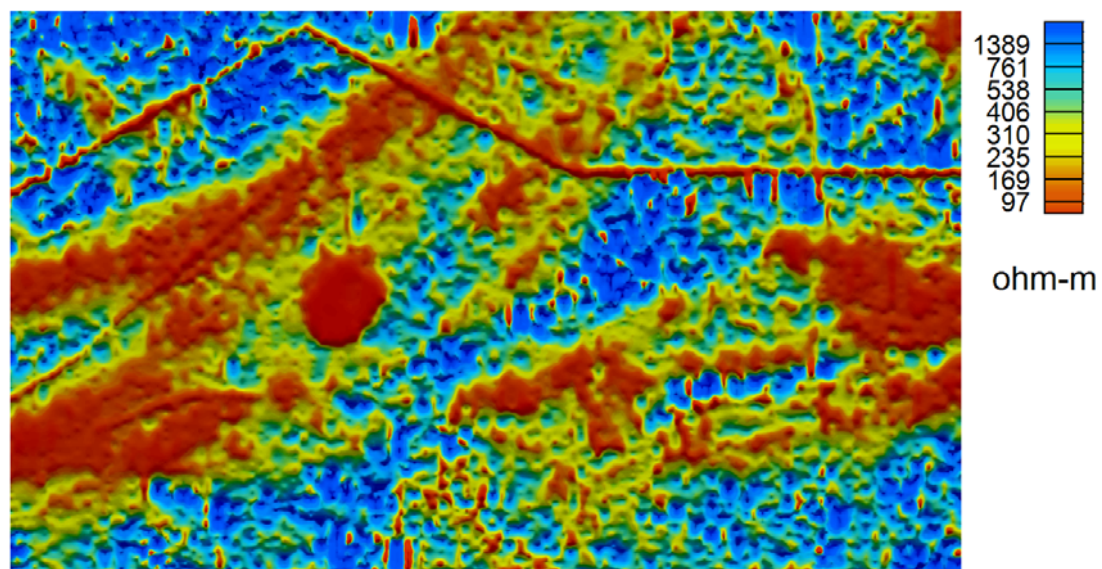
Appendix 2: Figure 48. Silvermines: Imaginary component, 24.5 kHz



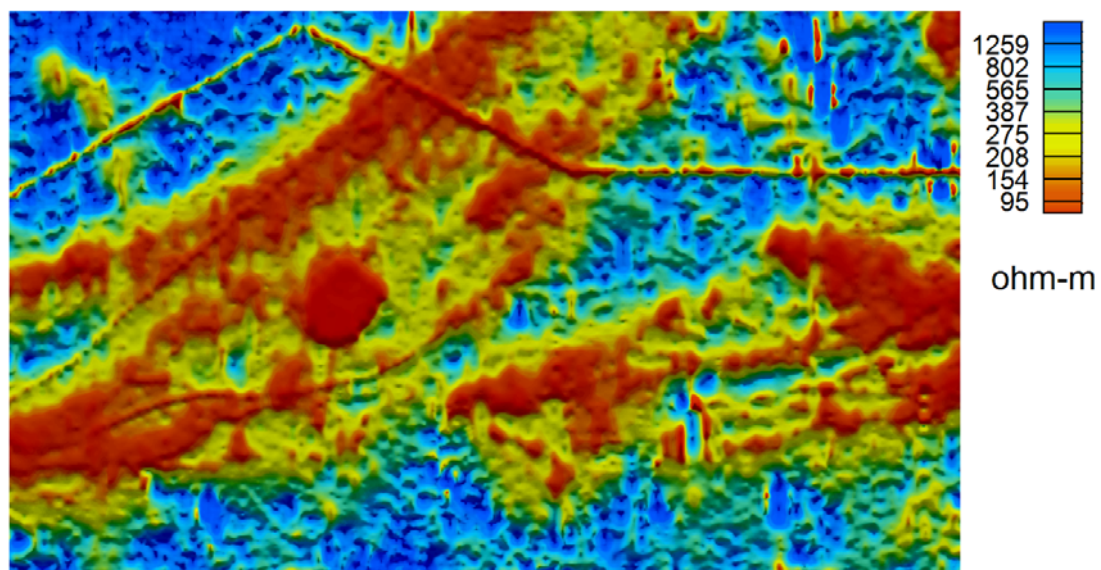
Appendix 2: Figure . Silvermines: Apparent resistivity, 0.9 kHz



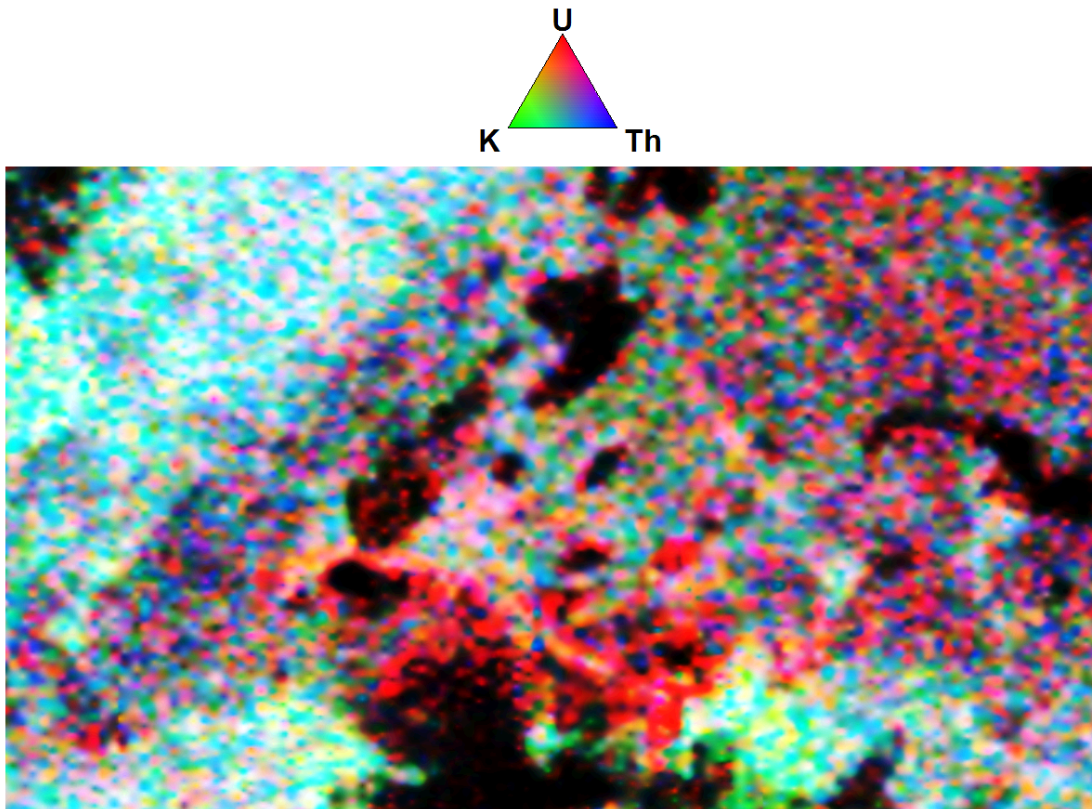
*Appendix 2: Figure 49. Silvermines: Apparent resistivity, 3 kHz*



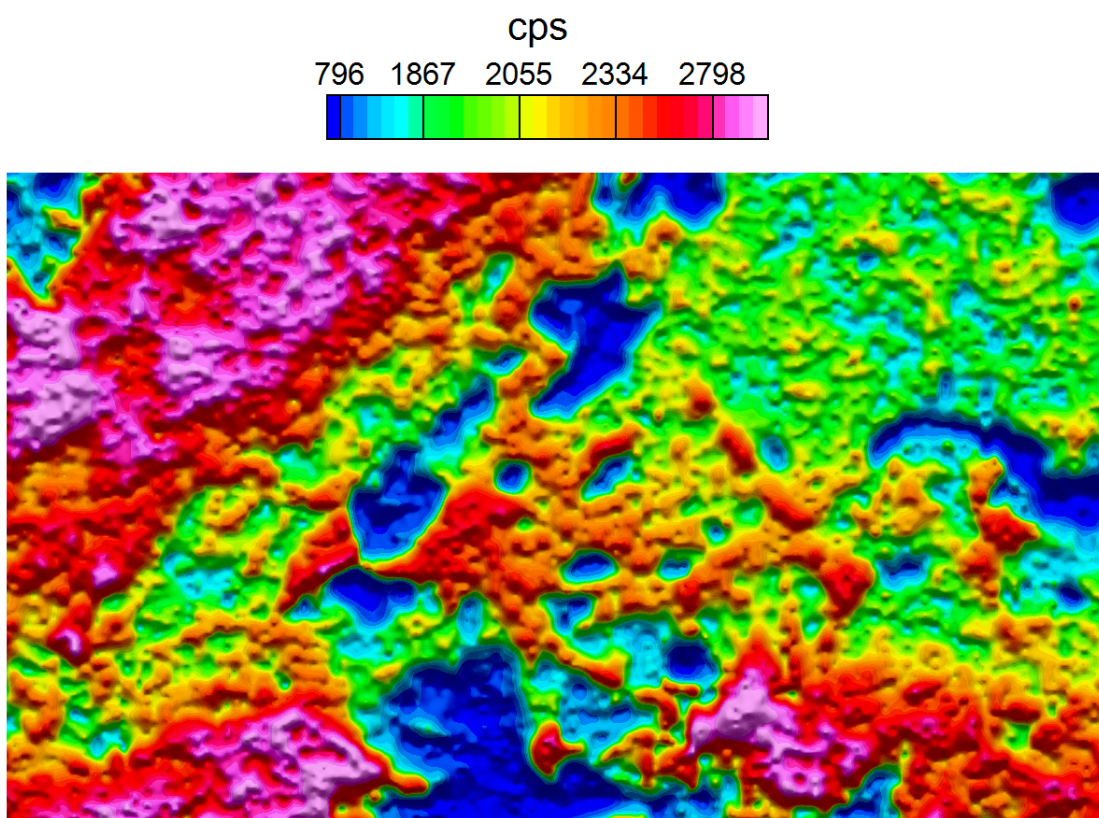
*Appendix 2: Figure 50. Silvermines: Apparent resistivity, 12 kHz*



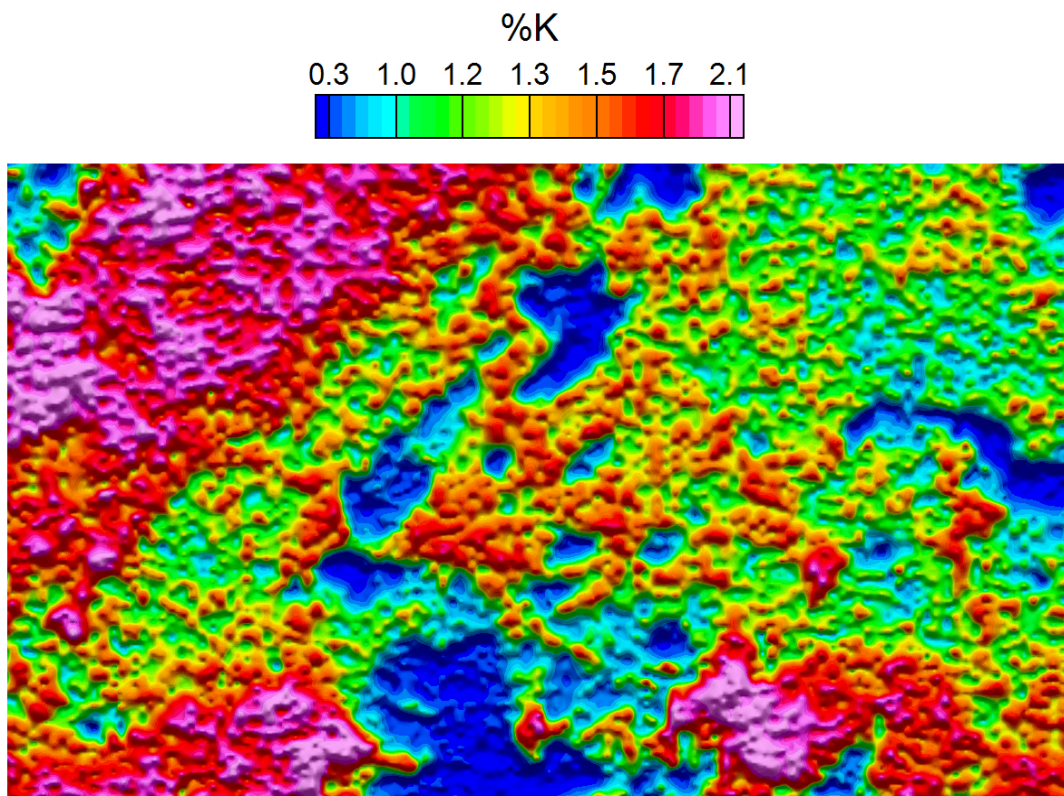
*Appendix 2: Figure 51. Silvermines: Apparent resistivity, 24.5 kHz*



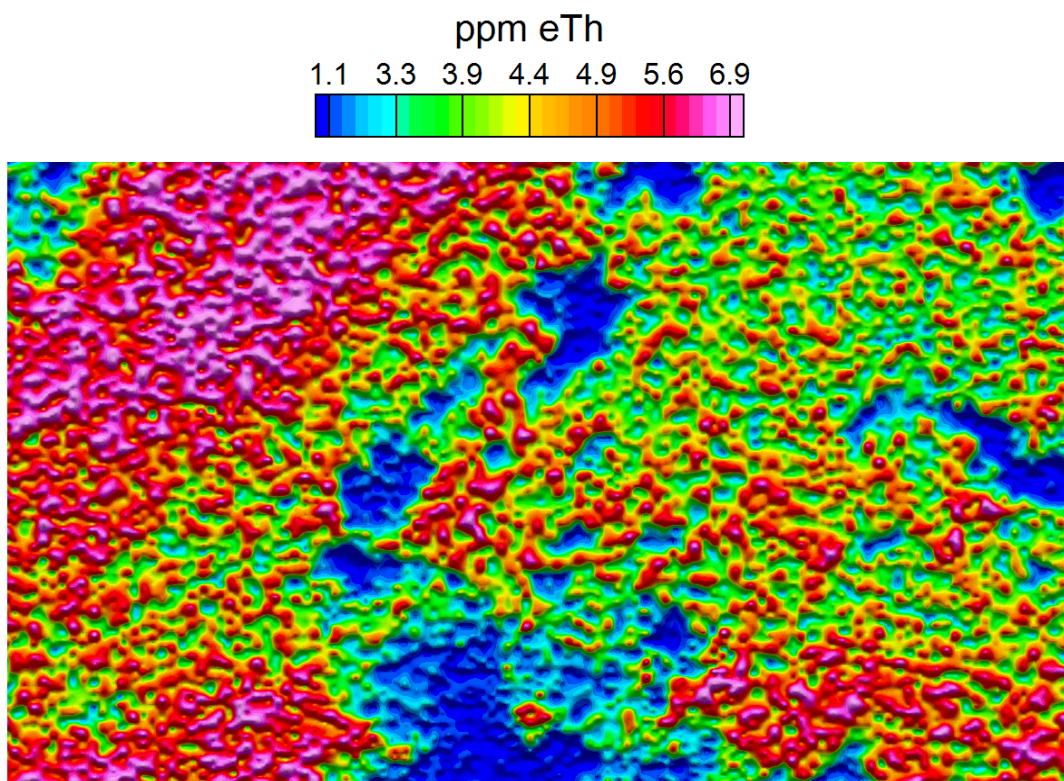
Appendix 2: Figure 52. Silvermines: Radiometric ternary image



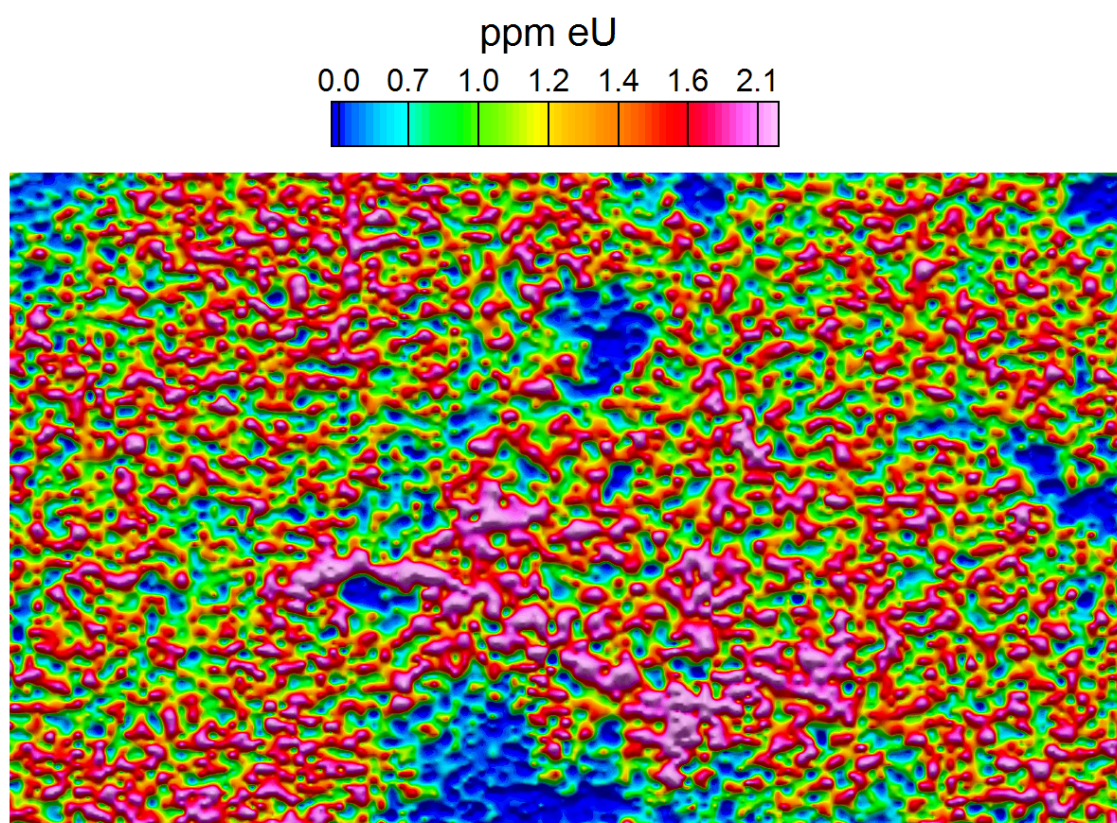
Appendix 2: Figure 53. Silvermines: Total radiation



*Appendix 2: Figure 54. Silvermines: Potassium concentration*



*Appendix 2: Figure 55. Silvermines: Thorium concentration*

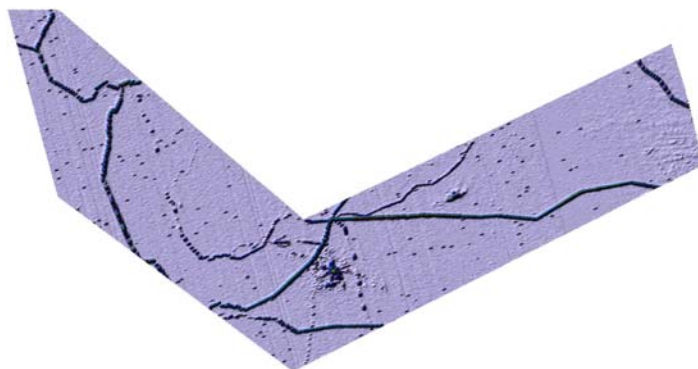
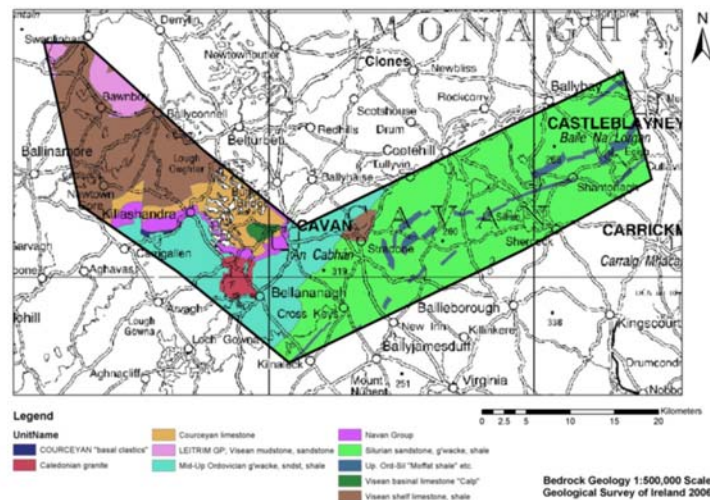


*Appendix 2: Figure 56. Silvermines: Uranium concentration*

## Appendix 3: Comments on the data

This Appendix provides some brief comments on the magnetic and radiometric images shown in Appendix 2. Rather than review the EM data in its entirety, images of half-space apparent conductivity are shown at 25 and 12 kHz, at two scales. Again comments are presented for the Cavan, Castleisland and Silvermines survey areas in turn.

### CAVAN-MONAGHAN-LEITRIM



Appendix 3: Figure 1. Upper: Bedrock geology. Lower: Power line monitor response.

### Cavan-Monaghan-Leitrim: Magnetics. With reference to Appendix 2: Figure 2.

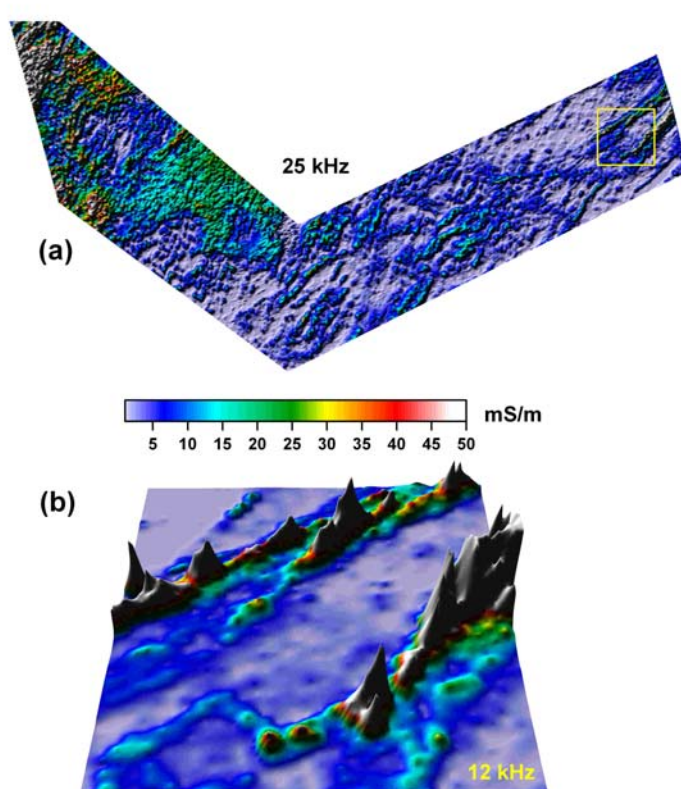
At the scale used, cultural perturbations, although they exist and are pervasive, are not prominent. The long wavelength feature in the west appears in association with the Carboniferous basin. The main easterly gradients appear to track the SE margin. Within this feature, at least two 'dyke' structures trend E-W across the whole survey area. The Caledonian granite is associated with highly detailed magnetic variation signatures. To the east of this feature, and centrally within the area, a number of

localised low amplitude structures are apparent. Regional scale, quasi-linear features occur throughout the eastern-most area in association with the Caledonian foreland.

### **Cavan-Monaghan-Leitrim: Radiometrics. With reference to Appendix 2: Figure 15 and Appendix 2: Figure 16**

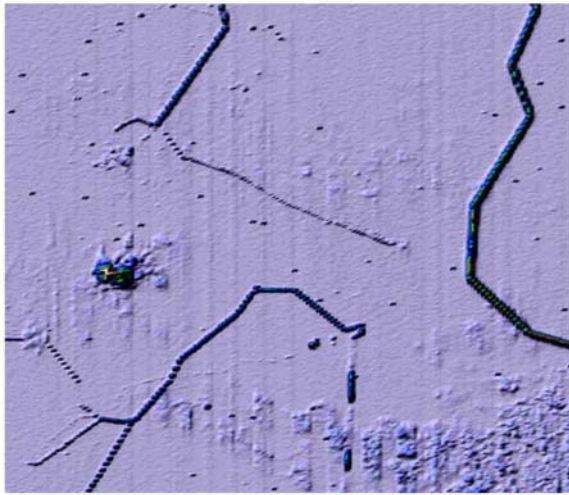
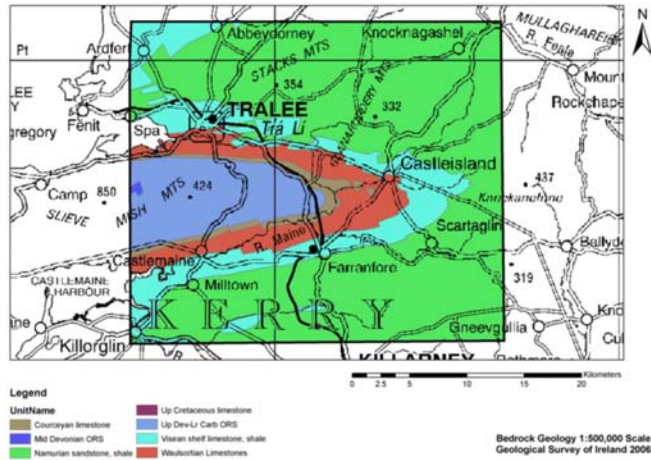
The Total Count image indicates a broad correlation with the bedrock units. In particular, the Caledonian foreland displays relatively high activity. The central Ordovician greywackes are reflected in consistent mid-range activity levels. Lows are apparent across the lake system. Geological low responses are observed in association with the Leitrim Group. Uranium activity becomes prevalent towards the west.

### **Cavan-Monaghan-Leitrim: Electromagnetics.**



*Appendix 3: Figure 2. EM Conductivity. (a) Apparent conductivity at 25 kHz for the whole survey. In the east, low conductivities ( $< 5$  mS/m) are associated with the Silurian greywacke sequence. Superimposed are sinuous conductive zones showing both trends and fabric. Typically these would be interpreted as shales. In the far east, a more conductive (towards 50 mS/m) band of cohesive ribbon-like conductors is observed. These have been interpreted (speculatively) as the Moffat shales which may be concealed (in part). The signature observed is repeated across the Caledonian foreland of Northern Ireland (Tellus project). In the west, elevated conductivities are associated with the Courcayan limestone while the Caledonian granite appears as a low conductivity zone due to the tight, low porosity matrix of the constituent rocks. (b) a 6x6 km detail defined by the square shown in (a). 12 kHz apparent conductivity shown as a perspective view from south to north.*

## CASTLEISLAND



*Appendix 3: Figure 3. Upper: Bedrock geology. Lower: Power Line monitor response*

### **Castleisland: Magnetics. With reference to Appendix 2: Figure 21**

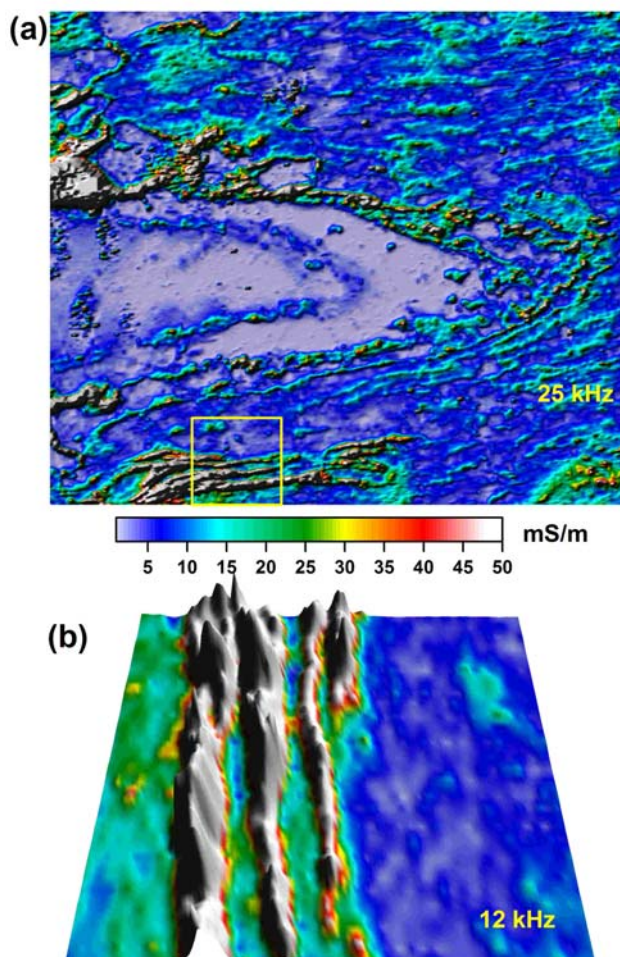
The high amplitude E-W axis follows the central high ground of the Slieve Mish mountains. The broad response of major gradients follows and outlines the geological trend of the anticline. Away from this dominant feature, some of the lower amplitude trends (semi-persistent arcuate features) can also be seen in the conductivity results presented later. The level of cultural perturbation is high and this results in a masking of low amplitude data features, when viewed at this scale.

### **Castleisland: Radiometrics. With reference to Appendix 2: Figure 34 and Appendix 2: Figure 35**

A comparison of the Total Count and Ternary images reveals that both provide useful summary interpretation information. The western wedge of low values occurs in association with the central Upper Devonian-Lower Carboniferous unit. This low can be seen to translate to higher activity levels (particularly in Uranium) in association

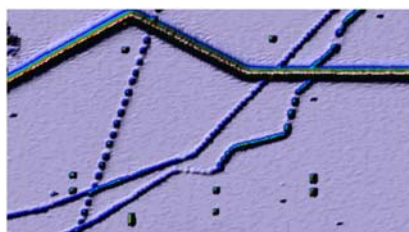
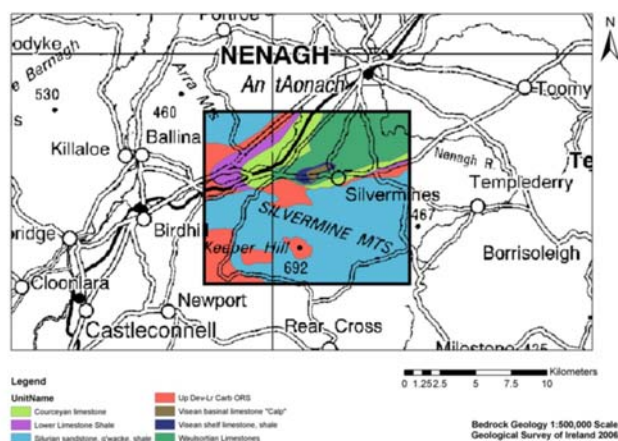
with the Viséan shale sequence. In detail, the radiometric data reveal complex patterns that require further investigation.

### Castleisland: Electromagnetics.



*Appendix 3: Figure 4. EM Conductivity. (a) Apparent conductivity at 25 kHz for the whole survey. Two areas of high conductivity seawater appear in the west. Perturbations due to power lines/roads appear to be minimal. The central zone, associated with the Upper Devonian-Lower Carboniferous unit, displays low conductivities. Again, Courceyan limestone may be identified with slightly enhanced conductivities, within this zone. A conductivity fabric/grain across the whole area is apparent. Various conductivity amplitudes may be associated with variations in depth below ground surface. A coherent set of conductors appear in the south (e.g. the 5x5 km square). These conductors have a distinct signature. An association between these conductors and the location of the Variscan Front is possible (speculative). (b) a 5x5 km detail defined by the square shown in (a). 12 kHz apparent conductivity shown as a perspective view from east to west.*

## SILVERMINES



Appendix 3: Figure 5. Upper: Bedrock geology. Lower: Power Line monitor response.

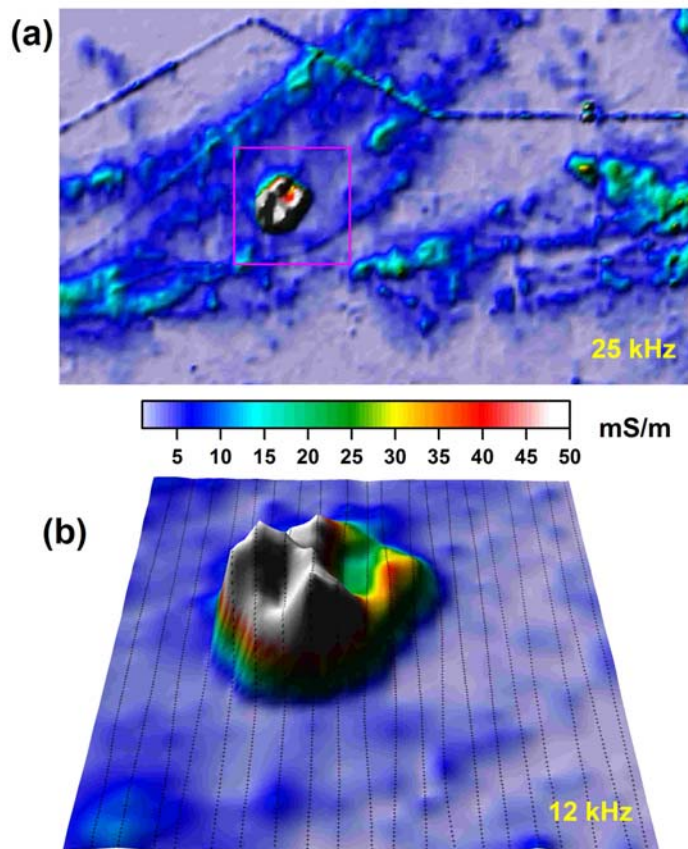
### Silvermines: Magnetics. With reference to Appendix 2: Figure 40.

The magnetic response across this small area is dominated by a N-S regional gradient. Further comments would require a more detailed investigation. Due to the scale used, cultural perturbations are very evident. An overlay of the topographic map on the magnetic image (not shown) indicates a close correlation between buildings/structures/power-line and localised distortions. The railway also produces a small perturbation at various locations along its length.

### Silvermines: Radiometrics. With reference to Appendix 2: Figure 52 and Appendix 2: Figure 53

The Total Count image shows large spatial variations at a number of scales that are not simply related to bedrock geology. The same information is repeated in the Ternary image. The central tailings area (assumed) is low in both Total Counts and in the Ternary image. A track of extensive lows also appears to the NE and south of this feature. The extensive low in the south central hills may be associated with drainage run-off (moisture) pattern (speculative). Broadly the information content of these data appears high and obviously worth further detailed investigation.

## Silvermines: Electromagnetics.



Appendix 3: Figure 6. EM Conductivity. (a) Apparent conductivity at 25 kHz for the whole survey. General background displays low conductivities ( $< 5$  mS/m). Superimposed are geological and cultural variations. A strong E-W power line effect is observed towards the north. Other linear/quasi-linear conductivity variations are associated with roads. Other, less localised, variations may be geological e.g. arcuate trend of enhanced conductivities in the NW quadrant may be associated with Courceyan limestone and/or shales. Main conductive anomaly (in 2x2 km square) shows internal detail and is highly confined spatially. It is assumed that this anomaly is associated with a tailings area. (b) a 2x2 km detail defined by the square shown in (a). 12 kHz apparent conductivity shown as a perspective view from south to north. Flight line sampling superimposed.